SCUOLA DI DOTTORATO

UNIVERSITÀ DEGLI STUDI DI MILANO-BICOCCA

Department of Medicine and Surgery

PhD program in Molecular and Translational Medicine

Cycle XXXIV

Biological conditions related to frailty and their effects on adult renal stem cells cultured as nephrospheres

Dr.ssa Grasselli Chiara
Matr. No. 808243
Tutor: Prof. Perego Roberto
Co-tutor: Dr.ssa Bombelli Silvia
Coordinator: Prof. Biondi Andrea

ACADEMIC YEAR 2020/2021

To my family

Table of contents

Chapter 1

General Introduction

1.1 Stem cells: why they are so important?

1.1.1 Definition and types of stem cells

Stem cells (SC) are rare and undifferentiated cells that are uniquely capable of both reproducing themselves through self-renewing and generating the differentiated cell types that are needed to perform specialized functions in the body; they generate all the cells that make up the tissues of an adult organism. From a more rigorous functional point of view, a *bona fide* stem cell can generate the different components of the tissue in which it is located throughout the life of the organism. These characteristics, therefore, play essential roles in organogenesis during embryonic development and in tissue regeneration.

There are two main types of stem cells: embryonic stem cells (ESC) and somatic stem cells (SSC).

The derivation of mouse embryonic stem cells (ESC) was first reported in 1981 [Evans, 1981], but that of human ESCs lines was reported only in 1998 [Thomson, 1998]. ESC are pluripotent stem cells derived from the undifferentiated inner cells mass (ICM) of the cleavage-stage embryo (blastocyst) and they are able to differentiate into all three embryonic germ layers: ectoderm, endoderm, and mesoderm; each of the cells of these cleavage-stage embryos is undifferentiated.

Additionally, under defined conditions, embryonic stem cells are capable of propagating themselves indefinitely.

With the progress of development, in the embryo appear somatic stem cells (SSC) for organogenesis? Although more differentiated than ESC the SSCs retain the feature of self-renewal. They become progressively restricted in development, giving rise to multiple lineages or unipotent, giving rise to single lineage cells destined to specific tissues. SSCs differ from ESCs for pluripotency; while ESCs can generate all cell types in the body, somatic stem cells are multipotent and can produce only a limited number of cell types. Although the proliferation and differentiation potentials decrease in the transition from the embryonic to the somatic stage, the reproductive capacity remains the same, the stem cell remains unchanged.

Therefore, the definition of stem cell is linked to the stage of development of the organism and to the context in which the cell is located. SSCs are tissue-specific and present in the different tissues of both the fetus and the adult organism, and are called fetal stem cells and adult stem cells respectively.

Adult stem cells, share at least two characteristics. First, they should be able of self-renewal for the lifetime of the organism. Second, they can give rise to mature cell types that have morphological characteristics and specialized functions. Typically, stem cells generate intermediate cell types (precursor or progenitor cells) before achieving their fully differentiated state. These cells are usually regarded as "committed" to a specific cell fate. Therefore, progenitor cells are early descendants of stem cells that can differentiate to form one or more kinds of cells but cannot divide and reproduce indefinitely. The maintained balance

between self-renewal and differentiation means that the main function of adult stem cells is to maintain the tissue homeostasis, intended as the capacity to replace cells dying under physiological or pathological conditions [Hunt, 1987].

Adult stem cells behavior is controlled by the integration of intrinsic factors with extrinsic signals supplied by the surrounding microenvironment, known as the stem cell niche. The underlying mechanisms that control this delicate balance are fundamental to understand stem cell regulation, the nature of cancer/tumor formation, and the therapeutic use of stem cells in human disease.

1.1.2 Potency of stem cells

The capacity to differentiate into specialized cell types and be able to give rise to any mature cell types is referred as potency. The potency of the stem cells specifies the differentiation potential, i.e. the potential to differentiate into different cell types. It is also described as the gene activation potential within a cell. In cell biology, cellular potency varies from toti-potency to uni-potency (Figure 1). Totipotent stem cells can differentiate into embryonic and extraembryonic cell types. These cells can give rise to a whole and viable organism. These cells are produced from the fusion of an egg and sperm cell. On the contrary, the pluripotent stem cells (PSCs) that are the ESC may give rise to all types of cells in an organism, but lack potential to contribute to the extra-embryonic cells such as placenta.

Another important class of stem cell is lineage-specific multipotent stem cells, which have limited differentiation potential and develop

only in their tissue. These can only differentiate into a limited number of cell types. For example, the bone marrow contains multipotent stem cells that give rise to all the cells of the blood but not to other types of cells. Oligopotent stem cells can differentiate into only a few cells, such as lymphoid or myeloid stem cells. Finally, the developmental potential of unipotent stem cells is further restricted, giving rise to a single cell type only and still retaining the self-renewal ability, which distinguishes them from non-stem cells.

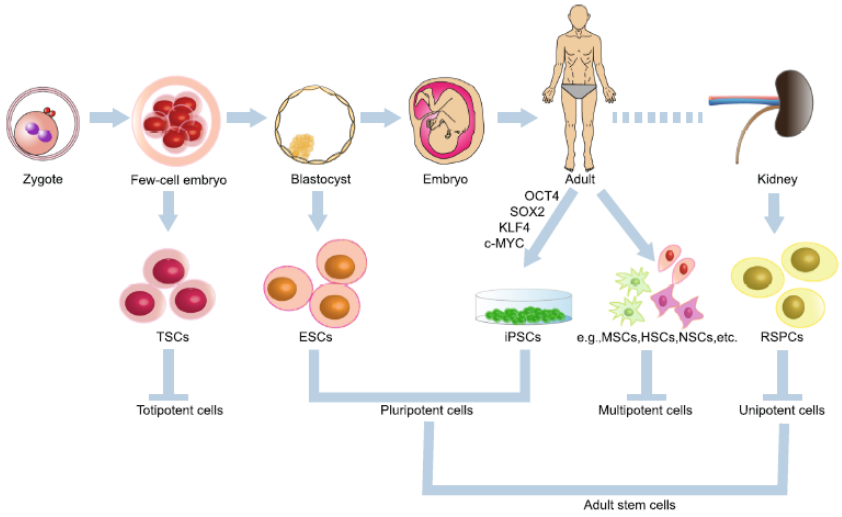

Figure 1. Schematic representation of the stem cell hierarchy based on stem cell potential. Liu C, Cheng F, Pan S et al. Stem cells: a potential treatment option for kidney diseases. Stem Cell Res Ther. 2020; 11(1): 249.

Thus, the traditional developmental dogma follows the differentiation of totipotent stem cells to PSCs, PSCs to multipotent stem cells, multipotent stem cells to unipotent stem cells and finally mature cells.

Both the self-renewal capacity and differential potential are reduced during their journey from totipotent to mature cell state. However, the discovery of nuclear reprogramming methods such as somatic cell nuclear transfer method and use of transcriptional factors to induce pluripotency in any cell type are demonstrated as powerful tools to reverse this hierarchy.

These findings show that the particular state of a somatic cell can be reprogrammed to achieve a pluripotent state called induced pluripotent stem cells (iPSCs) [Takahashi, 2006; Takahashi, 2007]. iPSC generated from patients have a great potential in disease modeling and regenerative medicine.

1.1.3 Physiological role and functional properties of stem cells

The principal function of a stem cell is to generate all of the differentiated cell types of the tissue in which it resides. During embryonic development this ability permits the rapid generation of the end-differentiated cells that will form the mature tissue and also in adulthood this capacity guarantees tissue homeostasis maintaining the stem compartment. Stem cells are generally quiescent cells, but they are able to activate and perform continuous proliferation over long periods of time (proliferative capacity) and to divide symmetrically or asymmetrically.

The maintenance of tissue homeostasis is controlled at multiple levels: (1) steady-state stem cells proliferation and self-renewal, as well as differentiation, ensures long-term maintenance of the stem cells pool

under physiological conditions; (2) acute induction of stem cells proliferation occurs in response to tissue damage; (3) reentry of stem cells into a quiescent or non-proliferative state after the tissue has been repaired or regenerated is necessary to re-establish the physiological equilibrium.

It is not always possible to assess all of these parameters simultaneously in a stem cell. As a consequence, different studies have pointed at different functional attributes as markers to identify a stem cell. Likely, the most important characteristic of a stem cell is its self-renewal capacity, i.e., ability to maintain the stem cell population at a steady state or to expand it under certain circumstances. At the single cell level, this can be achieved either by "asymmetric" division, generating one stem cell and one differentiated cell, or by "symmetric" division, where both progenies are identical to the mother stem cell [Alison and Islam, 2009]. In the former case, the overall stem cells number is maintained, whereas, in the latter, it increases. In a stem cell population as a whole, both mechanisms may occur. The balance between the different modes of division within the stem cells population determines its maintenance or expansion at each generation and can be genetically or epigenetically regulated. In this scenario, self-renewal is an essential feature of bona fide stem cells.

Multipotentiality is the capacity of a single self-renewing progenitor to generate the full array of organ-related lineages. Ideally, this feature is illustrated by the capacity of a single cell to replace all lost elements in the tissue of origin.

Proliferative plasticity of SSCs thus allows adapting the number of newly produced daughter cells to tissue demand [Biteau, 2011].

Differentiation, by definition, is the set of modifications that induce the progressive and stable acquisition of new functional and morphological competencies leading to the formation of defined phenotypes; i.e. it is a process of cell specialization. During the differentiation there is both qualitative and quantitative variation of markers, with the appearance of early and late markers.

A large number of interdependent factors, including transcription factors, epigenetic modification of developmental genes, including alterations in DNA methylation, histone modifications, polycomb gene group and non-coding RNA expression modulate this process. Other mechanisms that determine the fate commitment of stem cells are cytoplasmic determinants and communication between neighboring cells through signals that behave like morphogens.

Moreover, the implementation of the different functional properties of stem cells is flexible and dependent on the environment in which they are located, called niche. The stem cell niche is the *in vivo* microenvironment where stem cells both reside and receive stimuli that determine their fate. Therefore, the niche should not be considered simply a physical location for stem cells, but as the place where extrinsic signals interact and integrate to influence stem cell behavior. These stimuli include cell-to-cell and cell-matrix interactions and signals, molecules that activate and/or repress genes and transcription programs. As a direct consequence of this interaction, stem cells are maintained in a dormant state or induced to self-renewal and produce a cell committed to differentiate.

In summary, a positively identified adult stem cell would be a single self-renewing cell capable of generating progeny that can contribute to

the mature tissue with a sufficient number of newly differentiated cell types.

1.1.4 Aging and stem cells

Adult tissue stem cells have a pivotal role in regeneration and tissue maintenance throughout the lifespan of organisms. During aging the degenerative changes in tissue-specific stem cell number and function and in stem cell niches have been demonstrated to contribute to the age-related decline [Tümpel, 2019]. Therefore, stem cell exhaustion is considered as a hallmark of aging.

Understanding the molecular pathways involved in the age-dependent deterioration of stem cell function could be critical for developing new therapy strategies for aging diseases. Stem cell aging is characterized by many different cellular interactions often showing cross-talk in the determination of stem cell functions.

Pathways induced by reactive oxygen species (ROS) contribute to perturb stem cell functions and fate control in the context of aging. Accumulated cellular damage and declining mitochondrial integrity in aged cells lead to high ROS production leading to cell disfunction [Chaudhari, 2014].

Additionally, dysregulation of protein quality control, regulated by a complex protein network, can result in the accumulation of critically misfolded proteins affecting stem cell potential. Maintenance of the stem cell proteome is equally important for assuring stem cell identity [Saez, 2014]. Defects in proteostasis commonly lead to aberrant folding, toxic aggregation and accumulation of damaged proteins,

which can in turn cause cellular damage and tissue dysfunction [Tomaru, 2012].

There are also many studies that point to epigenetic regulation as important in determining stem cell function and further indicate that alterations in the epigenome that occur with aging can affect on cellular processes in aged organisms and their stem cells [Beerman, 2013].

Inflammation, in which an increase in pro-inflammatory cytokines occurs, can also impair the function of stem cells, ultimately reducing their ability to maintain homeostasis within the body.

Elevated levels of damaged DNA in aged stem cells could result from an accumulation of damage over time, an increase in long-term exposure to genotoxic assaults (both endogenous and exogenous source), a decrease in the capacity of repair in response to DNA damage or a combination of these possibilities [Behrens, 2014].

Aged human stem cells show compromised capacity to repair DNA damage, such as that produced by ionizing radiation [Rube, 2011]. These observations suggest that DNA damage response pathways, developed to safeguard genomic integrity and promoting survival of the organism, may show reduced activity in stem cells with age, leading to age-dependent loss of organ function and homeostasis.

As discussed above, stem cell aging is affected by different cell-intrinsic and cell-extrinsic pathways that contribute to a decline in stem cell function and depletion of the stem cell pool. Although, in some cases at least, these aging phenotypes can be reversed to restore the regenerative function of stem cells, aging is a major risk factor for many prelevant diseases [Sameri, 2020].

1.2 Renal stem cells

1.2.1 Renal tissue regeneration theory

It has been shown that the kidney is in no way a static organ, but it has a basal cellular regenerative potential. Renal cells are able to proliferate after injury, suggesting that kidney cells are able to regenerate under conditions of induced damage.

The complexity of the renal tissue in mammals, the lack of markers for adult cells which could retain stem properties in adult renal tissue and the reduced capacity of cell renewal make it difficult to study kidney regeneration mechanisms.

In this regard the debate is still going on, there are doubts about which cells are responsible for the recovery of tubular epithelium after injury [Huling, 2017]. Traditionally, tubular cells were considered as cells with regenerative potential, based on the quick functional recovery in animal models and on the robust proliferative activity observed in tubular tissue after injury [Basile, 2012]. Different hypotheses have been advanced about the nature of regenerative potential in the renal tissue.

The majority of studies attribute the basis of such regenerative potential to two main hypotheses, the dedifferentiation of the mature tubular epithelium or the presence of a resident pool of progenitor cells in the

kidney tissue [Lombardi, 2016]. Whether cells responsible for the regeneration of the kidney initially have stem-like properties or if they obtain a "progenitor phenotype" during dedifferentiation after an injury still stays the open question.

Dedifferentiation theory is based on the fact that at the steady state the differentiated epithelial cells of the proximal tubule are in the G1 phase of the cell cycle, ready to progress immediately in the cycle in case of injury in rats [Vogetseder, 2008]. In such scenario, fully differentiated tubular cells would transiently undergo dedifferentiation, loss of mature epithelium morphology and epithelial-mesenchymal transition, then proliferation to replace lost cells, migrate in correspondence of the damaged tubular base membrane and, ultimately, re-differentiation, replacing the lost tubular cells (Figure 2A).

The second hypothesis indicates the possible existence of a population of progenitor cells, so-called scattered tubular cells (STCs), in the adult kidney which have a more pronounced regenerative potential than differentiated tubular epithelium [Maeschima, 2003]. STCs would be in a quiescent state which is ready to re-enter the cell cycle to replace cell loss from tubular damage [Challen, 2006] (Figure 2B).

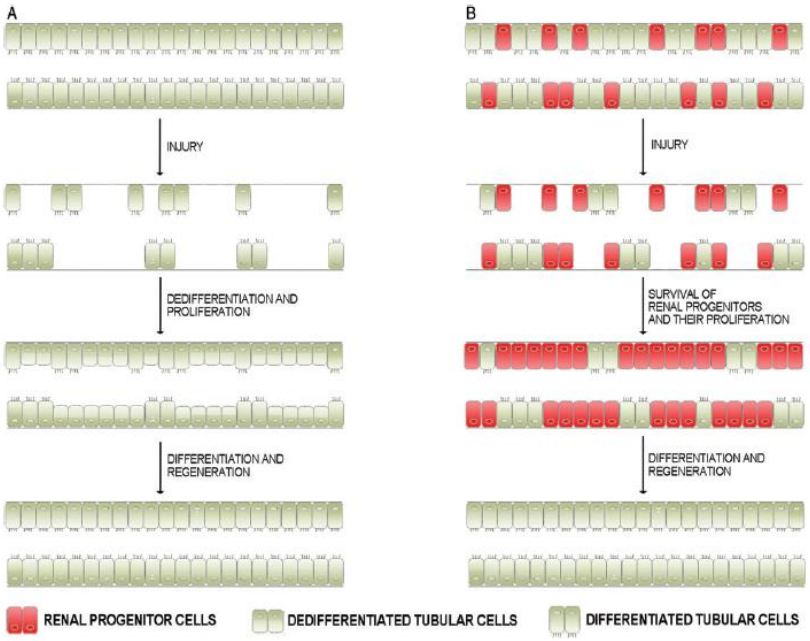

Figure 2. Schematic representation of tubular regeneration after injury. A Differentiated tubular cells surviving the injury dedifferentiate, proliferate, migrate and then differentiate, replacing the lost tubular cells; B Tubular progenitors are scattered among differentiated tubular cells. They are highly resistant to injury, so that they are able to survive, proliferate, migrate and then differentiate to replace lost tubular cells. Lombardi et al. Nephrol Dial Transplant. 2016; 31: 1243–1250.

1.2.2 Stem/Progenitor cells in kidney

Several studies have been made to identify and characterize renal stem/progenitor cells (RSPC) from differentiated cells in adult kidney, however what we actually know about RSPC is that there is no single *bona fide* marker.

First attempt was label-retaining assays because in general stem cells are quiescent cells; they have a slow turnover rate and show minimal physiologic differentiation. When labeled nucleic acids were incorporated, BrdU or 3H-thymidine, SCs retain the label for longer periods of time, while other cells lose them. Label-retaining cells (LRC) are believed to represent the SC compartment. The first evidence of the presence of progenitor cells in the kidneys arose in the study of Maeshima et al [Maeshima 2006]. They demonstrated the existence of LRCs in renal tubuli of normal rat kidneys. Oliver and collegues have identified LRCs in the mouse papilla [Oliver, 2003]. These cells form spheres in vitro as well as potentially differentiate towards other lineages. On a 3D gel substrate, they formed tubule-like or tubulocystic structures in response to growth factors treatment [Maeshima 2006] and, when LRCs were injected into cultured metanephros, formed nephrons and collecting ducts [Maeshima 2006].

In a recent study, the analysis of kidney progenitor cells was performed using transgenic mice with doxycycline-induced random labeling of all tubular epithelial cells by permanent recombination of a single-color-encoding gene. After an acute kidney injury they showed that tubules consisted of clones of cells with the same color. Only a small number of epithelial cells underwent mitosis, most of them were Pax-2-positive, the resident progenitors, whereas the rest of the tubular epithelium underwent an endoreplication cycle [Lazzeri, 2018]. This paper thus clarifies that in mice the renal functional recovery upon AKI involves both tubular cell hypertrophy via endocycle and a limited regeneration driven by progenitors.

In rats, the staining for vimentin, CD44 or transcription factor Sox9 carried out the search for stem/progenitor cells. However, the appearance *de novo* of vimentin-positive cells [Smeets, 2013] with atypical morphology or the expression of Sox9 by renal cells [Kang, 2016] occurs only after injury. Therefore, these processes may be only the result of the dedifferentiation of some renal cells.

Since lineage tracing in humans is not applicable, it is difficult to argue whether in humans there are the cell populations capable of the same regenerative abilities described in kidney mice and whether the human kidney cell phenotype is fixed or inducible. What we know is that, as well as in rodent kidneys, the presence of RSPCs has been demostrated in different portion of human kidney [Smeets, 2013; Bussolati, 2005]. A population of cells with morphology and progenitor properties, different from normal epithelial cells, were isolated in the proximal tubules. The main markers of this population were CD24, CD133 and vimentin, and cells were scattered throughout the proximal tubule in the normal human kidney. These cells had less cytoplasm compared to conventional ephitelial cells, fewer mitochondria, and had no brush border [Smeets, 2013].

A feature of human kidney progenitor cells, absent in rodent cells, is the presence of CD133, a specific marker of undifferentiated cells. Although CD133 is abundant in both immature and differentiated cells, specific glycosylated epitopes have been found only on immature cells in humans [Angelotti, 2010], such as hematopoietic stem/progenitor cells and tissue-specific progenitor cells [Corbeil, 2000]. The glycosylated form of CD133 has been shown to be expressed in human renal tissue. Thus, CD133 is a widely used marker of progenitors, but

for confirmation of the results of CD133 detection, cells often are examined for CD24, which usually co-expresses with CD133 [Romagnani, 2014].

Cells positive for CD24/CD133 have the ability to expansion, self-renewal and epithelial differentiation both in vitro and in vivo. In culture, they are able to differentiate into tubular epithelial cells and endothelial cells and to repair tubular structures [Sagrinati, 2006]. In vitro, they have the ability to form spheres, which is a specific feature of stem cells and to proliferate for a long time without signs of cell senescence [Lindregen, 2011]. In addition, CD24/CD133 positive cells have a pronounced regenerative potential when administered to mice with severe combined immunodeficiency (SCID) exposed to ischemia/reperfusion.

Ronconi et al. identified CD133+/CD24+ populations as arranged in a precise sequence within the Bowman's capsule (Ronconi, 2009). Angelotti et al. demonstrated the presence of small clusters of CD133+/CD24+/CD106+ cells that were localized at the urinary pole of Bowman's capsule that showed a high proliferative rate and could differentiate toward both podocytes and tubules. By contrast, CD133+/CD24+/CD106- were less proliferative and suggested a commitment toward the tubular lineage [Angelotti, 2012].

Apart from CD24 and CD133, other 49 proteins were expressed in the kidney in the same scattered pattern. Among them there are Pax-2 and Sox9, however, colocalization with CD24 or CD133 was shown only for vimentin, S100A6 and several other proteins (e.g., aldehyde dehydrogenase) [Lindgren, 2011].

Despite numerous studies, many questions remain open about RSPCs in both mouse and human.

1.2.3 Isolation and characterization of adult renal stem cells: the nephrosphere assay and PKH^{HIGH} cells

In the scenario described above, our group contributed to the debate for the definition of renal stem cells, isolating a pure population of multipotent stem-like cells by a functional approach [Bombelli, 2013]. Taking advantage from the ability of SC to grow as spheres, Bombelli et al. obtained nephrospheres (NS) containing cells at different level of maturation, i.e. both adult stem like cells and progenitors.

Spheres showed a clonal growth and sphere number was maintained along passages, so that the authors concluded that there is only a sphere initiating cell per nephrosphere.

Of note, sphere cells injected in nude mice were able to give rise to human epithelial tubular structures with characteristics of both proximal and distal tubules.

For the isolation of cells with stem properties within the NS, a lipophilic dye (PKH26) retained in quiescent stem cells after asymmetric division and diluted in proliferating progenitors, was used (Figure 3A).

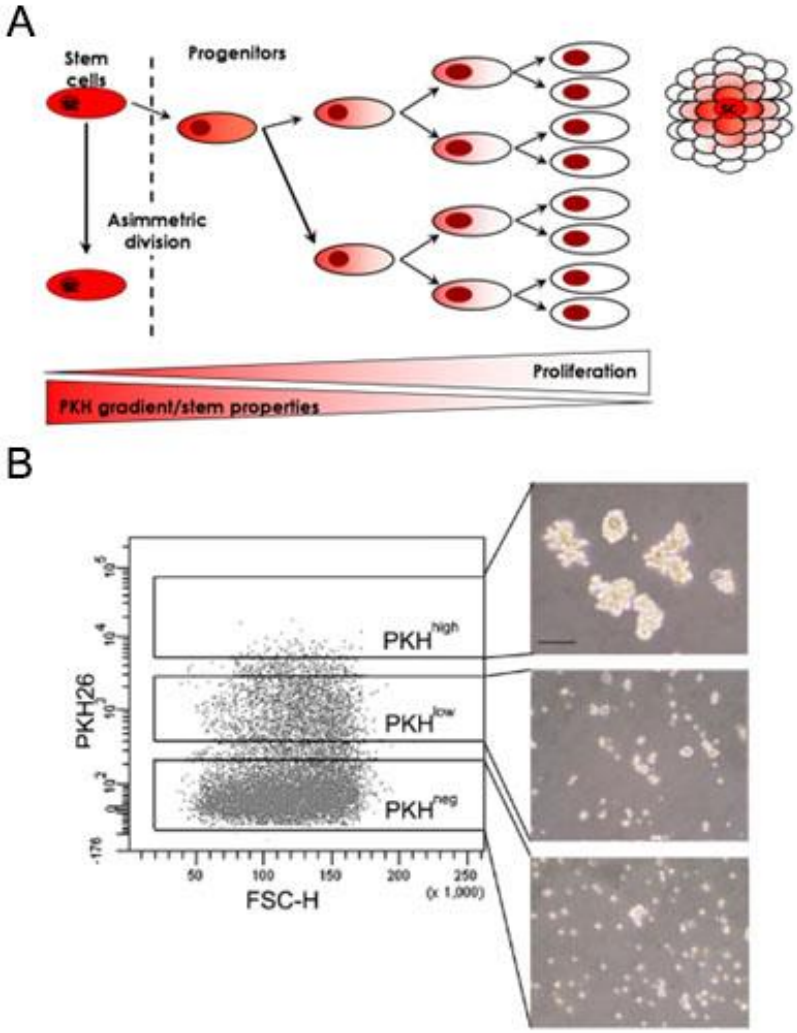

Figure 3. Illustration of cell proliferation using PKH26 and identification and isolation of PKH^{high} stem-like cells in the nephrospheres. A PKH26 is retained in quiescent stem cells and diluted in progenitors along proliferation; B PKH26-labeled nephrosphere cell population with gated populations and suspension cultures in sphere-forming conditions of FACS-sorted PKH^{high}, PKH^{low} and PKH^{neg} cells. Bombelli S et al. PKH^{high} cells within clonal human nephrospheres

provide a purified adult renal stem cell population. Stem Cell Res 2013, 11: 1163-1177.

Having stained cells before NS formation, the most fluorescent cells are the self-renewing quiescent cells with stem abilities. Based on PKH26 epifluorescence, three different populations were separated by cell sorting: PKH^{high}, PKH^{low} and PKH^{neg} cells (Figure 3B). Among these, only PKH^{high} cells showed self-renewal ability, in terms of reforming new secondary NS and multipotency, differentiating through three different renal lineages: epithelial, endothelial and podocytic. Instead, PKH^{low} and PKH^{neg} cells failed to differentiate both in podocytic and in endothelial lineages. PKH^{high} cells were then considered as cells with stem-like properties.

Investigating the expression of renal progenitor markers described in literature, (CD133 and CD24) an enrichment in CD133+/CD24- phenotype in the PKH^{high} population was observed. In addition, only PKH^{high}/CD133+/CD24- and PKH^{high}/CD133+/CD24+ showed the ability to self-renew, but only the first subpopulation could differentiate into epithelial, endothelial and podocytic renal lineages, while the second one failed the endothelial and podocytic differentiation.

It was finally concluded that PKH^{high}/CD133+/CD24- cells are those with stem-like properties within NSs.

In 2018 Bombelli et al have shown the capacity of immature NS cells to repopulate different nephron portions of decellularized human renal scaffolds comprising cortex, medulla and papilla. NS cells cultured on scaffolds with basal medium, without specific growth factors, were able to generate proximal and distal tubular structures as well as endothelial-

like structures expressing the specific differentiation markers. Furthermore, they were able to attach and proliferate in the peripheral areas of the glomerular space but not in the inner glomerular endothelium or epithelium [Bombelli, 2018]. Morover, in vitro, human adult renal stem-like PKH^{high}/CD133+/CD24− cells showed multipotency [Bombelli, 2020].

1.3 Kidney disease

1.3.1 kidney disease: definition, symptoms and causes

Kidney disease is a general expression for heterogeneous disorders affecting kidney function and structure. It has a progressive course that has a significant impact on the morbidity; abnormalities in measures of kidney structure and function are associated with increased risk for developing complications in other organ systems including increased mortality rates of the general population.

In recent years kidney diseases affect approximately 11% to 13% of adult population worldwide [Hill, 2016] and it is therefore considered a global public health problem. The only successful treatments for end stage chronic renal disease are dialysis and organ transplantation. However, the Italian Transplant Information System reports that 6039 individuals are on the wait-list for a kidney transplant, with only 1623 kidney transplants taking place during 2020 (26,87 %) (https://trapianti.sanita.it/ statistiche /home.asp). The average of waiting time for transplant is 3,4 years and the patient mortality during waiting time is relatively high (about 1,8%) (http://www.aido.it/dati_ statistici/liste.htm). The evident shortage of transplantable kidneys has driven researches towards bioengineering strategies for renal tissue regeneration.

Kidney diseases can be defined and classified according to many domains: structure, function, cause, duration, and outcomes. Generally, when kidney failure develops rapidly, from a few hours to a few days,

it is referred as “acute” and it is a life-threatening condition, but if recognized and treated properly, it can be reversible.

When kidney failure develops slowly, over the course of months or years, it is defined as “chronic”. It is an irreversible condition and the symptoms appear only late, when the disease is already advanced. The evolution of this condition can be slowed down but if it reaches its most advanced stage, it makes necessary the use of dialysis or kidney transplantation. However, a close interconnection with regard to their etiology has been recently highlighted [Ferenbach, 2016].

Kidney disease differs from most other disorders of organ systems in that it is often “silent”: there are few symptoms until late in the course of disease and even then, the symptoms are often nonspecific. Especially in chronic kidney disease (CKD) there are few kidney-specific clinical events; the symptoms become evident only when the damage developed is difficult to reverse.

Criteria to identify kidney failure include measures of kidney damage (albuminuria, abnormalities in the urine sediment, imaging, or biopsy) and function (decreased glomerular filtration rate, rising serum creatinine level, or decreased urine output).

Identifying the cause of kidney disease is not included in the definition of either chronic or acute kidney disease and they are often unknown.

1.3.2 Kidney dysfunction and renal stem cells

Stem cell-based therapy has been proposed as a potentially promising strategy for kidney disease, using stem cells as a therapeutic option for

regenerating damaged tissues and organs in an attempt to find innovative treatments to stimulate kidney regeneration

As said before, one of the most important features of stem cells is their capacity to divide and produce more stem cells (self-renewal potency) or differentiated precursors, which is associated with their potential to differentiate into different specialized cell types [Blanpain, 2014]. However, not all stem cell types have the same differentiative and therapeutic potential.

Adult stem cells are multipotent and the main role is to maintain tissue homeostasis throughout life by physiological cell turnover and by replacing damaged cells when necessary [Blanpain, 2014]. In human adult stem cells have been isolated from several different tissues including kidney. Progenitor cells capable of replacing glomerular cells, such as podocytes, and tubular epithelial cells have been identified [Maeschima, 2003; Bussolati, 2005; Bussolati, 2015; Dekel, 2006; Ronconi, 2009; Angelotti, 2012]. More recently, a new population of perivascular stromal cells has been isolated from the human kidney (kPSCs) [Leuning, 2017].

Several different populations of adult stem/progenitor cells have been tested to identify the most promising for stimulating the regenerative ability of the kidney [Marcheque, 2019]. MSCs have been described as one of the most efficient cell populations for activating the regeneration of the damaged kidney.

However, a number of studies have highlighted the potential that several renal precursor cell populations obtained from rodent and human kidneys have in the therapy of renal diseases, possibly by directly replacing injured cells [Bussolati, 2015; Lombardi, 2016;

Pleniceanu, 2018]. Of these, human kidney-specific progenitor cells were described as exerting a renoprotective effect in a glycerol-induced-AKI model due to their ability to counteract apoptotic stimuli and to directly generate novel tubular cells [Angelotti, 2012]. Moreover, kPSCs exhibited a transcriptional profile and stromal cell markers that are similar to human bone marrow cells but also exhibited a renal tissue-specific expression signature including HoxD10 and HoxD11 transcription factors, which are known to be crucial for nephrogenesis [Leuning, 2017]. Human kPSCs ameliorated kidney injury when injected into mice with glycerol-induced acute kidney injury without incorporating into tubular structures [Leuning, 2017].

Despite of the success of renal progenitor cell treatments in experimental kidney diseases, their limited sources and nephrogenic potential and their short life span limit the applicability of this approach.

1.4 Frailty

1.4.1 What is Frailty syndrome?

Frailty is a multidimensional geriatric syndrome that can be associated to aging. It is defined as a state of increased vulnerability resulting from severe decline of several physiological systems, loss of homeostatic mechanisms and functional reserves; so frail persons have a reduced capacity to compensate for internal and external stressors. It is a potentially reversible condition but, in most cases, it progresses towards disability and/or leads to several negative outcomes, including falls and fractures, hospitalizations, iatrogenic complications and mortality [Lang, 2009]. Importantly, the risk of adverse event can occur independently of the presence of comorbidity.

An early diagnosis of the syndrome would be crucial to prevent the complication related to frailty, considering its possible reversibility at the early stages [Tarazona-Santabalbina, 2016; Travers, 2019].

Weakness was the most common initial manifestation of the frailty phenotype. However, it evidenced only moderate predictive validity for incident frailty; the development of frailty is progressive and multisystemic and any one specific criterion alone, especially at an early stage in the process as in the case of weakness, may be neither sufficient nor specific for frailty prediction. Moreover, until now no molecular processes or biological indicators are available for the identification of a frail phenotype.

Putative frailty molecular indicators have been searched starting from comprehensive biomarkers of cellular ageing, inflammation and

immunosenescence [Collerton, 2012; Mitnitski, 2015] but the complex interactions between aging mechanisms and the studied molecules are not yet completely clear and can be confounding. Therefore, the search of eventual molecular indicators specific for frailty syndrome that can allow a timely and more objective identification of frail subjects is still ongoing.

A common feature of several clinical aspects involved in senescent organisms is the increment of oxidative stress that is described as one of the major cause of DNA damage accumulation, well documented in the different tissues of aged people [Sanchez-Flores 2017]. Likely, this accumulation can be implicated in frailty status [Dent 2016] because DNA damage can lead to molecular and cellular alterations (genomic instability, altered gene expression, loss of cell division potential, cell death, organ dysfunctions) [Rattan, 2006; Sanchez-Flores, 2017] that are a good background on which frailty can establish.

Studies show that the overall prevalence of frailty in community-dwelling older adults aged 65 or older ranges 17%, according to the WHO World Report on Ageing and Health [WHO, 2015]. In particular the prevalence of frailty increases with age from 3.9% in the 65-74 age group to 25% in the over 85 years group and was greater in women than men (8% vs. 5%) [Fried, 2001; Graham, 2009; Santos-Eggimann, 2009].

In our aging society, identifying frailty among community-dwelling older adults would certainly lead to stratify them according to their risk of negative outcomes, to prompt intervention strategies and ultimately to improve their quality of life (QoL) and outcomes [Henchoz, 2016]. The most hospitalized patients are frail or pre-frail. However, only frail

status (vs. pre-frail status) is associated with worse physical function and QoL, comorbidity and depression [Pandey, 2019] (Figure 4).

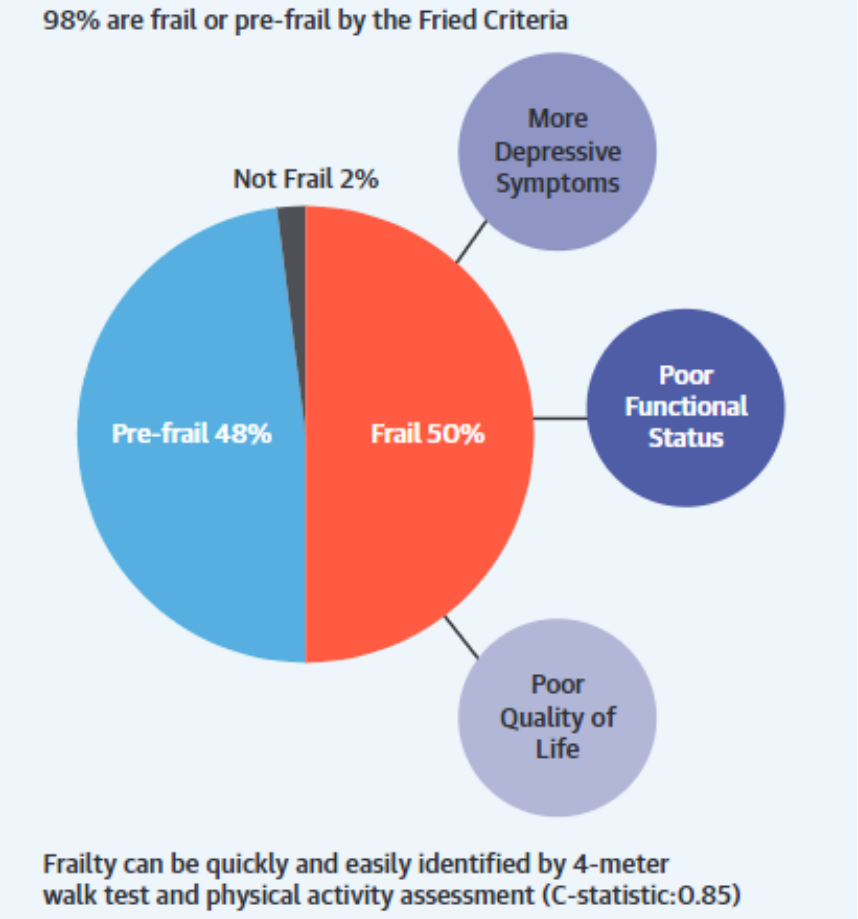

Figure 4. Illustration of the impact of frailty syndrome on the functional capacity of the subject and on the activity of daily living. Pandey, A. et al. J Am Coll Cardiol HF. 2019; 7(12):1079–88.

Given these premises, the identification of a frail phenotype could certainly be cost-effective given the cascade of events that lead and follow frailty, thus significantly improving the QoL [Marije, 2016].

1.4.2 How to identify frailty: Fried's criteria

In literature there are several evaluation methods to identify frailty but the most employed was described by Fried et al [Fried, 2001]. She proposed a frail phenotype characterized by at least three of the following five criteria:

- Unintentional weight loss over the last year (≥5%);
- Fatigue in activity of daily living. Exhaustion was measured using the question "In this last month, do you have less energy to do the things of daily living you want?" which was categorized as no exhaustion or yes exhaustion;
- Reduction of the walking speed. Subjects are considered frail if they employ more than 7 seconds to cover a distance of 4 meters [Guralnik, 1994];
- Low physical activity. It was assessed using Physical Activity Scale for the Elderly (PASE) over a one-week period. The PASE score combines information on leisure, household and occupational activity [Washburn, 1999];
- Reduction of muscle strength. Weakness was measured using the dynamometer handgrip strength for three consecutive times on dominant hand. The criterion is positive if the best value is less than cutoff value (<27 for males and <16 for females) [Cruz-Jentoft, 2019].

Patients who fulfilled none of the criteria were considered non-frail, patients were considered pre-frail if scoring in one or two criteria and frail if scoring three or more criteria. As we can see in Figure 5 the probability of incidence of disability was significantly higher in participants classified as frail compared with those classified as pre frail or non-frail [Makizako, 2015].

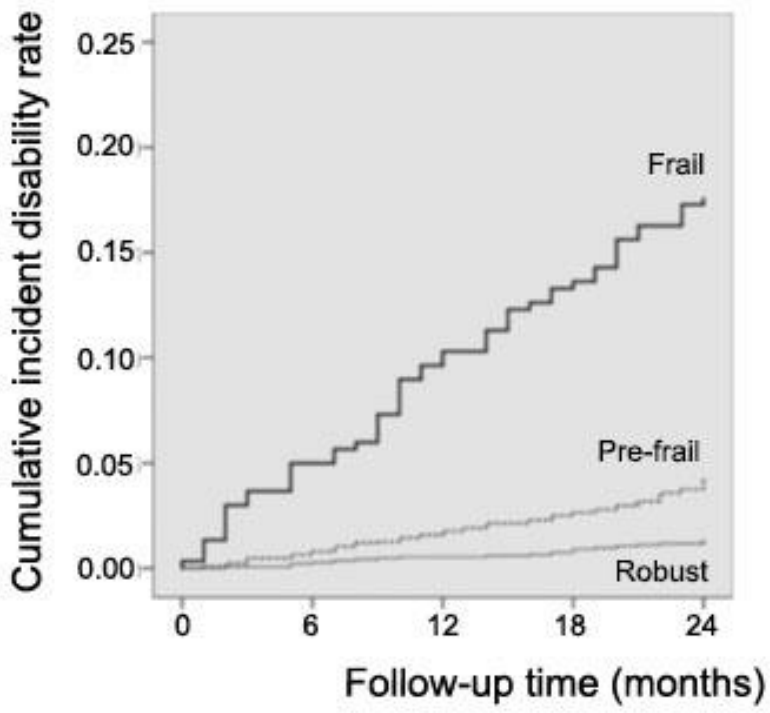

Figure 5. Representation of the cumulative incidence of disability in relation to the frail, pre-frail and robust subjects and the observation time. Makizako H et al. Impact of physical frailty on disability in community-dwelling older adults: a prospective cohort study. BMJ open 2015; 5: e008462.

Another approach is to calculate a frailty index based on clinical assessments and pathologies established by Rockwood et al [Rockwood, 2006]. They developed the rules-based frailty definition and the Frailty Index, a measure of frailty obtained by counting various clinical deficits. Afterward, they identified through Canadian Study on Health and Aging (CSHA) numerous items including signs, symptoms, clinical status and abnormal tests that, in their opinion, can characterize frailty. The goal was to create tools that could stratify elderly patients as to their relative degree of vulnerability (i.e., their risks of death and of entry into an institutional facility) with simple clinical descriptors. Rockwood's clinical frailty scale ranges from 1 (robust health) to 7 (complete functional dependence on others).

The methodologies of Rockwood and Fried identify frailty with different prevalences; however, the main limitation of both these criteria and methods is the late identification of frailty syndrome, which is possible only after the onset of clinical manifestations.

1.4.3 Kidney dysfunction and frailty

Frailty frequently occurs in CKD patients. In fact, the prevalence of frailty is > 60% in dialysis-dependent CKD patients, while is reported to be 11% in older adult population [Bao, 2012; Collard, 2012]. The phenotype of renal aging includes loss of kidney parenchymal mass, increased renal vascular resistance, reduced plasma flow and these characteristics are strongly increased in frail individuals [Daya, 2016]. However, the relationship between CKD and frailty is not completely understood.

What is known is that patients with advanced CKD often have a reduced energy intake that contributes to sarcopenia and, subsequently, physical frailty [Kim, 2013]. There is in fact a progressive decline in food intake with deteriorating kidney function [Carrero, 2013].

Physical activity tends to decrease with frailty syndrome and this it is more marked for individuals with CKD [Bowlby, 2016]. Furthermore, physical inactivity is associated with an increased risk of mortality in those with CKD and consequently the prevalence of frailty among individuals with CKD has increased early mortality [Wilhelm-Leen, 2009] (Figure 6).

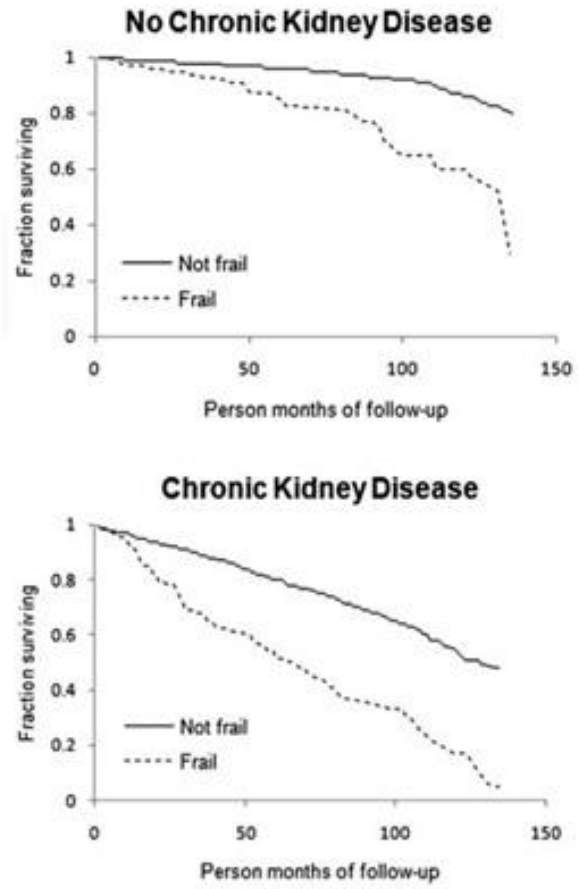

Figure 6. Relationship among frailty, chronic kidney disease and survival rate. Emilee R. Wilhelm-Leen et al. Frailty and Chronic Kidney Disease: The Third National Health and Nutrition Evaluation Survey. Am J Med. 2009; 122(7): 664–71.

Moreover, inflammation is associated with frailty in many chronic diseases [Jeffery, 2013]. In particular, the pro-inflammatory cytokines interleukin-6 and tumor necrosis factor alpha may have a role in age-related muscle atrophy and sarcopenia, which are key features of frailty [Hubbard & Woodhouse, 2010] and they are increased also in patients with CKD [Shlipak, 2003] suggesting a relationship between inflammation and frailty specifically in patients with CKD.

In conclusion, frailty was a significant predictor of adverse health outcomes, particularly in those with severe CKD stages.

Aim of the thesis

Frailty is a clinical geriatric syndrome closely linked to advanced age and a disease-related process. It is defined as a state of increased vulnerability resulting from decline of several physiological systems, so frail patients have a reduced capacity to compensate for external stressors. The identification of frailty occurs through five criteria defined by Fried, but this can be possible only after the onset of clinical manifestations without the possibility of a precocious diagnosis.

Several studies showed that there is a close association between frailty and CKD [Shlipak, 2004]. Of note, elderly individuals with CKD are two to three times more likely to be frail than those with normal renal function. However, the debate on these relationships is still ongoing [Chowdhury, 2017].

During aging the degenerative changes in tissue-specific stem cells, stem cell niches and function have been demonstrated to contribute to age-related decline [Tümpel, 2019]. Stem cell exhaustion is considered as a hallmark of aging and it is directly associated with an increased incidence of physical problems and diseases, including kidney dysfunction. It is worthwhile to understand whether the modulation of renal cell pool with stem-like property (RSC) has relation with frailty status.

Our group isolated a pure population of multipotent stem-like cells by a functional approach [Bombelli, 2013], taking advantage from the ability of RSC to grow as nephrospheres. Investigating the expression of renal progenitor markers described in literature (CD133 and CD24) [Bussolati, 2005; Sagrinati, 2006], our group identified in

nephrospheres a homogeneous cell population PKH^{high}/ CD133+/ CD24- displaying in vitro stem-cell properties [Bombelli, 2013], capacity to repopulate human decellularized renal scaffold [Bombelli, 2018] and multipotency (as shown in chapter 2) [Bombelli, 2020].

Given these premises, we wanted to test whether in the organism of aged and frail people there are biological conditions able to change the RSC behavior, justifying the high prevalence of chronic kidney dysfunction in the frail status and its severity.

Therefore, as shown in chapter 4, the aim of this 3-years project is **to study the effects of biological conditions related to frailty, such as oxidative stress and the alteration of inflammatory mediators, on adult RSC properties and evaluate if they are able to exhaust the SC pool and their functions.**

To achieve this main aim, the Geriatric Unit enrolled whole blood of frail, pre-frail and non-frail subjects, and young subjects as controls. The collected blood was separated into plasma and peripheral blood mononuclear cell (PBMC). In addition, samples of normal kidney tissue provided by pathologists as leftover tissue after nephrectomies in urological patients affected by renal carcinoma were used to establish NS cultures.

As we can see in chapter 3 DNA damage was evaluated both in PBMC and circulating hematopoietic progenitor stem cells (cHPSC) identified as CD34+/CD14-/CD3- by analyzing the phosphorylation of H2AX histone at serine 139 by FACS. PBMC and cHPSC from frail seniors showed a significant increased percentage of cells with DNA damage compared to all the other groups.

Also the mean fluorescence intensity (MFI) significantly increased in cHPSCs γH2AX+ of frail subjects compared to other subjects.

Subsequently, NS cultures, obtained from nephrectomies, have been treated with 10% plasma of enrolled frail, non-frail seniors and young controls. We first evaluated sphere forming efficiency (SFE), to test a possible change in RSC number and an effect on self-renewal abilities. We then evaluated DNA damage, proliferation, apoptosis and viability in renal stem/progenitor cells obtained after NS dissociation pre-treated with plasma. SFE statistically decreased in old people, both frail and non-frail seniors, compared to young controls and DNA damage increased in NS cells treated with plasma of frail seniors compared to those treated with the other plasmas.

Finally, we analysed the oxidative stress and the profile of 40 inflammatory cytokines on plasma of frail seniors, non-frail seniors and healthy young. We observed an increase of oxidative stress in frail compared to other groups and some cytokines are unique in frail seniors and others more present in frail subjects than in other groups.

References

Evans MJ, Kaufman MH. Establishment in culture of pluripotential cells from mouse embryos. Nature. 1981; 292: 154-156.

Thomson JA, Itskovitz-Eldor J, Shapiro SS et al. Embryonic stem cell lines derived from human blastocysts. Science. 1998; 282: 1145-1147.

Hunt P, Robertson D, Weiss D et al. A single bone marrow-derived stromal cell type supports the in vitro growth of early lymphoid and myeloid cells. Cell. 1987; 48: 997-1007.

Takahashi K, Yamanaka S. Induction of pluripotent stem cells from mouse embryonic and adult fibroblast cultures by defined factors. Cell. 2006; 126: 663-676.

Takahashi K, Tanabe K, Ohnuki M et al. Induction of pluripotent stem cells from adult human fibroblasts by defined factors. Cell. 2007; 131: 861-872.

Alison and Islam. Attributes of adult stem cells. J Pathol. 2009 Jan; 217(2):144-60.

Biteau B, Hochmuth CE, Jasper H. Maintaining tissue homeostasis: dynamic control of somatic stem cell activity. Cell Stem Cell. 2011; 9(5): 402-411.

Tümpel S, Rudolph KL. Quiescence: good and bad of stem cell aging. Trends Cell Biol. 2019; 29: 672- 685.

Chaudhari P, Ye Z, Jang YY. Roles of reactive oxygen species in the fate of stem cells. Antioxid Redox Signal. 2014; 20: 1881- 1890.

Saez I and Vilchez D. The Mechanistic Links Between Proteasome Activity, Aging and Age-related Diseases. Curr Genomics. 2014; 15(1): 38–51.

Tomaru U, Takahashi S, Ishizu A et al. Decreased proteasomal activity causes age-related phenotypes and promotes the development of metabolic abnormalities. Am J Pathol. 2012; 180:963–972.

Beerman I, Bock C, Garrison BS et al. Proliferation-dependent alterations of the DNA methylation landscape underlie hematopoietic stem cell aging. Cell Stem Cell. 2013; 12: 413- 425.

Behrens A, Van Deursen JM, Rudolph KL et al. Impact of genomic damage and ageing on stem cell function. Nat Cell Biol. 2014; 16:201–207.

Rube CE, Fricke A, Widmann TA et al. Accumulation of DNA damage in hematopoietic stem and progenitor cells during human aging. PLoS ONE. 2011; 6: e17487.

Sameri S, Samadi P, Dehghan et al. Stem Cell Aging in Lifespan and Disease: A State-of-the-Art Review. Curr Stem Cell Res Ther. 2020;15(4):362-378.

Huling, J, Yoo JJ. Comparing adult renal stem cell identification, characterization and applications. J. Biomed. Sci. 2017, 24, 32.

Basile DP, Anderson MD, Sutton TA. Pathophysiology of acute kidney injury. Compr Physiol 2012; 2: 1303–1353.

Lombardi D, Becherucci F, Romagnani P. How much can the tubule regenerate and who does it? An open question. Nephrol Dial Transplant. 2016 Aug;31(8):1243-50.

Vogetseder A, Picard N, Gaspert A et al. Proliferation capacity of the renal proximal tubule involves the bulk of differentiated epithelial cells. Am J Physiol Cell Physiol 2008; 294: C22–C28.

Maeshima A, Yamashita S, Nojima Y. Identification of renal progenitor-like tubular cells that participate in the regeneration processes of the kidney. J. Am. Soc. Nephrol. 2003, 14, 3138–3146

Challen GA, Bertoncello I, Deane JA et al. Kidney Side Population Reveals Multilineage Potential and Renal Functional Capacity but also Cellular Heterogeneity. J. Am. Soc. Nephrol. 2006, 17, 1896–1912.

Maeshima A, Sakurai H, Nigam SK. Adult kidney tubular cell population showing phenotypic plasticity, tubulogenic capacity, and integration capability into developing kidney. J. Am. Soc. Nephrol. 2006, 17, 188–198.

Oliver JA, Maarouf O, Cheema FH et al. The renal papilla is a niche for adult kidney stem cells. J. Clin. Invest. 2004.

Lazzeri E, Angelotti ML, Peired A et al. Endocycle-related tubular cell hypertrophy and progenitor proliferation recover renal function after acute kidney injury. Nat. Commun. 2018, 9.

Smeets B, Boor P, Dijkman H et al. Proximal tubular cells contain a phenotypically distinct, scattered cell population involved in tubular regeneration. J. Pathol. 2013, 229, 645–659.

Kang HM, Huang S, Reidy, K et al. Sox9-Positive Progenitor Cells Play a Key Role in Renal Tubule Epithelial Regeneration in Mice. Cell Rep. 2016.

Bussolati B, Bruno S, Grange C et al. Isolation of renal progenitor cells from adult human kidney. Am. J. Pathol. 2005, 166, 545–555.

Angelotti ML, Lazzeri E, Lasagni L et al. Only anti-CD133 antibodies recognizing the CD133/1 or the CD133/2 epitopes can identify human renal progenitors. Kidney Int. 2010, 78, 620–621.

Corbeil, D, Röper, K, Hellwig A. The human AC133 hematopoietic stem cell antigen is also expressed in epithelial cells and targeted to plasma membrane protrusions. J. Biol. Chem. 2000, 275, 5512–5520.

Romagnani P, Lasagni L, Remuzzi G. Nephrons are generated via a series of committed progenitors. Nat Rev Nephrol. 2014; 10: 491.

Sagrinati C, Netti GS, Mazzinghi B et al. Isolation and characterization of multipotent progenitor cells from the Bowman's capsule of adult human kidneys. J. Am. Soc. Nephrol. 2006, 17, 2443–2456.

Lindgren D, Boström AK, Nilsson K et al. Isolation and characterization of progenitor-like cells from human renal proximal tubules. Am J Pathol. 2011 Feb;178(2):828-37.

Ronconi E, Sagrinati C, Angelotti ML et al. Regeneration of Glomerular Podocytes by Human Renal Progenitors. J. Am. Soc. Nephrol. 2009; 20: 322–332.

Angelotti ML, Ronconi E, Ballerini L et al. Characterization of renal progenitors committed toward tubular lineage and their regenerative potential in renal tubular injury. Stem Cells 2012, 30, 1714–1725.

Bombelli S, Zipeto MA, Torsello B et al. PKHhigh cells within clonal human nephrospheres provide a purified adult renal stem cell population. Stem Cell Res 2013, 11: 1163-1177.

Bombelli S, Meregalli C, Scalia C et al. Nephrosphere-Derived cells are induced to multilineage differentiation when cultured on human decellularized kidney scaffolds. Am J Pathol. 2018; 188(1):184-195.

Bombelli S, Meregalli C, Grasselli C et al. PKHhigh/CD133+/CD24− Renal Stem-Like Cells Isolated from Human Nephrospheres Exhibit In Vitro Multipotency. Cells. 2020; 9: 1805.

Hill NR, Fatoba ST, Oke JL et al. Global Prevalence of Chronic Kidney Disease - A Systematic Review and Meta-Analysis. PLoS One. 2016; 11(7): e0158765.

Ferenbach DA, Bonventre JV. Acute kidney injury and chronic kidney disease: From the laboratory to the clinic. Nephrol. Ther. 2016; 12: (Suppl. 1) (Suppl. 1), S41–S48.

Blanpain C, Fuchs E. Stem cell plasticity. Plasticity of epithelial stem cells in tissue regeneration. Science. 2014; 344: 1242281.

Bussolati B, Camussi G. Therapeutic use of human renal progenitor cells for kidney regeneration. Nat. Rev. Nephrol. 2015; 11: 695–706.

Dekel B, Zangi L, Shezen E et al. Isolation and characterization of nontubular Sca-1^{+}Lin^{-} multipotent stem/progenitor cells from adult mouse kidney. J. Am. Soc. Nephrol. 2006; 17: 3300–3314.

Leuning DG, Reinders MEJ, Li J et al. Clinical-Grade Isolated Human Kidney Perivascular Stromal Cells as an Organotypic Cell Source for Kidney Regenerative Medicine. Stem Cells Transl. Med. 2017; 6: 405–418.

Marcheque J, Bussolati B, Csete M et al. Concise Reviews: Stem Cells and Kidney Regeneration: An Update. Stem Cells Transl. Med. 2019; 8: 82–92.

Pleniceanu O, Omer D, Harari-Steinberg O et al. Renal lineage cells as a source for renal regeneration. Pediatr. Res. 2018; 83: 26-274.

Lang PO, Michel JP, Zekry D. Frailty syndrome: a transitional state in a dynamic process. Gerontology. 2009; 55(5): 539-49.

Tarazona-Santabalbina FJ, Gómez-Cabrera MC, Pérez-Ros P et al. A Multicomponent Exercise Intervention that Reverses Frailty and Improves Cognition, Emotion, and Social Networking in the Community-Dwelling Frail Elderly: A Randomized Clinical Trial. J Am Med Dir Assoc. 2016; 17(5): 426-33.

Travers J, Romero-Ortuno R, Bailey J et al. Delaying and reversing frailty: a systematic review of primary care interventions. Br J Gen Pract. 2019; 69(678): e61-e69.

Collerton J, Martin-Ruiz C, Davies K et al. Frailty and the role of inflammation, immunosenescence and cellular ageing in the very old: cross-sectional findings from the Newcastle 85+ Study. Mech Ageing Dev. 2012; 133(6): 456-66.

Mitnitski A, Collerton J, Martin-Ruiz C et al. Age-related frailty and its association with biological markers of ageing. BMC Medicine. 2015; 13: 161.

Sánchez-Flores M, Marcos-Pérez D, Costa S et al. Oxidative stress, genomic features and DNA repair in frail elderly: A systematic review. Ageing Res Rev. 2017; 37: 1-15.

Dent E, Kowal P, Hoogendijk EO. Frailty measurement in research and clinical practice: A review. Eur J Intern Med. 2016; 31: 3-10.

Rattan SIS. Increased molecular damage and heterogeneity as the basis of aging. Biol Chem. 2008; 389(3): 267-72.

Fried LP, Tangen CM, Walston J et al. Frailty in Older Adults: Evidence for a Phenotype. The Journals of Gerontology: Series A. 2001; 56(3): M146–M157.

Graham JE, Snih SA, Berges IM et al. Frailty and 10-year mortality in community-living Mexican American older adults. Gerontology. 2009; 55(6):644–651.

Santos-Eggimann B, Cuenoud P, Spagnoli J et al. Prevalence of frailty in middle-aged and older community-dwelling Europeans living in 10 countries. The journals of gerontology. 2009;64(6):675–681.

Henchoz Y, C Büla C, Guessous I et al. Association between Physical Frailty and Quality of Life in a Representative Sample of Community-Dwelling Swiss Older People. J Nutr Health Aging. 2017; 21(5): 585-592.

Pandey A, Dalane K, Whellan DJ et al. J Am Coll Cardiol HF. 2019;7(12):1079–88.

Marije H, Kallenberg, Hilda A et al. Functional and Cognitive Impairment, Frailty, and Adverse Health Outcomes in Older Patients Reaching ESRD—A Systematic Review. CJASN. 2016; 11(9): 1624-1639.

Guralnik JM, Simonsick EM, Ferrucci L et al. A short physical performance battery assessing lower extremity function: association with self-reported disability and prediction of mortality and nursing home admission. J Gerontol. 1994; 49(2): M85-94.

Washburn RA, McAuley E, Katula J et al. The physical activity scale for the elderly (PASE): evidence for validity. J Clin Epidemiol. 1999; 52(7):643-51.

Cruz-Jentoft AJ, Bahat G, Bauer J et al. Sarcopenia: revised European consensus on definition and diagnosis. Age and Ageing. 2019; 48(1): 16-31.

Makizako H, Shimada H, Takehiko D et al. Impact of physical frailty on disability in community-dwelling older adults: a prospective cohort study. BMJ open 2015; 5: e008462.

Rockwood K, Mitnitski A, Song X et al. Long-term risks of death and institutionalization of elderly people in relation to deficit accumulation at age 70. J Am Geriatr Soc. 2006; 54(6): 975-9.

Bao Y, Dalrymple L, Chertow GM et al. Frailty, dialysis initiation, and mortality in end-stage renal disease. Archives of Internal Medicine. 2012; 172(14): 1071– 1077.

Collard RM, Boter H, Schoevers RA et al. Prevalence of frailty in community-dwelling older persons: a systematic review. J Am Geriatr Soc. 2012; 60(8): 1487-92.

Daya N, Voskertchian A, Schneider ALC et al. Kidney Function and Fracture Risk: The Atherosclerosis Risk in Communities (ARIC) Study. Am J Kidney Dis. 2016; 67(2): 218-226.

Kim JC, Kalantar-Zadeh K, Kopple JD. Frailty and proteinenergy wasting in elderly patients with end stage kidney disease. J Am Soc Nephrol. 2013; 24: 337–351.

Carrero JJ, Stenvinkel P, Cuppari L et al. Etiology of the protein-energy wasting syndrome in chronic kidney disease: a consensus statement from the International Society of Renal Nutrition and Metabolism (ISRNM). J Ren Nutr. 2013; 23: 77–90.

Bowlby W, Zelnick LR, Henry C et al. Physical activity and metabolic health in chronic kidney disease: a cross sectional study. BMC Nephrol. 2016; 17: 187.

Wilhelm-Leen ER, Hall YN, Tamura MK et al. Frailty and Chronic Kidney Disease: The Third National Health and Nutrition Evaluation Survey. Am J Med. 2009; 122(7): 664–71.

Jeffery C A, Shum DW, Hubbard RE. Emerging drug therapies for frailty. Maturitas. 2013; 74(1): 21–25.

Hubbard RE, Woodhouse K W. Frailty, inflammation and the elderly. Biogerontology. 2010; 11(5): 635–641.

Shlipak MG, Fried LF, Crump C et al. Elevations of inflammatory and procoagulant biomarkers in elderly persons with renal insufficiency. Circulation 2003; 107(1): 87–92.

Shlipak MG, Stehman-Breen C, Fried et al. The presence of frailty in elderly persons with chronic renal insufficiency. Am J Kidney Dis. 2004; 43(5): 861-7.

Chowdhury R, Peel NM, Krosch M et al. Frailty and chronic kidney disease: a systematic review. Arch Gerontol Geriatr 2017; 68: 135-142.

Chapter 2

PKH^{high}/CD133+/CD24- renal stem-like cells isolated from human nephrospheres exhibit in vitro multipotency

Silvia Bombelli[1]*, Chiara Meregalli[1], Chiara Grasselli[1], Maddalena M. Bolognesi[1], Antonino Bruno[2], Stefano Eriani[1], Barbara Torsello[1], Sofia De Marco[1], Davide P. Bernasconi[1], Nicola Zucchini[3], Paolo Mazzola[1,4], Cristina Bianchi[1], Marco Grasso[5], Adriana Albini[1,2], Giorgio Cattoretti[1,3] and Roberto A. Perego[1]*

[1] School of Medicine and Surgery, Milano-Bicocca University, Via Cadore 48, 20900 Monza, Italy; silvia.bombelli@unimib.it (S.B.); c.meregalli4@campus.unimib.it (C.M.); c.grasselli@campus.unimib.it (C.G.); maddalena.bolognesi@unimib.it (M.M.B.); s.eriani@campus.unimib.it (S.E.); barbara.torsello@unimib.it (B.T.); s.demarco8@campus.unimib.it (S.D.M); davide.bernasconi@unimib.it (D.P.B.); paolo.mazzola@unimib.it (P.M.); cristina.bianchi@unimib.it (C.B.); giorgio.cattoretti@unimib.it (G.C.); albini.adriana@gmail.com (A.A.); roberto.perego@unimib.it (R.A.P.)

[2] IRCCS MultiMedica, Milan, 20138, Italy; antonino.bruno@multimedica.it (A.B.)

[3] Pathology Unit, 4Geriatric Unit and 5Urology Unit, ASST Monza, San Gerardo Hospital Via G. B. Pergolesi 33, 20900 Monza, Italy. n.zucchini@asst-monza.it (N.Z.); m.grasso@asst-monza.it (M.G.)

* Correspondence: roberto.perego@unimib.it (R.A.P.); Tel. +390264488303 (R.A.P.); silvia.bombelli@unimib.it (S.B.); Tel. +390264488326 (S.B.)

Cells. 2020; 9, 1805. DOI: 10.3390/cells9081805.

Funding: This research was supported by grants to R.A.P.: from Ministero dell'Istruzione, dell'Università e della Ricerca-Progetti di Rilevante Interesse Nazionale [number 20060669373_004]; Fondo di Ateneo per la Ricerca [numbers 17656, 10069]; Fondo di Ateneo quota competitiva [number ATESP0107]; partially from Fondazione Cariplo [grant 2017-0577]. S.D.M. (grant DR 1596/2016) and C.G. (grant 76466/18) are recipients of PhD fellowships and S.B. was partially supported by a postdoctoral fellowship (grant 2-18-5999000-5) from Ministero dell'Istruzione, dell'Università e della Ricerca. M.M.B. is supported by a fellowship of Fondazione Cariplo [grant 2017-0577]. This work has also been partially supported by the Italian Ministry of Health Ricerca Corrente - IRCCS MultiMedica

Abstract

The mechanism upon which human kidneys undergo regeneration is debated, though different lineage tracing mouse models have tried to explain the cellular types and the mechanisms involved. Different sources of human renal progenitors have been proposed, but it is difficult to argue whether these populations have the same capacities that have been described in mice. Using the nephrosphere model, we isolated the quiescent population of adult human renal stem-like PKH^{high}/CD133+/CD24- cells (RSC). The aim of this paper was to deepen the RSC in vitro multipotency capacity. RSC, not expressing endothelial markers, generated secondary nephrospheres containing CD31+/vWf+ cells and cytokeratin positive cells, indicating the coexistence of endothelial and epithelial commitment. RSC cultured on decellularized human renal scaffolds generated endothelial structures together with the proximal and distal tubular structures. CD31+ endothelial committed progenitors sorted from nephrospheres generated spheroids with endothelial-like sprouts in Matrigel. We also demonstrated the double commitment toward endothelial and epithelial lineages of single RSC. The ability of the plastic RSC population to recapitulate the development of tubular epithelial and endothelial renal lineages makes these cells a good tool for the creation of organoids with translational relevance for studying the parenchymal and endothelial cell interactions and developing new therapeutic strategies.

Keywords: human adult stem cell; kidney; endothelium; scaffold; nephrosphere; multipotency

Introduction

Neonephrogenesis does not occur in the adult human kidney, but the kidney retains some regenerative potential to replace the loss of cells during physiological processes, in which about 70,000 cells from different nephron segment are lost every hour and excreted with urine [1]. Even after acute kidney injury (AKI), regeneration is present and AKI is considered reversible as documented by the recovery of urine production and the biomarkers of renal function [2]. Lineage tracing studies in mice have helped clarify the mechanisms underlying the recovery after renal injury. Humphreys and collegues [3], demonstrated that after AKI all new epithelial cells originate from within the renal epithelium itself, and not from extrarenal sources. Some years later, Rinkevich and colleagues, in a "rainbow" mouse model, demonstrated the formation of new tubular cells via clonal expansion of specific tubular cell subpopulation in a segment-restricted manner [4]. It has long been known that in the kidney some tubular cells can undergo hypertrophy and some hyperplasia [5]. However, it remained to be determined whether any differentiated tubular cell under specific conditions is capable to give rise to dedifferentiation and clonal proliferation of tubular cells, or if only a specific predetermined fraction of cells (stem/progenitor cells) is endowed with this potential within the nephron [6,7]. Lazzeri and colleagues [8] identified and characterized the tubular cells that undergo the endocycle-mediated hypertrophy and the small subset of Pax2+ tubular progenitor cells that have proliferative capacity in conditional Pax8/FUCCI2aR mice. With their paper they demonstrated in mice that the renal functional recovery upon AKI involves both tubular cell hypertrophy via endocycle and a limited

regeneration driven by progenitors. They also observed the presence of endocycling cells as a dominant tubular epithelial response in human kidney biopsies from patients with chronic kidney disease after AKI [8]. However, the specific cell phenotype eventually responsible for tubular regeneration in human kidneys is still debated. In fact, different sources of multipotent renal progenitors have been described in different portions of the nephron, mainly based on CD133 expression, alone [9,10] or coupled with CD24 marker [11,12]. Since lineage tracing in humans is not applicable, it is difficult to argue whether these populations are capable of the same regenerative abilities described in mice and whether their phenotype is fixed or inducible [13].

In this scenario, we contributed to the debate by isolating a human cell population with stem features using the sphere-forming functional approach [14] that it has been recently described as a good model able to entails a genetic program that recapitulates renal development [15]. We identified the quiescent PKH26-retaining human renal stem-like cells (PKH^{high}) isolated from clonal nephrospheres (NS) and demonstrated, in 2D culture, their ability to self-renew and differentiate into tubular and podocytic lineages as well as endothelial cells14. We also evidenced that 70% of PKH^{high} cells have the PKHhigh/CD133+/CD24- phenotype associated with stem-like properties [14]. Recently, we showed that our NS cells are able to repopulate tubular and endothelial structures, when cultured on decellularized human renal scaffolds [16].

In order to better understand whether, among the NS cells, the PKHhigh/CD133+/CD24- adult human renal stem-like cells (RSC) are the cellular players that drive repopulation and multipotency, the aim

of this paper was to investigate in depth the in vitro multipotency of this cell subpopulation using different in vitro tests. In addition, aiming to give more insight on the cellular and molecular basis of renal regeneration, we also studied the in vitro multipotency capacity of RSC at the single cell level.

Materials and Methods

Tissues

Normal kidney tissue was obtained from 20 patients (male 14, female 6; median age 70 years, range 38-88 years) following nephrectomy for renal tumors. Discarded normal tissues far away from the tumor and exceeding the diagnostic needs were collected, de-identified and processed. The tissue was collected from the healthy region of the kidney without any presence of cancer and judged as normal by experienced pathologists. The procedures were approved (No 1532, 17th Nov 2011) by the institutional local Ethical Committee "Comitato Etico Azienda Ospedaliera San Gerardo" and patient informed consent was obtained. All procedures were performed in accordance with the Declaration of Helsinki, the relevant guidelines and regulations. NS cultures were established from fresh renal tissue samples. Frozen pieces of renal tissue, comprising cortex, medulla and papilla were stored at -80° C until use.

Nephrosphere cultures

The preparation of suspension of single cells from renal tissue [17] and the establishment of NS cultures [14] were performed as previously described. Cells before NS culture were stained with PKH26 lipophilic

dye as described [14]. The floating NS grown in non-adherent conditions in dishes coated with poly-Hema (Sigma Aldrich) were collected for use after 10-12 days. NS cells were dissociated enzymatically for 5 minutes in TrypLE Express (Life Technologies) and then mechanically by repetitive pipette syringing to generate a single cell suspension [14].

Immunofluorescence and FACS analysis

Cytospin for immunofluorescence (IF) staining were prepared using cells after dissociation of NS or after sorting of specific cell subpopulations from dissociated NS. The slides were prepared spinning 5,000 cells at 800 g for 15 minutes on Heraeus Multifuge 3S+ centrifuge (Thermo Scientific). IF was performed as described [18] using the rabbit anti-von Willebrand factor (vWf, DAKO; 1:2000), mouse monoclonal anti-Cytokeratin 8.18 (CK 8.18, clone 5D3, Thermo Fisher Scientific; 1:50) and mouse monoclonal anti-CD31 (clone JC70A, DAKO, 1:25) primary antibodies and Alexa Fluor 488 conjugated anti-mouse and Alexa Fluor 594 conjugated anti-rabbit IgG secondary antibodies (Molecular Probes Invitrogen, 1:100). IF micrographs were obtained at 400x magnification using a Zeiss LSM710 confocal microscope and Zen2009 software (Zeiss).

The FACS procedure was performed as described [19] on NS preparations and trypsinised clones, and analysis was performed with a MoFlo Astrios cell sorter and Kaluza 2.1 software (both from Beckman Coulter). For FACS analysis the following antibodies were used: rabbit monoclonal anti-Cytokeratin 7 (CK7, clone EPR1619Y, Abcam; 1:20), mouse monoclonal APCH7-conjugated anti-CD10 (clone HI10a,

Becton Dickinson; 1:20), mouse monoclonal APC-conjugated anti-CD31 (clone WM59, Biolegend; 1:20), mouse monoclonal FITC-conjugated anti pan CK (clone CK3-CH5, Miltenyi Biotech, 1:10), mouse monoclonal APC-conjugated anti-CD133 (clone AC133, Miltenyi Biotech, 1:10), mouse monoclonal FITC-conjugated anti CD24 (clone ML5, Biolegend, 1:20). Alexa Fluor 488 conjugated anti-rabbit (Molecular Probes Invitrogen, 1:100) was used as secondary antibody for Cytokeratin 7.

FACS sorting

The cell suspension obtained from PKH26 stained NS [14] was FACS sorted with a MoFlo Astrios cell sorter on the basis of PKH fluorescence intensity. We isolated the cellular population with the highest PKH fluorescence (PKH^{high}) gated on the basis of the sphere forming efficiency (SFE) percentage, which is described to be around 1%. $PKH^{low/neg}$ cells, with intermediate or without fluorescence, were gated as 80-90% of the total cell population [14]. Within the PKH^{high} cells, we also isolated the CD133+/CD24- cell subpopulation (RSC) by FACS sorting, described to be around 70% of PKH^{high} cells [14], and within the $PKH^{low/neg}$ cells we isolated the CD31+ cells (gated as about 1%) and the CD31- cells (gated as about 90%). Single cell sorting of RSC population was performed on 96-well plates and the presence of a single cell per well was assessed under contrast phase microscope (Leica). An average sorting rate of 500-1000 events per second at a sorting pressure of 25 psi with a 100μm nozzle was maintained.

RSC cultured on decellularized extracellular matrix (ECM) kidney scaffolds and 3D staining

Frozen human renal tissues were cut into approximately 2 mm thick slices maintaining all kidney regions. Slices were decellularized as described [16] and a portion of the scaffold was routinely tested for complete decellularization by H&E staining on multiple formalin fixed, paraffin embedded (FFPE) sections. 15,000 FACS sorted RSC were seeded on the decellularized renal scaffold, obtained from the same patient, and cultured with basal medium (DMEM low glucose supplemented with 10% FBS, both from Euroclone) in 96-well poly-Hema coated plates. Five different experiments, each representing one individual tissue patient were performed. The cells were allowed to attach to the ECM scaffold for 5 days while only adding the medium without changing it, then the medium was changed every 2 days. The cultures were stopped at 30 days, formalin fixed for at least 16 hours and paraffin embedded for histological analysis or processed for 3D staining as follow.

A small portion of two of the different 30-day-cultured scaffolds was cut and fixed in formalin for 1 hour. The two scaffold samples were incubated with Alexa Fluor 680–phalloidin (1:100 in PBS; Molecular Probes Invitrogen) for 15 minutes and with 4',6-Diamidino-2-Phenylindole (DAPI) (Sigma-Aldrich) for 10 minutes, then mounted between a glass coverslip and glass slides. Immunofluorescence micrographs were obtained at ×400 magnification using the Zeiss LSM710 confocal microscope and Zen2009 software. Z-stack function was used to acquire sequential micrographs every 1.2 μm, covering the

entire thickness of the chosen structures and then 3D reconstruction was assembled using the specific ImageJ software 3D plugin.

Histologic characterization

The decellularized scaffolds, on which RSC had been cultured, were FFPE, sectioned (2 µm thick) and Hematoxylin and Eosin (H&E) stained in order to assess the cellular repopulation and to evaluate the morphological features. Images were acquired using the Hamamatsu Nanozoomer S60 scanner (Nikon). The S60 scanner has two six-filters wheels, one for excitation the other for emission filters, a three-cube turret and is equipped with a Plan Apochromat Lambda 20x NA 0.75 objective (Nikon), a Fluorescence Imaging Module L13820 equipped with a mercury lamp (Hamamatsu Photonics), and an ORCA-Flash 4.0 digital CMOS camera (Hamamatsu Photonics). IF staining of histologic sections was performed as described [16], using mouse monoclonal anti-Aquaporin (AQP1, clone B-11, Santa Cruz, 1:50), rabbit polyclonal anti-CD13 (Santa Cruz, 1:200), mouse monoclonal anti-N-Cadherin (NCAD, clone 32, Beckton Dickinson, 1:50) proximal tubular markers; rabbit monoclonal anti-Cytokeratin 7 (CK7, clone EPR1619Y, Abcam; 1:200), mouse monoclonal anti-Calbindin-D28k (CALB, clone CB-955, Sigma Aldrich, 1:200), mouse monoclonal anti- E-Cadherin (ECAD, clone 36, Beckton Dickinson, 1:50) distal tubular markers; mouse monoclonal anti-Cytokeratin 8.18 (CK 8.18), epithelial marker (clone 5D3, 1:50); von Willebrand factor (vWf), endothelial marker (1:2000) primary antibodies, and Alexa Fluor 680 conjugated goat anti-mouse and Alexa Fluor 594 conjugated goat anti-rabbit IgG secondary antibodies (1:100). DAPI dilactate 5.45 µM (Sigma) was added for

nuclear counterstaining. The immunofluorescent images were acquired using the S60 scanner or the Zeiss LSM710 confocal microscope and Zen2009 software (Zeiss). In cases of sequential IF staining, the sections were subjected to elution of the previous antibodies by incubation in a shaking water bath at 56°C for 30 minutes in a 2% SDS, 114 mM 2-Mercaptoethanol, 60 mM Tris-HCl pH 6.8 solution [20].

In vitro single cell differentiation

The single sorted RSC were grown in different media. The epithelial medium consisted in DMEM-F12 (Lonza) supplemented with 10% FBS, ITS supplement (5 µg/ml Insulin, 5 µg/ml Transferrin, 5 ng/ml sodium selenite), 36 ng/ml Hydrocortisone, 40 pg/ml Triiodothyronine (all from Sigma Aldrich), 20 ng/ml EGF (Cell Signaling) and 50 ng/ml HGF (Cell Signaling). The endothelial medium was composed of endothelial cell basal medium (EBM™, Lonza) supplemented with EGM™SingleQuots™ (Lonza), 10% Fetal Bovine Serum. FACS analysis with the appropriate antibodies was performed on the trypsinised cells of obtained clones.

3D culture on Matrigel and staining

96 well plates were precoated with 75µl of 10 mg/ml growth factor reduced, Phenol-Red free Matrigel® Matrix (Corning). 10,000 cells each of the following RSC, CD31-/PKH$^{low/neg}$, CD31+/PKH$^{low/neg}$ cell subpopulations were FACS sorted after dissociation of NS and seeded on Matrigel in the endothelial medium described above to perform morphogenesis assay as described [21]. Contrast phase images were obtained at 6 hours and at different time points starting at 24 hours to

follow the growth. Matrigel plugs were subjected to 3D IF staining with a protocol modified from Lee et al. [22]. Plugs were fixed with 4% paraformaldehyde (Thermo Fisher scientific) at room temperature (RT) for 10 minutes and treated with PBS glycine (100mM) (Euroclone) for other 10 minutes and then incubated with 0.5 mg/ml of Proteinase K (Sigma Aldrich) for 5 minutes at RT. A blocking solution composed by IF buffer (0.5% Triton, 0.1% BSA, 0.05% Tween20 in PBS) with 10% normal goat serum (Euroclone) was added for 1 hour and half at RT with shaking. Incubation with rabbit monoclonal anti CK8.18 (clone EP17/EP30, DAKO, 1:25), mouse monoclonal CD31 (clone JC70A, 1:25), mouse monoclonal E-Cadherin (clone 36, Becton Dickinson, 1:50) and rabbit polyclonal vWf primary antibodies diluted in IF buffer was performed at RT for 2 hours and then with Alexa Fluor 488 conjugated goat anti-mouse and Alexa Fluor 594 conjugated goat anti-rabbit IgG secondary antibodies (1:100). IF micrographs were obtained at 400x magnification using a Zeiss LSM710 confocal microscope and Zen2009 software.

Statistical analysis

For FACS analysis of CD31 and CK7/CD10 expression, the chi-squared test was used to compare the overall proportion of positive cells among the three subpopulations PKH^{high}, PKH^{low}, and PKH^{neg}. Pairwise comparisons were performed again with the chi-squared test with Holm correction for multiplicity. These tests take into account the differences in the numbers of the analyzed events between the three cell subpopulations examined. The chi-squared test was again used for the FACS analysis of CD31 and pan Cytokeratin expression on the cells

within the clones cultured in epithelial or endothelial medium to assess the statistical differences and $p < 0.01$ was considered significant.

Results

Human RSC cultured on human decellularized scaffolds.

RSC (PKH^{high}/CD133+/CD24- cells) were obtained by FACS sorting from NS cultured for 10 days. PKH^{high} cells represent the PKH26 most fluorescent cells, gated as about 0.8-1% of the total NS population. This percentage of PKH^{high} cells corresponds to the usual sphere forming efficiency (SFE) observed [14]. The RSC were gated as about 70% of PKH^{high} cells on the basis of CD133+/CD24- phenotype [14] and represented those with higher stem-like capacity PKH^{high}/CD133+ cells, while the PKH^{high}/CD133- cells do not have self-renewal capacity [14]. We seeded 15,000 sorted cells of RSC (the maximum number of yielded cells) on decellularized scaffolds placed in poly-Hema coated 96 well plates [16]. After 5 days the cells, which could not attach to the plastic because of Poly-Hema, were into the scaffold since no cells were observed in the area of well not covered by the scaffold. The limited number of cells did not repopulate completely the scaffold, however, our aim was to investigate the differentiation abilities of RSC and their capability to settle in specific nephron portions and not to entirely repopulate the scaffolds. With this purpose, the small number of cells on the scaffold had the advantage to mimic a situation close to a clonal-like condition in which theoretically single cells could attach, proliferate and differentiate to generate a specific structure. The 3D staining of small scaffold portions, after 30 days of culture with RSC in presence of a basal medium without any other additional growth factor,

showed the presence of cells demonstrating the nontoxicity of the decellularized matrix and the capability of the RSC to proliferate and differentiate into the scaffolds (Figure 1a). In addition, the RSC showed the capacity to localize at different specific portions of the scaffold, as evidenced by haematoxylin and eosin (H&E) staining (Figure 1b). H&E showed the presence of simple cuboidal epithelial-like cells, typical of the renal tubular portion (Figure1b, top panels) as well as flat cells, similar to simple squamous endothelial-like cells, located on the big vessel basement membrane (Figure 1b, bottom panels). No cells were visible after 30 days of culture in the control scaffold in which we did not plate any cells (Supplementary Figure S1a).

Using the sequential immunofluorescence (IF) staining [21], which permitted us to evaluate several markers on the same repopulated structure, we documented that the different morphology acquired in the scaffold by RSC cells corresponded to different renal cell phenotypes. This capacity, already described for the whole cells present in NS [16], is now demonstrated to be associated to the stem-like cells. The epithelial (CK8.18), proximal (AQP1, CD13 and N-Cadherin) and distal (CK7, Calbindin D-28k and E-Cadherin) tubular and endothelial (vWf) markers were evaluated. RSC, after 30 days of culture on decellularized scaffolds, mostly generated cells showing epithelial proximal or distal tubular- or endothelial-like phenotype localized on the tubular or vascular spaces of the scaffold respectively (Figure 1c). In fact, the cells in tubular structures expressed the epithelial CK8.18 and proximal and distal tubular markers in a mutually exclusive way indicating a specific lineage differentiation (Figure1c, upper and middle panels; Supplementary Figure S3). Endothelial vWf was not detectable

in the structures with cells expressing tubular markers (Figure 1c, upper and middle panels). Instead, other structures had cells expressing endothelial vWf, lacking the expression of CK8.18 epithelial and AQP1 and CK7 tubular markers (Figure 1c, lower panels). 75% of the structures formed by RSC presented epithelial-like phenotype and 18% presented endothelial-like phenotype. Of note, few structures (8%) repopulated with RSC presented cells that co-expressed markers of different lineages, suggesting a still immature cell phenotype or a transitional state. In fact, some of them co-expressed epithelial CK8.18, tubular AQP1/CK7 and endothelial vWf markers (Supplementary Figure S1b). These data show that RSC organized in structures containing cells expressing epithelial or endothelial markers, supporting the multipotency of these progenitors isolated from human kidneys.

$PKH^{low/neg}$ progenitors were cultured on decellularized scaffolds as controls. H&E staining showed only the presence of simple cuboidal epithelial-like cells, typical of the renal tubular portion and not of endothelial-like cells (Supplementary Figure S2a). Sequential immunofluorescence staining confirmed the epithelial tubular-like phenotype. In fact, $PKH^{low/neg}$ cells, after 30 days of culture on decellularized scaffolds, only generated cells showing epithelial proximal or distal tubular-like phenotype. No vWf+ cells within the structures has been observed. In tubular structures were present cells expressing the epithelial CK8.18 and tubular markers, proximal AQP1 or distal CK7, in a mutually exclusive way indicating a specific lineage differentiation (Supplementary Figure S2b) or together indicating a still immature phenotype (Supplementary Figure S2c).

Cell commitment toward epithelium and endothelium

The PKH^{high} cells obtained dissociating NS showed the co-expression of proximal CD10 and distal CK7 tubular markers (42.53%±7.54 weighted mean ±standard deviation), which dramatically decreased in PKH^{low} (22.34%± 2.73) and PKH^{neg} (7.81%±2.85) cells (Figure 2a, upper panels), suggesting the intrinsic plasticity of these progenitors. The co-expression of CD10 and CK7 markers was also observed in RSC, gated as about 70% of PKH^{high} cells, before seeding on decellularized scaffold (data not shown). More surprisingly, although the PKH^{high} cells did not express the endothelial CD31 marker (0%), their PKH^{low} and PKH^{neg} cell progeny inside the NS expressed CD31 (0.81%± 0.14 and 2.29%±0.60 respectively), suggesting that CD31 expression increased within the spheres in relation to proliferation assessed by PKH26 dye fluorescence decrement (Figure 2a, lower panels). Even on cytospinned PKH^{high} cells, the total negativity of vWf and CD31 endothelial markers and the positivity of epithelial marker CK8.18 was documented (Figure 2b, upper panels). On the contrary, the presence of few cells with an endothelial phenotype (vWF+ and CD31+) was confirmed in the cytospinned $PKH^{low/neg}$ cells (Figure 2b, white arrow in lower panels). About 20% of the CD31+ cells in the $PKH^{low}$and PKH^{neg} cells showed a co-expression with Cytokeratin (data not shown), indicating a transitional state of differentiation inside the NS that we already noted in repopulated scaffold structures (Supplementary Figure S1b). Therefore, these data suggest the existence of a differentiation gradient within the NS starting from immature PKH^{high} cells toward different lineage commitment evidenced in PKH^{low} and PKH^{neg} progeny.

To demonstrate that the RSC, about 70% of PKH^{high} cells, have the capacity to generate the CD31+ cells, we sorted CD31- RSC from NS and plated them for ten days to form new secondary NS (Figure 3a). FACS analysis of cells from these secondary NS revealed again that the PKH^{high} cells retained the CD31- phenotype, while only some of PKH^{low} and PKH^{neg} cell progeny expressed CD31 (Figure 3b), likely due to the presence of a lineage commitment within NS. Even in secondary NS, as in primary NS (Figure 2a), there was a gradient of enrichment in CD31+ cells along proliferation/differentiation from the quiescent PKH^{high} cells to the proliferating PKH^{low} and PKH^{neg} cells. Furthermore, the expression of the endothelial marker vWf has been detected by IF in some cells of secondary NS generated from the RSC negative for endothelial markers (Figure 3c). These data support the observation that RSC were able to give rise to endothelial cells, suggesting an intrinsic multipotency capacity.

Morphogenesis 3D assay

The behaviour of the endothelial committed cells within the NS has been analysed by a morphogenesis 3D assay in Matrigel using three different cell subpopulations sorted from NS. We analysed the CD31- RSC, the CD31-/$PKH,^{low/neg}$ progenitors and the CD31+/$PKH^{low/neg}$ progenitors committed to an endothelial lineage. At 6 hours of culture, all our cell subpopulations started organizing as spheroids (Figure 4a). Extending the time of culture, only the endothelial-committed CD31+/$PKH^{low/neg}$ population generated sprouts similar to capillary-like structures [23] (Figure 4b) at different time points and in the following days these sprouts increased over time (Figure 4c). RSC

generated bigger and more organized spheroids than CD31-/PKH$^{low/neg}$ cells and both without any sprouts (Figure 4b, upper and middle panels). In addition, 3D IF staining evidenced the presence of CD31+ and vWf+ cells in structures generated by CD31+/PKH$^{low/neg}$ progenitors. We did not observe the colocalization of CD31 and vWf endothelial markers with CK8.18 and E-Cadherin epithelial markers (Figure 4d). CD31 was localized in the sprout-like extensions, as indicated by the arrows (Figure 4d, upper panels). This morphogenesis assay provided further observations indicating that in NS the CD31- RSC can generate endothelial committed CD31+/PKH$^{low/neg}$ progenitor cells, which are able to differentiate into an endothelial-like phenotype.

Single cell differentiation

To confirm the multipotency ability of CD31- RSC, their capacity to differentiate into both tubular epithelial and endothelial lineages has been assessed at single cell level in 2D culture. Starting from NS, obtained from three different patients, one single RSC was sorted into wells containing specific epithelial (48 wells) or endothelial (48 wells) media. One 96-well plate for each patient sample was used, and the single cell presence in the wells has been assessed under contrast phase microscope (Figure 5a, left panel). We were able to obtain cell clones (Figure 5a, right panel) from 34% (range 18.7%-62.5%) of single RSC in epithelial medium and from 22% (range 12.5%-37.5%) of single RSC in endothelial medium. The expression of Cytokeratin epithelial marker and CD31 endothelial marker has been evaluated by FACS at 10 days of confluent clone culture. With both media, most of the cells (>90%) evaluated in 16 of the obtained clones expressed Cytokeratin,

indicating the commitment toward epithelial lineage (Figure 5b). In all 16 clones tested, a few cells expressed CD31 alone (range 0.05%-2.83%) or together with Cytokeratin (range 0.12%-4.72%), indicating a differentiation toward endothelial lineage or a transitional status respectively (Figure 5b, left and middle panels). However, the mean percentage of CD31+/CK- endothelial cells as well CD31+/CK+ cells was significantly higher in the clones obtained in endothelial medium (0.99%±0.76 and 2.35%±0.76, respectively, weighted mean ± SD) compared to those in epithelial medium (0.14±0.11 and 0.56±0.54, respectively) (Figure 5c). Extending the culture time to 23 days for two clones grown in endothelial medium, the percentage of CD31+ cells was much higher than 10 days (Figure 5a, right panel). With this experiment we demonstrate that from one single CD31- RSC it was possible to obtain clones that contain both epithelial like (CK+) and endothelial like (CD31+) cells, as evidence of the multipotency of the single RSC. This capacity is unique to RSC, since single $PKH^{low/neg}$ progenitor cells can generate clones containing only epithelial like (CK+) cells (Supplementary Figure S2d).

Discussion

The aim of this study was to investigate the *in vitro* multipotency of human adult renal stem-like PKH^{high}/CD133+/CD24- cells (RSC) using different *in vitro* tests. Our data evidenced that RSC subpopulation, able to generate NS, had the capacity to attach to tubular and vascular segments of renal scaffolds differentiating in epithelial- and endothelial-like lineages respectively. RSC were cultured on renal scaffold with a medium without any growth factor or external stimuli,

so RSC may have proliferated and differentiated responding to the growth factors preserved in the ECM [23, 24] as well as to the basement membrane composition [25].

RSC did not present any ability to repopulate the glomerular endothelium and epithelium. In fact, visceral epithelium and a differentiation towards podocytes were not present, although we previously demonstrated that RSC were able to differentiate *in vitro* into podocytes upon appropriate stimuli [14]. In our model, RSC are seeded on the scaffold in a static system and do not integrate into the glomerulus probably due to the physic obstacle represented by the capillary matrix [26]. Moreover, it is described [27] that glomerular endothelium appears important for the induction of the final maturation of podocytes. A few structures presented cells co-expressing markers, which are specific for these different lineages of differentiation, as a possible evidence of a transient and immature phenotype.

In addition, RSC not expressing CD31 and vWf endothelial markers were able to generate NS, which contained some CD31+ filial cells. These CD31+ cells, sorted from NS, generated in matrigel 3D spheroids that branched in capillary-like sprouts exhibiting an endothelial-like behaviour. In fact, spheroid sprouting is typical of endothelial cells and it is considered a reliable 3D angiogenesis assay [28]. The fact that only spheroids obtained from CD31+ $PKH^{low/neg}$ cells could generate sprouts in a 3D assay can be an indication of their endothelial commitment. PKH^{high} cells were also enriched in cells co-expressing proximal and distal tubular markers. This co-expression decreased in the $PKH^{low/neg}$ cells, the progeny of PKH^{high} cells, while CD31+ cells increased. These data may indicate a differentiation gradient within NS, in which

$PKH^{low/neg}$ progeny represents the subpopulation committed to proximal and distal tubular and endothelial phenotype. The presence of a differentiation gradient inside the spheres was also described in mammospheres [29]. Moreover, the capacity of a single RSC to commit into both epithelial and endothelial lineage has been demonstrated by an in vitro single cell differentiation assay. This commitment of single RSC into both epithelial and endothelial lineages was surprising. In fact, we were dealing with a single adult epithelial stem-like cell that was not expected to differentiate into endothelial lineage. Multipotent capacity has been demonstrated to be unique of RSC, since $PKH^{low/neg}$ progenitors are neither able to generate endothelial-like structures on the scaffolds nor to exhibit multipotency at single cell level.

The repeated appearance of this result indicates that the endothelial commitment and differentiation of RSC, which lack not only endothelial but also mesenchymal and hematopoietic markers (data not shown), can be possible. There is some support for this possibility in literature. Little and McMahon [30], reviewing the development of mammalian kidney, assessed that vascular progenitors exist within the metanephric mesenchyme and may actively populate newly forming vasculature through a vasculogenic process. In addition, 3D organoids obtained from iPSC reprogrammed into intermediate mesoderm contain both epithelial and vascular compartments [31, 32]. Therefore, we can speculate that also our RSC, though they are adult stem cells, can somehow acquire multipotency and differentiate into epithelial and endothelial lineages, even though there is no current evidence of such a behaviour in vivo in lineage tracing mouse models [4,8]. A possible explanation of this observed intriguing phenomenon of multipotency

can be found in the study published by Gonçalves and collegues [33]. The authors evidenced that angiomyolipoma cells derive from a multipotent cancer stem cell that is generated by a renal epithelial cell. Becherucci and Romagnani commented on this paper, suggesting the possibility that in the renal epithelium there might be a differentiation capacity that goes behind the epithelial phenotype [34]. In fact, it has been proposed that in different conditions, specific stem cells can be exposed to factors that are different from those of their specific tissue niches [35]. In the same way, renal epithelial stem cells could exhibit lineage restricted capacity when evaluated with in vivo models of lineage tracing under their steady-state conditions, but in some different conditions, such as *in vitro* culture, they could show cellular plasticity. We can thus hypothesise that multipotency capacity is something intrinsic but dormant in resident stem cells in the healthy human kidney, while the NS microenvironment can establish a new niche exposing the RSC to new and different factors able to rouse multipotency capacities. Based on these observations, our model can be promising because it allows us to isolate a plastic population of human renal stem-like cells which is able to grow as NS and to recapitulate the development of different renal lineages. In this scenario, the RSC can be a good tool for the creation of renal organoids, and the ability of RSC to differentiate into endothelium and epithelium may eventually have translational relevance for studying the parenchymal and endothelial cell-cell interactions and developing new therapeutic strategies.

Author Contributions: Conceptualization, Silvia Bombelli and Roberto A Perego; Data curation, Silvia Bombelli, Cristina Bianchi, Adriana Albini, Giorgio Cattoretti and Roberto A Perego; Formal analysis, Silvia Bombelli, Davide P Bernasconi, Cristina Bianchi, Adriana Albini, Giorgio Cattoretti and Roberto A Perego; Funding acquisition, Roberto A Perego; Investigation, Silvia Bombelli, Chiara Meregalli, Chiara Grasselli, Antonino Bruno, Stefano Eriani, Barbara Torsello and Sofia De Marco; Methodology, Silvia Bombelli and Maddalena M Bolognesi; Project administration, Roberto A Perego; Resources, Antonino Bruno, Nicola Zucchini, Paolo Mazzola and Marco Grasso; Software, Maddalena M Bolognesi and Davide P Bernasconi; Supervision, Roberto A Perego; Validation, Silvia Bombelli and Roberto A Perego; Visualization, Silvia Bombelli; Writing – original draft, Silvia Bombelli; Writing – review & editing, Silvia Bombelli and Roberto A Perego.

Acknowledgments: We would like to thank Maureen Quinn for English revision.

Conflicts of Interest: The authors declare no conflict of interest.

Figure Legends

Figure 1. *Histological characterization of the decellularized scaffolds repopulated with RSC (PKH^{high}/CD133+/CD24- cells).* (a) Representative Z-stack 3D reconstruction of images after DAPI (blue) and phalloidin (purple) immunofluorescence staining of the scaffolds at 30 days after RSC seeding. Total thicknesses of the shown structure were 31,2 µm Original magnification, ×400. (b-c) Five independent experiments of human kidney scaffold repopulation for 30 days with RSC in presence of basal medium were performed. (b) Representative H&E staining of FFPE repopulated scaffold sections. Scale bars, 100 µm. (c) Representative sequential IF analysis of the FFPE repopulated scaffolds with the antibodies against the indicated markers that recognise specific tubular or vascular phenotypes. The different antibodies combinations identify proximal tubules (top), distal tubules (middle) and endothelium (bottom). Scale bars, 50 µm. CK: Cytokeratin; AQP: Aquaporin; vWf: von Willebrand Factor; Blue:DAPI.

Figure 2. *Immunophenotypical characterization of nephrosphere cell subpopulations.* (a) FACS analysis of NS cell subpopulations PKH^{high}, PKH^{low}, PKH^{neg} gated on PKH26 fluorescence. PKH^{high} cells were the brightest PKH-positive cells and gated as 0.8–1% of the total population. PKH^{low} cells, with intermediate fluorescence, were gated as 15–20% of the total cell population, and the PKH^{neg} cells, without fluorescence, as 60–70% of the total cell population. The antibodies against the indicated markers were used. For each

subpopulation the overall weighted mean percentages ± SD referred to three (top) and four (bottom) independent experiments, are reported in the dot plots. CK: Cytokeratin; FSC: Forward scatter. Chi-squared test $p<0.001$. (b) IF analysis of PKH^{high}, $PKH^{low/neg}$ cells sorted from dissociated NS and then cytospinned. The indicated markers have been evaluated. Blue: DAPI. Results are representative of at least three independent experiments. Original magnification 400x. Scale bars, 50 µm. Arrows: vWf+ (left panel) and CD31+ (right panel) cells.

Figure 3. *Characterization of secondary NS generated from FACS sorted CD31- RSC*. (a) Contrast phase image of secondary NS generated from CD31- RSC FACS sorted from primary NS. (b) FACS analysis of CD31 expression in PKH^{high}, PKH^{low}, PKH^{neg} cell subpopulations of secondary NS cells gated on PKH26 fluorescence. (c) IF analysis of cytospinned cells obtained from secondary NS dissociation. Antibody against vWf was used. Blue: DAPI. Original magnification 400x. Scale bar, 50 µm. Arrow: vWf+ cells.

Figure 4. *Morphogenesis 3D assay*. (a) Contrast phase images of RSC (left), CD31-/$PKH^{low/neg}$ (middle), and CD31+/$PKH^{low/neg}$ (right) at 6 hours of culture. Scale bars, 100 µm. (b) Contrast phase images of structures obtained in Matrigel at 6-7 days of culture from the 3 different samples #1, #2, #3 of RSC (top), CD31-/$PKH^{low/neg}$ (middle), CD31+/$PKH^{low/neg}$ (bottom). Scale bars, 100 µm. (c) Percentage of structures with sprouts in the three different samples of CD31+/$PKH^{low/neg}$ at different time points. (d) 3D IF

staining of the structures obtained from CD31+/PKH$^{low/neg}$ cells with the antibodies against the indicated markers. Two different fields for each staining are shown. CK: Cytokeratin; ECAD: E-Cadherin; vWf: von Willebrand Factor; Blue: DAPI. Original magnification 400x. Scale bars, 50 µm. Arrows: CD31+ cells in the sprout-like extensions.

Figure 5. *Single cell differentiation.* (a) Contrast phase images of a representative single sorted RSC (left panel) and the representative clone generated at day 10. Original magnification: 100X. Insert: 2X digital zoom. (b) FACS analysis of two representative clones obtained from single RSC at ten days of culture in epithelial (left panel) and endothelial (middle panel) media. FACS analysis at 23 days of culture of one representative clone in endothelial medium (right panel). The CD31 and Cytokeratin markers were evaluated. (c) Graphic representation of CD31+/CK- and CD31+/CK+ cell percentage within the clones obtained after 10 days of culture in specific media. Weighted mean ± SD is referred to four independent experiments of 10 clones grown in epithelial medium and 6 in endothelial medium. Chi-squared test, *$p<0.01$.

Figure 1

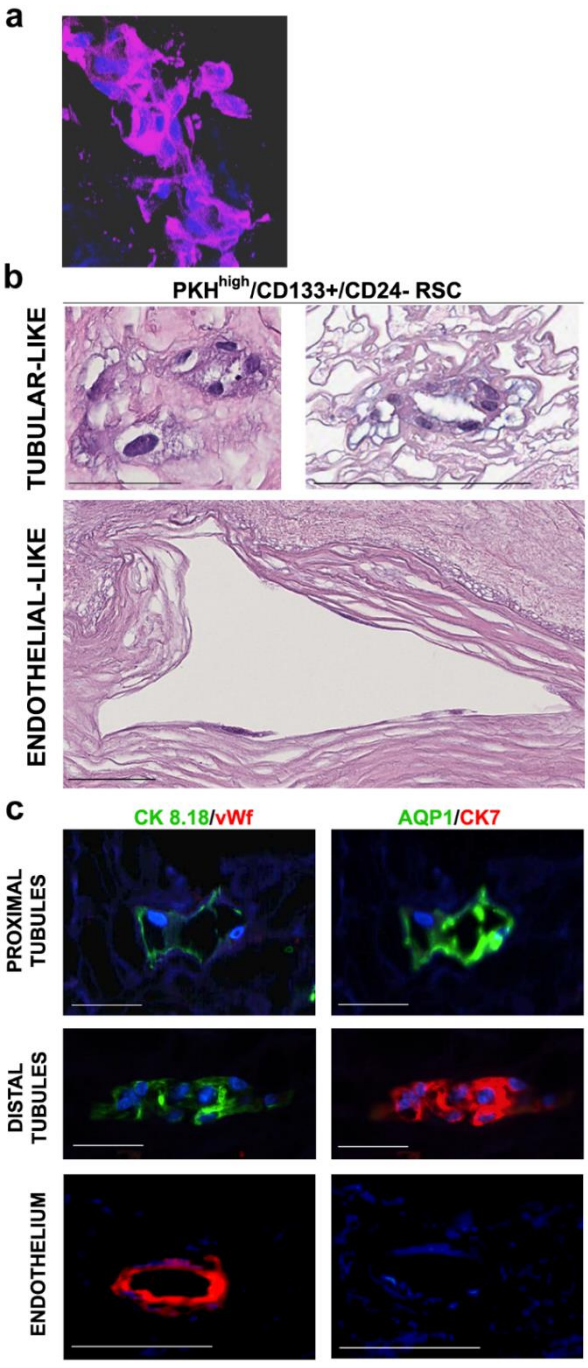
a
b
PKH^high/CD133+/CD24- RSC
TUBULAR-LIKE
ENDOTHELIAL-LIKE
c
CK 8.18/vWf
AQP1/CK7
PROXIMAL TUBULES
DISTAL TUBULES
ENDOTHELIUM

Figure 2

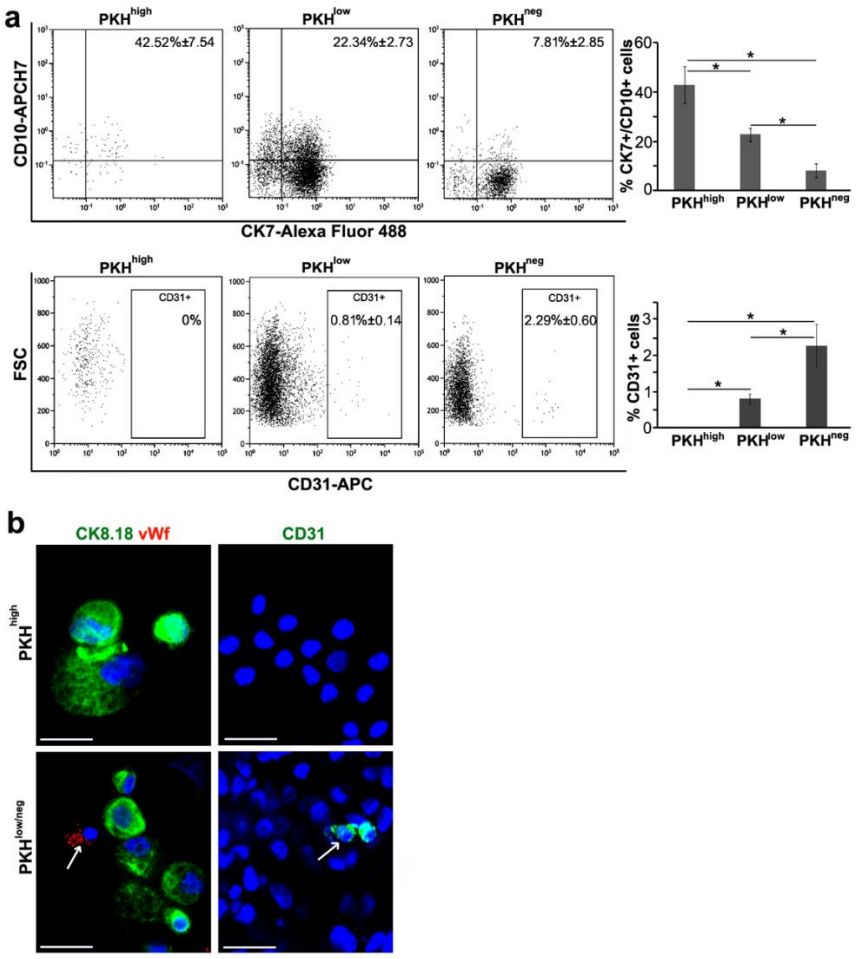
a
PKH^high
PKH^low
PKH^neg
42.52%±7.54
22.34%±2.73
7.81%±2.85
CD10-APCH7
CK7-Alexa Fluor 488
% CK7+/CD10+ cells
CD31+
0%
0.81%±0.14
2.29%±0.60
FSC
CD31-APC
% CD31+ cells
b
CK8.18 vWf
CD31
PKH^high
PKH^low/neg

Figure 3

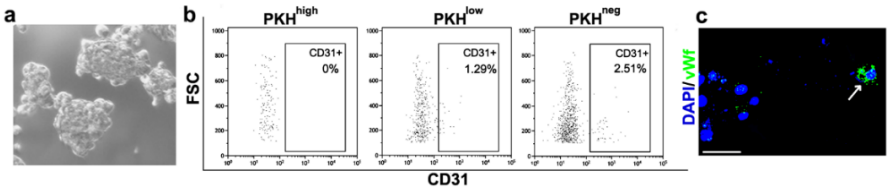

Figure 4

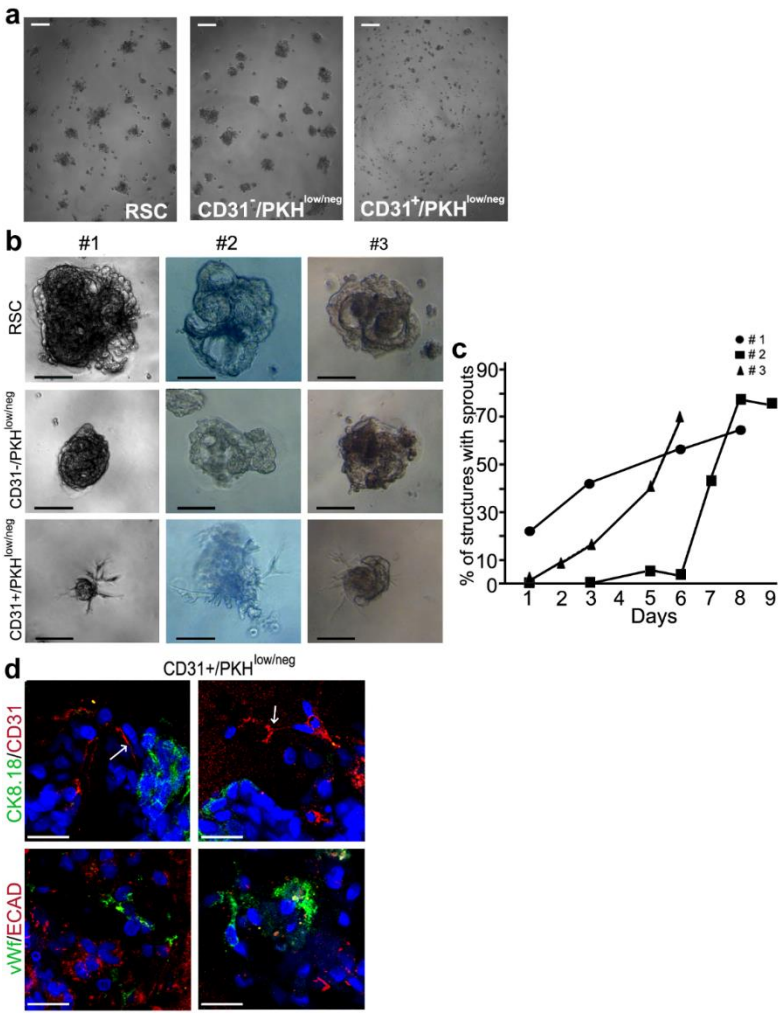

Figure 5

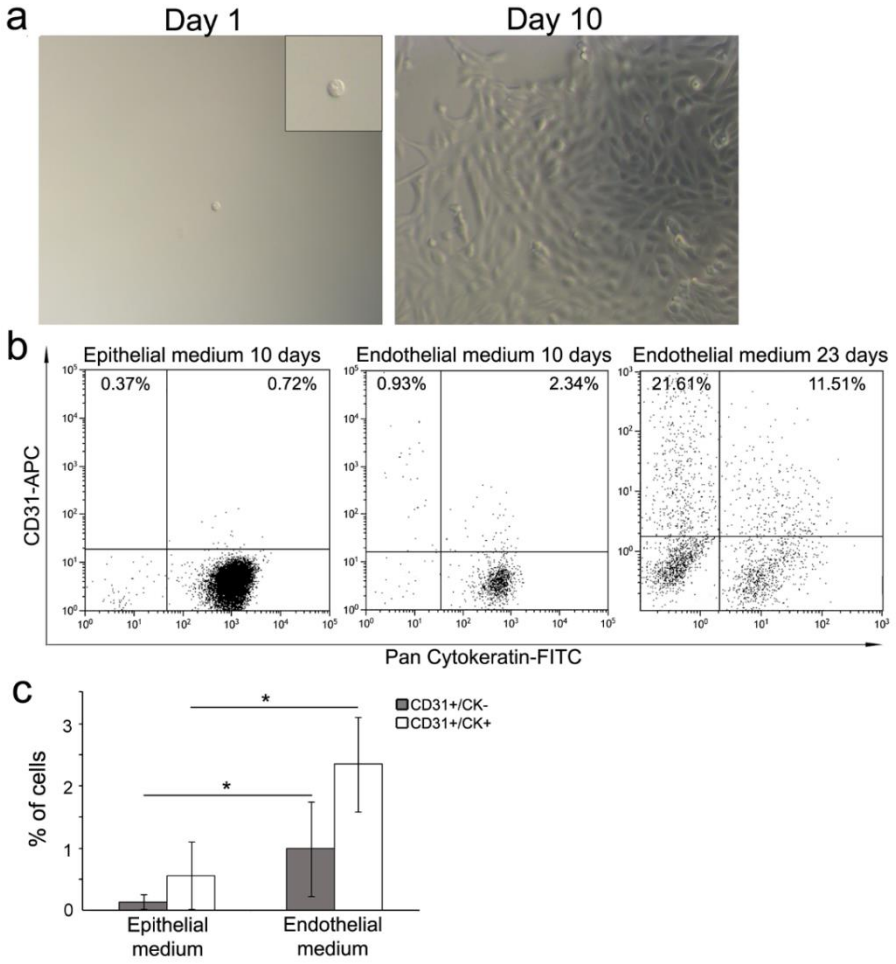
a
Day 1
Day 10
b
Epithelial medium 10 days
Endothelial medium 10 days
Endothelial medium 23 days
0.37%
0.72%
0.93%
2.34%
21.61%
11.51%
CD31-APC
Pan Cytokeratin-FITC
c
CD31+/CK-
CD31+/CK+
% of cells
Epithelial medium
Endothelial medium
*
*

Supplemental figure legends

Supplementary Figure S1: *Histological characterization of decellularized scaffolds repopulated with RSC*. (a) Representative H&E staining of FFPE scaffold sections after 30 days without seeding any cells. Scale bars, 100 µm. (b) Representative IF analysis of FFPE scaffolds repopulated with RSC. The antibodies against the indicated markers recognise cells that co-express specific tubular epithelial and endothelial markers. Sequential immunostaining has been performed. Scale bars, 100 µm. CK: Cytokeratin; AQP: Aquaporin; vWf: von Willebrand Factor; Blue:DAPI.

Supplementary Figure S2: *Differentiation abilities of PKH$^{low/neg}$ progenitor cells*. (a-b-c) Five independent experiments of human kidney scaffold repopulation for 30 days with PKH$^{low/neg}$ cells in presence of basal medium were performed. (a) Representative H&E staining of FFPE repopulated scaffold sections. Scale bars, 50 µm. (b-c) Representative sequential IF analysis of the FFPE repopulated scaffolds with the antibodies against the indicated markers that recognise specific tubular or vascular phenotypes. Scale bars, 50 µm. CK: Cytokeratin; AQP: Aquaporin; CALB: Calbindin D-28k; vWf: von Willebrand Factor; Blue:DAPI**.** (d) FACS analysis of representative clones obtained from single PKH$^{low/neg}$ cells at ten days of culture in epithelial and endothelial media. The CD31 and Cytokeratin markers were evaluated.

Supplementary Figure S3: *Histological characterization of decellularized scaffolds repopulated with RSC.* Representative sequential IF analysis of the FFPE repopulated scaffolds with the

antibodies against the indicated markers that recognise specific proximal (AQP1, CD13, N-Cadherin) or distal (CK7, CALB, E-Cadherin) tubular phenotypes. CK: Cytokeratin; AQP: Aquaporin; CALB: Calbindin D-28k.

Supplementary Figure S1

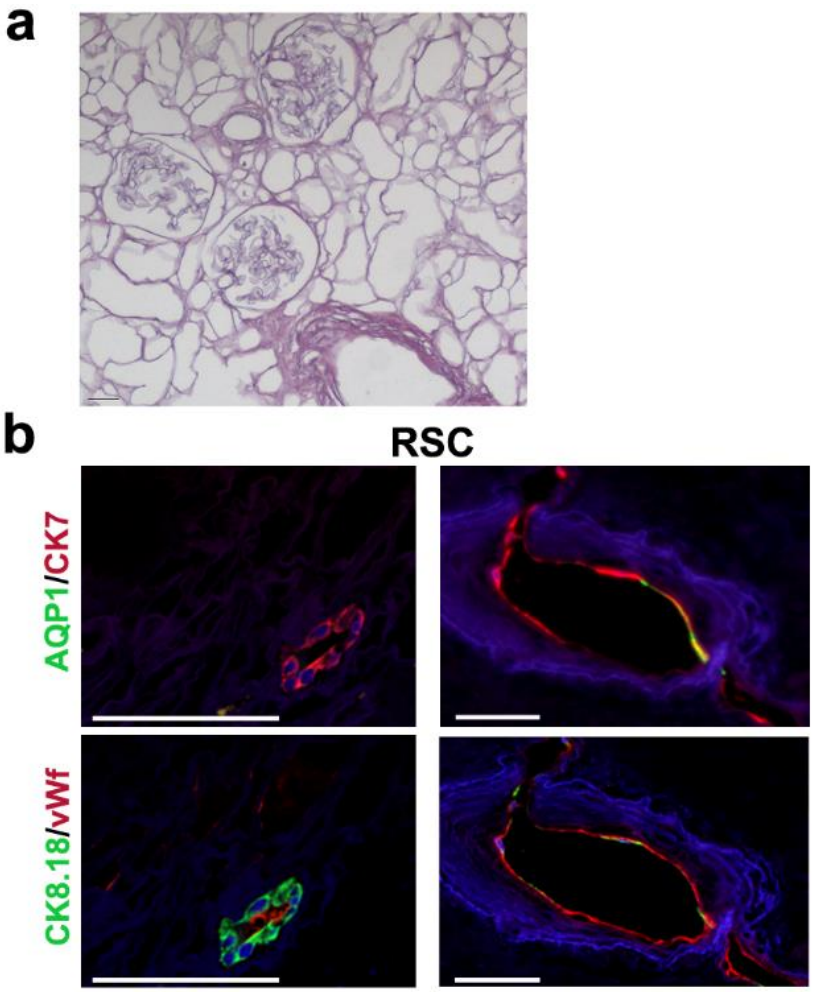

Supplementary Figure S2

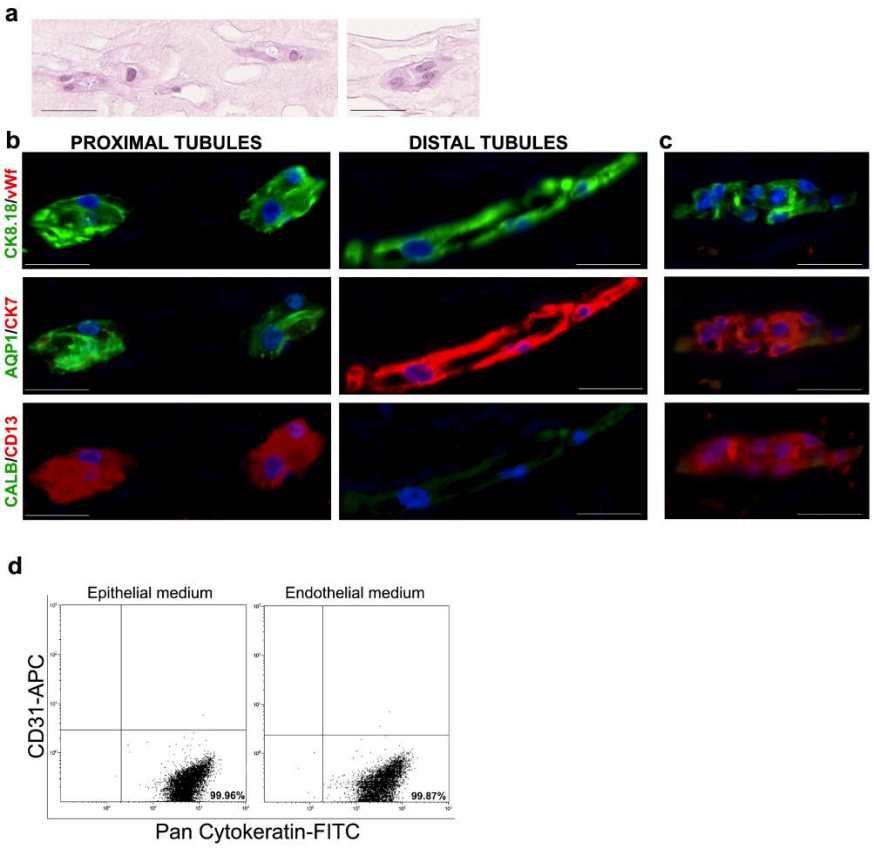

Supplementary Figure S3

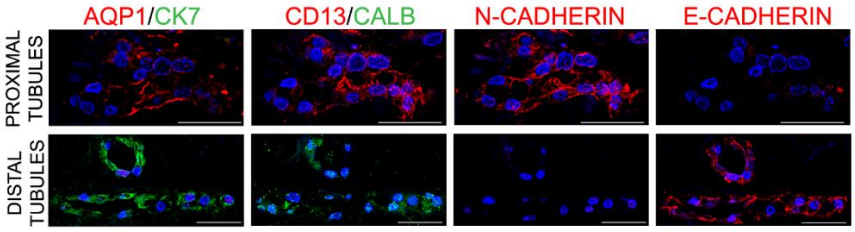

References

1. Prescott, L.F. The normal urinary excretion rates of renal tubular cells, leucocytes and red blood cells. *Clin. Sci*. **1966**, 31, 425–435.
2. Lameire, N.H.; Bagga, A.; Cruz, D.; De Maesneer, J.; Endre, Z.; Kellum, J.A.; Liu, K.D.; Mehta, R.L.; Pannu, N.; Van Biesen, W.; Vanholder, R. Acute kidney injury: an increasing global concern. *Lancet*. **2013**, 382(9887), 170-179; DOI: 10.1016/S0140-6736(13)60647-9.
3. Humphreys, B.D.; Valerius, M.T.; Kobayashi, A.; Mugford, J.W.; Soeung, S.; Duffield, J.S.; McMahon, A.P.; Bonventre, J.V. Intrinsic epithelial cells repair the kidney after injury. *Cell Stem Cell*. **2008**, 2(3), 284-291; DOI: 10.1016/j.stem.2008.01.014.
4. Rinkevich, Y.; Montoro, D.T.; Contreras-Trujillo, H.; Harari-Steinberg, O.; Newman, A.M.; Tsai, J.M.; Lim, X.; Van-Amerongen, R.; Bowman, A.; Januszyk, M.; Pleniceanu, O.; Nusse, R.; Longaker, M.T.; Weissman, I.L.; Dekel, B. In vivo clonal analysis reveals lineage-restricted progenitor characteristics in mammalian kidney development, maintenance, and regeneration. *Cell Rep*. **2014**, 7(4), 1270-1283; DOI: 10.1016/j.celrep.2014.04.018.
5. Johnson, H.A.; Vera Roman, J.M. Compensatory renal enlargement. Hypertrophy versus hyperplasia. *Am J Pathol*. **1996**, 49(1), 1-13.
6. Lombardi, D.; Becherucci, F.; Romagnani, P. How much can the tubule regenerate and who does it? An open question. Nephrol. *Dial. Transplant*. **2016**, 31(8), 1243-1250; DOI: 10.1093/ndt/gfv262.

7. Pleniceanu, O.; Omer, D.; Harari-Steinberg, O.; Dekel, B. Renal lineage cells as a source for renal regeneration. *Pediatr. Res*. **2018**, 83(1-2), 267-274; DOI: 10.1038/pr.2017.255.
8. Lazzeri, E.; Angelotti, M.L.; Peired, A.; Conte, C.; Marschner, J.A.; Maggi, L.; Mazzinghi, B.; Lombardi, D.; Melica, M.A.; Nardi, S.; Ronconi, E.; Sisti, A.; Antonelli, G.; Becherucci, F.; De Chiara, L.; Romero Guevara, R.; Burger, A.; Schaefer, B.; Annunziato, F.; Anders, H.; Lasagni, L.; Romagnani, P. Endocycle-related tubular cell hypertrophy and progenitor proliferation recover renal function after acute kidney injury. *Nat. Commun*. **2018**, 9(1), 1344-1362; DOI: 10.1038/s41467-018-03753-4.
9. Bussolati, B.; Bruno, S.; Grange, C.; Buttiglieri, S.; Deregibus, M.C.; Cantino, D.; Camussi, G. Isolation of renal progenitor cells from adult human kidney. *Am. J. Pathol*. **2005**, 166(2), 545-555; DOI: 10.1016/S0002-9440(10)62276-6.
10. Bussolati, B.; Moggio, A.; Collino, F.; Aghemo, G.; D'Armento, G.; Grange, C.; Camussi, G. Hypoxia modulates the undifferentiated phenotype of human renal inner medullary CD133+ progenitors through Oct4/miR-145 balance. *Am. J. Physiol. Renal. Physiol*. **2012**, 302(1), F116-F128; DOI: 10.1152/ajprenal.00184.2011.
11. Sagrinati, C.; Netti, G.S.; Mazzinghi, B.; Lazzeri, E.; Liotta, F.; Frosoli, F.; Ronconi, E.; Meini, C.; Gacci, M.; Squecco, R.; Carini, M.; Gesualdo, L.; Francini, F.; Maggi, E.; Annunziato, F.; Lasagni, L.; Serio, M.; Romagnani, S.; Romagnani, P. Isolation and characterization of multipotent progenitor cells from the Bowman's capsule of adult human kidneys. *J. Am. Soc. Nephrol*. **2006**, 17(9), 2443-2456; DOI: 10.1681/ASN.2006010089.

12. Angelotti, M.L.; Ronconi, E.; Ballerini, L.; Peired, A.; Mazzinghi, B.; Sagrinati, C.; Parente, E.; Gacci, M.; Carini, M.; Rotondi, M.; Fogo, A.B.; Lazzeri, E.; Lasagni, L.; Romagnani, P. Characterization of renal progenitors committed toward tubular lineage and their regenerative potential in renal tubular injury. *Stem Cells*. **2012**, 30(8), 1714-1725; DOI: 10.1002/stem.1130.
13. Bussolati, B.; Camussi, G. Therapeutic use of human renal progenitor cells for kidney regeneration. *Nat. Rev. Nephrol*. **2015**, 11(12), 695-706; DOI: doi: 10.1038/nrneph.2015.126.
14. Bombelli, S.; Zipeto, M.A.; Torsello, B.; Bovo, G.; Di Stefano, V.; Bugarin, C.; Zordan, P.; Viganò, P.; Cattoretti, G.; Strada, G.; Bianchi, C.; Perego, R.A. PKH^{high} cells within clonal human nephrospheres provide a purified adult renal stem cell population. *Stem Cell Res*. **2013**, 11(3), 1163-1177; DOI: 10.1016/j.scr.2013.08.004.
15. Steinberg, O.H.; Omer, D.; Gnatek, Y.; Pleniceanu, O.; Goldberg, S.; Cohen-Zontag, O.; Pri-Chen, S.; Kanter, I.; Ben Haim, N.; Becker, E.; Ankawa, R.; Fuchs, Y.; Kalisky, T.; Dotan, Z.; Dekel, B. Ex Vivo Expanded 3D Human Kidney Spheres Engraft Long Term and Repair Chronic Renal Injury in Mice. *Cell. Rep*. **2020**, 30(3), 852-869; DOI: 10.1016/j.celrep.2019.12.047.
16. Bombelli, S.; Meregalli, C.; Scalia, C.; Bovo, G.; Torsello, B.; De Marco, S.; Cadamuro, M.; Viganò, P.; Strada, G.; Cattoretti, G.; Bianchi, C.; Perego, R.A. Nephrosphere-derived cells are induced to multilineage differentiation when cultured on human decellularized kidney scaffolds. *Am. J. Pathol*. **2018**, 188(1), 184-195.; DOI: 10.1016/j.ajpath.2017.09.012.

17. Bianchi, C.; Bombelli, S.; Raimondo, F.; Torsello, B.; Angeloni, V.; Ferrero, S.; Di Stefano, V.; Chinello, C.; Cifola, I.; Invernizzi, L.; Brambilla, P.; Magni, F.; Pitto, M.; Zanelli, G.; Mocarelli, P.; Perego, R.A. Primary cell cultures from human renal cortex and renal-cell carcinoma evidence a differential expression of two spliced isoforms of Annexin A3. *Am. J. Pathol*. **2010**, 176(4), 1660-1670; DOI: 10.2353/ajpath.2010.090402.

18. Torsello, B.; Bianchi, C.; Meregalli, C.; Di Stefano, V.; Invernizzi, L.; De Marco, S.; Bovo, G.; Brivio, R.; Strada, G.; Bombelli, S.; Perego, R.A. Arg tyrosine kinase modulates TGF-β1 production in human renal tubular cells under high-glucose conditions. *J Cell Sci*. **2016**, 129(15), 2925-36; DOI: 10.1242/jcs.183640.

19. Di Stefano, V.; Torsello, B.; Bianchi, C.; Cifola, I.; Mangano, E.; Bovo, G.; Cassina, V.; De Marco, S.; Corti, R.; Meregalli, C.; Bombelli, S.; Viganò, P.; Battaglia, C.; Strada, G.; Perego, R.A. Major Action of Endogenous Lysyl Oxidase in Clear Cell Renal Cell Carcinoma Progression and Collagen Stiffness Revealed by Primary Cell Cultures. *Am. J. Pathol*. **2016**, 186(9), 2473-85; DOI: 10.1016/j.ajpath.2016.05.019.

20. Bolognesi, M.M.; Manzoni, M.; Scalia, C.R.; Zannella, S.; Bosisio, F.M.; Farretta, M.; Cattoretti, G. Multiplex Staining by Sequential Immunostaining and Antibody Removal on Routine Tissue Sections. *J. Histochem. Cytochem*. **2017**, 65(8), 431-444; DOI: 10.1369/0022155417719419.

21. Bruno, S.; Bassani, B.; D'Urso, D.G.; Pitaku, I.; Cassinotti, E.; Pelosi, G.; Boni, L.; Dominioni, L.; Noonan, D.M.; Mortara, L.; Albini, A. Angiogenin and the MMP9-TIMP2 axis are up-

regulated in proangiogenic, decidual NK-like cells from patients with colorectal cancer. *FASEB J*. **2018**, 32(10), 5365-5377; DOI: 10.1096/fj.201701103R.

22. Lee, G.Y.; Kenny, P.A.; Lee, E.H.; Bissell, M.J. Three-dimensional culture models of normal and malignant breast epithelial cells. *Nat. Methods*. **2007**, 4(4), 359-65; DOI: 10.1038/nmeth1015.
23. Peloso, A.; Ferrario, J.; Maiga, B.; Benzoni, I.; Bianco, C.; Citro, A.; Currao, M.; Malara, A.; Gaspari, A.; Balduini, A.; Abelli, M.; Piemonti, L.; Dionigi, P.; Orlando, G.; Maestri, M. Creation and implantation of acellular rat renal ECM-based scaffolds. *Organogenesis.* **2015**, 11: 58-74; DOI:10.1080/15476 278.2015 .1072661.
24. Caralt, M.; Uzarski, J.S.; Iacob, S.; Obergfell, K.P.; Berg, N.; Bijonowski, B.M.; Kiefer, K.M.; Ward, H.H.; Wandinger-Ness, A.; Miller, W.M.; Zhang, Z.J.; Abecassis, M.M.; Wertheim, J.A. Optimization and critical evaluation of decellularization strategies to develop renal extracellular matrix scaffolds as biological templates for organ engineering and transplantation. *Am J Transplant.* **2015**, 15: 64-75; DOI: 10.1111/ajt.12999.
25. Sciancalepore, A.G.; Portone, A.; Moffa, M.; Persano, L.; De Luca, M.; Paiano, A.;, Sallustio, F.; Schena, F.P.; Bucci, C.; Pisignano, D. Micropatterning control of tubular commitment in human adult renal stem cells. *Biomaterials.* **2016**, 94: 57-69. DOI: 10.1016/j.biomaterials.2016.03.042.
26. Remuzzi, A.; Figliuzzi, M.; Bonandrini, B.; Silvani, S.; Azzollini, N.; Nossa, R.; Benigni, A; Remuzzi, G. Experimental Evaluation

of Kidney Regeneration by Organ Scaffold Recellularization. *Sci Rep*. **2017**, 7;7:43502. DOI: 10.1038/srep43502.

27. Pavenstädt, H.; Kriz, W; Kretzler, M. Cell biology of the glomerular podocyte. *Physiol Rev***. 2003,** 83: 253-307, DOI: 10.1152/physrev. 00020.2002.
28. Heiss, M.; Hellström, M.; Kalén, M.; May, T.; Weber, H.; Hecker, M.; Augustin, H.G.; Korff, T. Endothelial cell spheroids as a versatile tool to study angiogenesis in vitro. *FASEB J*. **2015**, 29, 3076–3084; DOI: 10.1096/fj.14-267633.
29. Pece, S.; Tosoni, D.; Confalonieri, S.; Mazzarol, G.; Vecchi, M.; Ronzoni, S.; Bernard, L.; Viale, G.; Pelicci, P.G.; Di Fiore, P.P. Biological and molecular heterogeneity of breast cancers correlates with their cancer stem cell content. *Cell*. **2010**, 140(1), 62-73; DOI: 10.1016/j.cell.2009.12.007.
30. Little, M.H.; McMahon, A.P. Mammalian kidney development: principles, progress, and projections. *Cold Spring Harb. Perspect. Biol.* **2012**, 4(5), a00830; DOI: 10.1101/cshperspect.a008300.
31. Takasato, M.; Er, PX.; Chiu, HS.; Maier, B.; Baillie, GJ.; Ferguson, C.; Parton, RG.; Wolvetang, EJ.; Roost, MS.; Chuva de Sousa Lopes, SM.; Little, MH. Kidney organoids from human iPS cells contain multiple lineages and model human nephrogenesis. *Nature*. **2015**, 526(7574), 564-568; DOI: 10.1038/nature15695.
32. Homan, K.A.; Gupta, N.; Kroll, K.Y.; Kolesky, D.B.; Skylar-Scott, M.; Miyoshi, T.; Mau, D.; Valerius, M.T.; Ferrante, T.; Bonventre, J.V.; Lewis, J.A.; Morizane, R. Flow-enhanced vascularization and maturation of kidney organoids in vitro. *Nat. Methods*. **2019**, 16(3), 255-262; DOI: 10.1038/s41592-019-0325-y.

33. Gonçalves, A.F. Evidence of renal angiomyolipoma neoplastic stem cells arising from renal epithelial cells. *Nat. Commun*. **2017**, 8(1), 1466-1482; DOI: 10.1038/s41467-017-01514-3.

34. Becherucci, F.; Romagnani, P. Angiomyolipoma: a link between stemness and tumorigenesis in the kidney. *Nat. Rev. Nephrol*. **2018**, 14(4), 215-216; DOI: 10.1038/nrneph.2018.16.

35. Batlle, E.; Clevers, H. Cancer stem cells revisited. *Nat. Med*. **2017**, 23, 1124-1134; DOI: 10.1038/nm.4409.

Chapter 3

DNA damage in circulating hematopoietic progenitor stem cells as promising biological sensor of frailty

Chiara Grasselli MSc[1*], Silvia Bombelli PhD[1*], Stefano Eriani MSc[1], Giulia Domenici MD[2], Riccardo Galluccio MD[1,2], Chiara Tropeano BcSc[1,3], Sofia De Marco PhD[1], Maddalena M Bolognesi MSc[1], Barbara Torsello PhD[1], Cristina Bianchi PhD[1], Antolini Laura PhD[1], Fabio Rossi MD[4], Paolo Mazzola MD[1,2], Valerio Leoni MD PhD[1,3], Giuseppe Bellelli MD[1,2], Roberto A Perego MD[1]

[1] School of Medicine and Surgery, University of Milano Bicocca, Monza, Italy

[2] Acute Geriatric Unit, San Gerardo Hospital, ASST-Monza, Monza, Italy

[3] Laboratory of Clinical Chemistry, Hospital of Desio, ASST-Brianza, Desio, Italy

[4] Immunotransfusional Unit, San Gerardo Hospital, ASST-Monza, Monza, Italy

* Equal contribution

Corresponding author:
Roberto A. Perego, MD
School of Medicine and Surgery, University of Milano Bicocca,
Via Cadore 48, 20900 Monza (MB) - Italy
Phone +39 02 6448 8303
e-mail: roberto.perego@unimib.it

Submitted on *Journals of Gerontology: Biological Sciences*. 2021.

Funding: This work was supported by Fondazione Cariplo Milano (Italy) by the grant 2017-0577 to RAP

Abstract

Frailty is an age-related syndrome that exposes individuals to increased vulnerability. Although it is potentially reversible in most cases leads to negative outcomes, including mortality. The several methods proposed identify frailty only after the onset of clinical manifestations. An early diagnosis might give the possibility to manage better the frailty progression. The frailty pathophysiology is still unclear although mechanisms, linked to inflammation and immunosenescence, have been investigated. A common feature of several clinical aspects involved in senescent organisms is the increase of oxidative stress, described as one of the major causes of DNA damage accumulation in aged cells including the adult stem cell compartment. Likely, this accumulation might be implicated in frailty status. The oxidative status of our frail, pre-frail and non-frail population was characterized. In addition, the DNA damage in hematopoietic cells was evidenced analyzing the peripheral blood mononuclear cells (PBMC) and their T lymphocyte, monocyte, circulating hematopoietic progenitor stem cell (cHPSC) subpopulations. The phosphorylation of C-terminal of histone H2AX at amino acid Ser 139 (γ-H2AX), which occurs at the DNA double strand break focus, was evaluated. In our frail population an increased oxidative stress and a high level of DNA damage in cHPSC was found. This study may have potential implications because the increment of DNA damage in cHPSC could be suggestive of an organism impairment preceding the evident frailty. In addition, it may open the possibility for attenuation of frailty progression throughout specific drugs acting on preventing DNA damage or removing damaged cells.

Keywords: γ-H2AX, Biology of aging, Oxidative stress, Cellular senescence.

Introduction

Frailty is an age-related syndrome, which results from a decline in physiological capacities across several organ systems and exposes the individual to an increased vulnerability towards internal and external stressors (1). It is a potentially reversible condition, but in most cases it progresses towards disability and/or leads to several negative outcomes, including falls and fractures, hospitalizations, iatrogenic complications, and mortality (1-3). The risk of these adverse events can occur independently of the presence of comorbidity (4). Several methods have been proposed to assess frailty in research and clinical practice, without clear evidence that one method is preferable to the others. Fried et al. (4) developed the phenotype model of frailty that is one of the most employed in clinical research. It considers frailty as a biological entity and classifies the individuals as frail when three or more of the following five criteria are present: unintentional weight loss, exhaustion, slow walking speed, low physical activity and low muscle strength. A classification of pre-frailty is also possible when only one or two of these criteria are present. The pathophysiological mechanisms underlying the frailty phenotype are still unclear although mechanisms, in particular linked to inflammation and immunosenescence, have been investigated (5, 6). However, the complex interactions during aging between the studied molecules and these mechanisms are yet to be defined.

A common feature of several clinical aspects involved in senescent organisms is the increase of the oxidative stress that is described as one of the major causes of DNA damage accumulation, well documented in the different tissues of older people (7). Likely, this accumulation might

be implicated in frailty status (8) because DNA damage can lead to molecular and cellular alterations (genomic instability, altered gene expression, loss of cell division potential, cell death, organ dysfunctions) (7, 9) that are a good background on which frailty can establish.

The phosphorylation of the C-terminal of histone H2A, variant H2AX, at the highly conserved amino acid Ser 139 (γ-H2AX) is an early response to DNA double strand breaks (DSB), γ-H2AX and DSB correlate in 1:1 manner (10). In the cells can be present transient and persistent γ-H2AX foci. In the persistent foci, DSB are not repairable and appear to be common in senescent cells and increase in older subjects (11-13). γ-H2AX foci detection is one of the most sensitive way to examine the DNA damage (14). In recent years the role of DNA damage has been investigated on whole blood (15) and lymphocytes (16), evaluating the relationship between the level of persistent γ-H2AX foci and frail status of older patients.

With our study we wanted to deepen the characterization of DNA damage in hematopoietic cells, analyzing the peripheral blood mononuclear cells (PBMC) and the T lymphocyte, monocyte, circulating hematopoietic progenitor stem cell (cHPSC) subpopulations present in PBMC of frail, pre-frail and non-frail seniors.

Materials and Methods

Study population

A group of 85 subjects (40 Frail, 13 Pre-Frail, 32 Non-Frail) aged 65 years old and above were recruited from the Geriatrics Unit, San Gerardo Hospital ASST Monza. All of them were outpatients. The exclusion criteria for the recruited subjects were: a) illiteracy, b)

psychiatric disorders, c) Parkinson's disease, d) cognitive function impairment, e) Multiple Sclerosis, f) neurodegenerative diseases, g) hip fracture or other severe trauma affecting mobility. The identification of frail phenotype in all subjects occurred at recruitment and was based on the presence of five criteria (4): 1) Shrinking, which was determined as an unintentional weight loss of 5% or more than usual, over the last year; 2) Self-reported exhaustion, which was measured as present or absent by asking the individual: "In the last month, do you have less energy to do the things of daily living you want?"; 3) Slow walking speed, which was defined as present if an individual took more than 7 seconds to cover a distance of 4 meters (17); 4) Low physical activity, which was assessed using Physical Activity Scale for the Elderly (PASE) over a one-week period. The PASE score combines information on leisure, household and occupational activity (18); 5) Weakness, which was measured using the dynamometer handgrip strength for three consecutive times on dominant hand. The criterion is positive if the best value is less than cutoff value (<27 for males and <16 for females) (19). Participants were considered frail if they fulfilled three or more criteria, pre-frail if scoring in one or two criteria and robust or non-frail with no criteria scored. Forty-six young subjects, aged between 25 and 35 years old, without functional disability, acute pathologies in progress or abuse of drugs, alcohol, smoke and with healthy lifestyle, were recruited among blood donors as control group. The study was conducted according to the principles of the Declaration of Helsinki II and approved by the Ethics committee Brianza (Monza, Italy) code FRA-ARSC March 22nd, 2018. The participation in the

study was voluntary, all subjects were fully informed on the aims of the study, the nature of participation and signed the informed consent.

Comprehensive geriatric assessment

After recruitment, all 85 older adults underwent a comprehensive geriatric assessment (CGA) including demographics (age and sex), life habits (smoking and alcohol consumption), and several tools to evaluate nutritional, cognitive, functional, and somatic health status. Nutritional status was evaluated using the Mini Nutritional Assessment-short form (MNA-sf) (20) and cognitive status using the Mini Mental State Examination (MMSE) (21). The functional status was assessed with the modified Barthel Index (22), the Lawton and Brody's Instrumental Activity of Daily Living (IADL) (23) and the Short Physical Performance Battery (SPPB) (17). Lastly, the somatic health status was assessed with the Charlson Comorbidity Index (CCI) (24). The number of drugs taken at home was determined.

PBMC collection, Cell characterization, DNA damage evaluation

Whole blood from frail, pre-frail, non-frail and young subjects was collected into BD Vacutainer CPT Cell Preparation Tubes with sodium heparin (Becton Dickinson, Franklin Lakes, NJ, USA). The isolation of PBMC by Ficoll-Paque (GE Healthcare Bio-SciencesAD, Uppsola, Sweden) density gradient separation was performed according to manufacturer's instructions. The PBMC isolated were suspended in blocking solution (PBS with 5% Fetal Bovine Serum) at room temperature (RT) for 15 minutes then treated following a protocol modified by Beaton et al (25). Briefly, membrane cell staining was

performed for 15 minutes at RT with the following antibodies: APC Mouse Anti-Human CD3 (Clone UCHT1; BD Pharmingen, San Jose, CA, USA; 1:200), T lymphocyte marker; APC-H7 Mouse anti-Human CD14 (Clone MφP9; BD Pharmingen; 1:200), monocyte marker; PE Mouse Anti-Human CD34 (Clone 8G12; BD Pharmingen; 1:100), hematopoietic progenitor stem cell (HPSC) marker. The stained PBMC were then centrifuged, suspended, fixed with 4% Methanol free Formaldehyde (Thermo Fisher Scientific, Waltham, MA, USA) and permeabilized with 0.1% Triton X-100 (Sigma-Aldrich, St. Louis, MO, USA). After centrifugation, 70% cold methanol was added dropwise while vortexing the cellular pellet, then the samples were stored at -20°C for 24 hours. Successively, these samples were washed and stained for 2 hours at 4°C with Anti-phospho-Histone H2AX (Ser139) FITC conjugate (Clone JBW301; Millipore, Burlington, MA, USA; 2.5mg/mL) to identify DNA double-strand break. The samples were then analyzed with a MoFlo Astrios cell sorter and Kaluza 2.1 software (both from Beckman Coulter, Miami, FL, USA). Based on the gating strategy (Supplementary Fig 1) used on the PBMC (a minimum of 10^5 events were acquired), the percentage of T lymphocytes CD3+, monocytes CD14+ and circulating HPSC (cHPSC) CD34+/CD3-/CD14- were evaluated as well as the respective cells positive for γ-H2AX. The mean fluorescence intensity (MFI) calculated as the median of the fluorescence intensity values of the γ-H2AX+ cells (represented on the X axis of Figure 1 and Supplementary Figure 1) has also been evaluated. MFI provides information on the amount of DNA damaged foci in the cells.

For the characterization of cHPSC on fresh whole blood, 700 µl of peripheral blood were lysed using erythrocyte lysis buffer (Biolegend, San Diego, CA, USA). Then the white blood cells underwent membrane cell staining as described above using the following antibodies: APC anti-human Lineage cocktail against CD3/CD14/CD16/ CD19/ CD20/ CD56 (Lin1) (Biolegend; 1:5); APC/Fire^{TM} 750 anti-human CD45 (Clone 2D1, Biolegend; 1:20); PE anti-human CD34 (Clone 8G12; BD Pharmingen; 1:100). Flow cytometry analysis was performed based on the gating strategy described in Supplementary Figure 2. A minimum of 2 x10^5 events were acquired in the PBMC region.

Evaluation of oxidative stress

Oxysterols as markers of oxidative stress and 8-hydroxy-2-deoxy Guanosine (8-OH-dG) as marker of oxidative DNA damage were analyzed in a set of randomly chosen samples of plasma collected from frail, pre-frail, non-frail and young individuals. 7-keto-cholesterol (7KC), 7β-hydroxycholesterol (7βOHC), 5a6a-epoxycholesterol, 5β,6β.epoxycholsterol, 3β,5α,6β-3OH-cholesterol (triol) were quantified by isotope dilution mass spectrometry (26) as cholesterol oxidation and cholesterol autoxidation products resulting from oxidative stress (27-29). The 8-hydroxy-2-deoxy Guanosine (8-OH-dG) was analyzed in duplicate by enzyme-linked immunosorbent assay (ab201734, 8-hydroxy-2-deoxy Guanosine ELISA kit, Abcam, Cambridge, UK), *according to* literature (30) and *manufacturer instructions*.

Statistical analysis

Continuous variables were reported as mean ± standard deviation and as median with first quartile-third quartile. Categorical variables were reported as absolute and relative frequencies. The comparison between groups was performed with the Oneway ANOVA with Tukey's test correction and with Pairwise Multiple Comparison Procedures (Holm-Sidak method), with Wilcoxon-Mann-Whitney test in case of non-Gaussian distribution. When significant, the single pairs (frail, pre-frail, non-frail and young) were also compared. Significance was for $P < 0.05$. Receiver operating characteristic (ROC) curve analysis were done using one-way analysis (Wilson-Brown method) and the results were reported as fraction. The GraphPad Prism program has been used (GraphPad Software, Inc., La Jolla, CA, USA).

Results

Study population

Among the 85 subjects recruited, 40 were frail (Male 17, Female 23); 13 pre-frail (Male 4, Female 9), 32 non-frail (Male 21, Female 11), these subjects underwent the CGA (Table 1) and lab analyses (Supplementary Table 1). Forty-six young subjects (Male 17, Female 29; mean age±SD 29.9±2.9 years; median age 29.5 years) were also recruited.

As expected, age was higher in frails and pre-frails in comparison to non-frails. Furthermore, frail and pre-frail subjects had lower scores at the MNA-sf, were more impaired in cognitive and functional status and had a higher CCI score. Lastly, non-frail subjects took a lower number of drugs if compared to both frails and pre-frails. The distribution of

chronic diseases (most of them used to calculate the CCI score) and the classes of drugs taken in the frail, pre-frail and non-frail groups are described in the Supplementary Table 2.

Hematological data of study population

The hematological parameters were obtained on fresh blood of the 85 seniors and 46 youngs (Supplementary Table 1). There were no differences in all variables considered, with two exceptions. The hemoglobin levels of older adults were lower in frails (11.0 ± 1.6 g/dL) than in pre-frails (12.9 ± 1.3 g/dL), non-frails (14.1 ± 1.0 g/dL) and youngs (14.7 ± 1.3 g/dL). The lymphocytes counts were lower in frails. In a set of randomly chosen frail (5 samples), non-frail (4 samples) and young (5 samples) subjects, we analyzed the cHPSC (Lin1-/CD45+/CD34+) present in the gate of mononucleated cells (Supplementary Figure 2). The results showed a percentage of cHPSC in the range of 0.040-0.071 (Supplementary Table 1). In all 85 older adults and 46 young (Table 2), we performed the separation of PBMC by Ficoll-Paque sedimentation, with a yield around 40%. By FACS analysis, using the gating strategy shown in supplementary Figure 1, we evaluated the PBMC, T lymphocytes as CD3+ cells, monocytes as CD14+ cells, the CD3-/CD14- cells considered B-lymphocytes for the majority and the cHPSC as CD3-/CD14-/CD34+ cells (Table 2). In the Ficoll-Paque isolated PBMC of the different subject groups the ratio between the T and B lymphocytes was maintained in favor of T lymphocytes. There was a slight reduction of monocytes in the separated PBMC (Table 2) respect to monocytes of the fresh whole blood (Supplementary Tab 1), probably because of their typical

stickiness. Anyway, there were not significant differences in the monocyte counts of the different subject groups but only a trend toward higher counts in frail patients. The percentage of the cHPSC CD34+/CD3-/CD14- subpopulation was around 0.073-0.099 (Table 2). This percentage is close to the one seen in the fresh whole blood, in which the more restricted Lin1-/CD45+/CD34+ phenotype has been evaluated (Supplementary Table 1). In conclusion, the separation by Ficoll-Paque maintained the reciprocal ratios among the different cell populations in the different groups.

DNA damage in PBMC and in the respective cell subpopulations

We detected the percentage of cells positive for ɣH2AX foci in the frail, pre-frail, non-frail older adults and young individuals, assessing the DNA damage in the Ficoll-Paque isolated PBMC (Figure 1). We evaluated by FACS the C-terminal phosphorylation of H2AX histone at serine 139 (γ-H2AX), the early event in response of DSB, using the gating strategy shown in Supplementary Figure 1. Our data showed an evident significant increase of cells positive for γ-H2AX in the PBMC, cHPSC and T cells of the frail patients (Figure 1). The difference between frails and pre-frails was significant only in cHPSC and not in PBMC and CD3+ T cells. The percentage of γ-H2AX+ cells in CD14+ monocytes increased in the frail group without a statistical significance with respect to all the other groups (Figure 1). However, this finding was also strengthened by the non-significant differences in the amount of monocytes in the PBMC of all studied groups, after Ficoll-Paque sedimentation (Table 2). In monocytes the DNA damage in pre-frail and non-frail subjects had the same level of the young individuals.

We also evaluated the mean fluorescence intensity (MFI) (Figure 2) assessing the amount of DNA damage foci per cell in each individual cell population of the specific subject group. The quantification of the MFI provided a distinct and additional parameter to the percent of DNA damaged positive cells. In PBMC, CD3+ and CD14+ cells, we observed higher MFI in frail subjects compared to other groups, although non significantly different (Figure 2). Instead, the MFI significantly increased in cHPSCs γ-H2AX+ of frail subjects compared to both pre-frail and non-frail seniors and to young individuals (Figure 2). ROC curve analysis (Supplemental Figure 3) assessing the percentage of DNA damaged cHPSC in our frail and non-frail subjects showed that the area under curve (AUC) was 0.835 (95% C.I. 0.740-0.931), suggesting a good discriminating power of the percentage of DNA damaged cHPSC to potentially discriminate between frail and non-frail subjects. The Youden Index that determines the optimal cut-off value was 0.611. The comparison between frails and pre-frails gave an AUC of 0.780 (95% C.I. 0.640-0.920) with a Youden Index of 0.548. These data showed that cHPSC of frails had both a higher percentage of cells with DNA damage and an increased MFI, as indicator of the median number of γ-H2AX foci per cell, compared to the other groups.

Increment of oxidative stress in frail population

We evaluated the oxidative status in a set of plasma of our subjects to verify whether in the frail subjects an increase of oxidative stress was detectable. We observed significant increments of auto-oxidation of oxysterols 7KC and 7βOHC, markers of oxidative stress (27-29) in the frail plasma with respect to pre-frail and non-frail plasma (Fig 3A),

together with increments of 5α,6α-epoxycholesterol, 5β,6β epoxycholsterol, 3β,5α,6β-3OH-cholesterol (triol) in plasma of frail subjects (data not shown). These findings were suggestive for an increased oxidative stress in frail compared to pre-frail, not frail and young individuals.

To reinforce the hypothesis that the DNA damage found in the hematopoietic cells had an oxidative origin we also evaluated in a different set of plasma the 8-OH-dG, which is produced by the oxidative damage of DNA (30). We observed a significant increase of 8-OH-dG in frail compared to pre-frail, non-frail and young subjects (Fig 3B) as with 7KC and 7bOHC.

Discussion

The daily intake of drugs, malnutrition, together with comorbidity are significantly represented in our frail patients and these may contribute for the shift to a higher level of their oxidative metabolism. In fact, the oxysterols analysis evidenced increased oxidative stress in frail individuals. We found that the increased oxidative status and the increased 8-OH-dG matched with DNA damage in the hematopoietic cells of frail patients. We observed a trend of increased DNA damage in the PBMC and in the CD34+ cHPSC and CD3+ T lymphocytes of non-frail seniors in comparison to young controls. This finding was in accordance with the literature (31, 32) and can be considered as an event associated with aging. However, our work also showed a significant percentage increment of PBMC, as well as CD34+ cHPSC and CD3+ T cells with DNA damage in frail in comparison to non-frail individuals

and in case of cHPSC this significant increment is evident even in comparison to pre-frails. Instead, CD14+ monocytes in the frail group showed only a trend to the increment of DNA damage with respect to the other older adult groups. It was similarly very interesting that the number of DNA damage foci per cell, evidenced by the MFI, was significantly higher in the CD34+ cHPSC of frail patients with respect to pre-frails, non-frails and youngs. In PBMC, CD3+ T lymphocytes and CD14+ monocytes the MFI value was higher in frail but not significantly. It has to be noted that T lymphocytes are considered long-lived and quiescent cells (33) and their high DNA damage level may represent the accumulation of DNA damage foci taken place over the lifespan. Instead, the monocytes are typically proliferating short-lived cells (34, 35) and DNA damage foci occur in the cells that however die precociously and likely do not have time to accumulate foci during lifespan, except in the frail period in which the risk for DNA damage increases. In aging, genomic instability has raised a great and persistent interest and it is also recognized as a determinant of age-related stem cell decline that accelerates age-related pathologies in several tissues and organs (36, 37). It is known that genomic alterations accumulate in human HPSC in life in a linear rate, similarly to adult stem cell of other tissues (31). The hematopoietic stem cells CD34+ are long-lived cells that accumulate DNA damages over life and particularly during aging when they come out of their dormant state by cell-intrinsic mechanisms (38) and by the shift of the basal metabolism to a higher level of oxidative metabolism (39-40). Both, the loss of dormant status and the increment of ROS, may have a direct consequence in the progressive increase of γ-H2AX towards frailty status. It has to be mentioned that

in mice part of the γ-H2AX foci found in aged hematopoietic stem cells can be due to ineffective dephosphorylation rather than persistent DNA damage, however, this situation pushes the cells to transcriptional silencing and functional decline (41). In conclusion, in our frail population, the clinical characteristics (age, malnutrition, drug intake) and comorbidity (diabetes mellitus, cardiovascular diseases, kidney diseases, obstructive pulmonary diseases) causing oxidative stress can justify the high level of DNA damage in cHPSC. In addition, the oxidative DNA damage likely affects several other adult stem cells and the DNA damage, as a process interconnected with other biological processes, may induce an amplification of dangerous effects. Therefore, our findings suggest that in the tissues of older adults, the occurrence of DNA damage accumulation, the DNA damage repair deficiency as well as the cellular functional decline can limit the adult stem cell compartment functions (42). All this may be implicated in the decline of tissue renewal capacity, in the appearance of aging-related pathology (43) and in a frailty more severe and progressive. Our study has potential implications: i) the increment of DNA damage in cHPSC might be a suggestive signal of organism impairment that precedes the evident frailty in older people. Although the evaluation of cHPSC CD34+/γ-H2AX+ can be improved for its eventual clinical use, it is promising that the ROC curve analysis showed the possibility to distinguish the frails from non-frails and pre-frails by the percentage of DNA damaged cells in the hematopoietic adult stem cell compartment. ii) if future studies will replicate or corroborate our findings, it will be possible to hypothesize that progression of frailty may be attenuated throughout specific drugs that act on preventing DNA damage or on

removing the damaged cells. Indeed, drug therapies (for example, geroprotectors, senolytic drugs and repurposed drugs) have been shown to attenuate frailty in preclinical and/or clinical studies (44).

Conflict of interest

None declared

Acknowledgments

We thank Prof Cattoretti G. from University of Milano-Bicocca for the helpful discussion.

Table 1. *Comprehensive Geriatric Assessment of 85 older adults, according to frail, pre-frailty or non-frail status.*

Characteristics	Frail (n=40)	Pre-frail (n=13)	Non-frail (n=32)	p value[a]	p value[b]	p value[c]
Age, years mean±SD median (1st-3rd quartile)	 81.9± 6.2 82 (78-86)	 79.5 ± 6.9 81 (73.5-84)	 73.8 ± 6.7 71 (67-77)	 .197 .109	 <.001 <.001	 .059 .004
Females, n (%)	23 (57.5)	9 (69.2)	11 (34.4)	.415	.090	.044
Smoke, n (%)						
Current smoker	3 (7.5)	1 (7.7)	1 (3.1)	.872	.397	.337
Past smoker	12 (30)	5 (38.5)	7 (21.9)			
Alcohol, n (%)						
moderate consumption	12 (30)	5 (38.5)	19 (59.4)	.595	.014	.175
consumption of >1 unit (males) or >½ unit (females)	2 (5)	-	-			
History of allergies, n (%)	4 (10)	2 (15.4)	3 (9.4)	.616	.868	.537
Mini Nutritional Assessment - short form, median (1st-3rd quartile)	11 (9-12)	13 (12-14)	14 (13-14)	<.001	<.001	.800
Mini-Mental State Examination, median (1st-3rd quartile)	26 (23-28)	27 (26-28.5)	30 (28-30)	.510	<.001	.002
Modified Barthel Index, median (1st-3rd quartile)	65 (60-90)	98 (90-100)	100 (100-100)	<.001	<.001	-
Instrumental Activities of Daily Living, median (1st-3rd quartile)	4 (3-5)	7 (5-7)	7 (6-8)	.010	<.001	.083
Short Physical Performance Battery, median (1st-3rd quartile)	5 (3-6)	7 (6.5-8.5)	12 (10-12)	<.001	<.001	.001
Charlson Comorbidity Index, median (1st-3rd quartile)	2 (1-4)	1 (0-1)	0 (0-1)	.006	<.001	.080
Number of drugs, median (1st-3rd quartile)	7 (5-9)	4 (3-7)	3 (1-3.5)	.199	<.001	.004

Notes. Values are expressed as mean ± standard deviation, unless otherwise specified.
[a] comparison between pre-frail vs. frail.
[b] comparison between non-frail vs. frail.
[c] comparison between non-frail vs. pre-frail

Table 2. *Ficoll-Paque isolated PBMC and the respective mononucleated cell subpopulations analyzed by FACS with the gating strategy shown in Supplementary Figure 1.* Samples obtained from 85 older adults divided according to the frail, pre-frail, non-frail status and from a group of 46 young subjects.

	Frail 40 pts	**Pre-Frail 13 pts**	**Non-Frail 32pts**	**Young 46 pts**
PBMC n [a]	800503±784393 474416 (205072-1168448)	942967±763245 812920 (343009-1315235)	846580.5±696317 595650 (286251-1321378)	1068624±766984 807084 (400997-1856148)
T cells CD3+ %	57.4±14.1 58.6 (50-69)	59.2±17.7 66.2 (49-72)	59.1±9.5 56.6 (52-67)	62.2±12.0 62.6 (56-70)
Cells CD3-/ CD14- %	33.8±12.0 33.5 (24-40)	32.2±17.8 24 (17-40)	33.2±9.7 34.7 (25-39)	31.1±12.0 29.4 (23-35)
Monocytes CD14+ %	7.0±4.6 6.6 (4-8)	5.9±3.5 5.5 (7-3)	6.3±4.3 5 (3-7)	5.5±3.5 4.5 (3-7)
cHPSC CD3-/ CD14- /CD34+ %	0.076±0.070 0.062 (006-0.09)	0.099±0.068 0.092 (0.03-0.14)	0.068±0.040 0.05 (0.04-0.09)	0.081±0.072 0.07 (0.03-0.10)

Notes. Values are expressed as mean ± standard deviation and median (1st-3rd quartile). Statistical analysis was not significant among all groups.

[a] PBMC were analyzed with the non-parametric test Wilcoxon-Mann-Whitney.

Figure Legends

Figure 1. *DNA damage in PBMC isolated by Ficoll-Paque and in the respective cell subpopulations: cHPSC CD34+/CD3-/CD14-, T lymphocytes CD3+, monocytes CD14+*. Representative FACS analysis of γ-H2AX dot plots of the different studied groups (40 frail, 13 pre-frail, 32 non-frail, 46 young). Histograms represent the percentage of cells positive for DNA damage (γ-H2AX) in the different groups. SSC: Side scatter. Data expressed as means ± SEM. *p<0.05

Figure 2. *Mean fluorescence intensity (MFI) of DNA damage in PBMC isolated by Ficoll-Paque and in the respective cell subpopulations: cHPSC CD34+/CD3-/CD14-, T lymphocytes CD3+, monocytes CD14+*. Histograms represent the averaged median values of MFI in the different study groups (40 frail, 13 pre-frail, 32 non-frail, 46 young). Data expressed as means ± SEM. *p < 0.05.

Figure 3. *Representation of oxidative stress evaluated in plasma:* A) Level of 7KC (left) and 7βOHC (right) in 17 frail, 9 pre-frail, 18 non-frail, 10 young samples. B) Level of 8-OHdG in 10 frail, 9 pre-frail, 10 non-frail, 10 young samples. * p<0.01. Data expressed as means±SD.

Figure 1

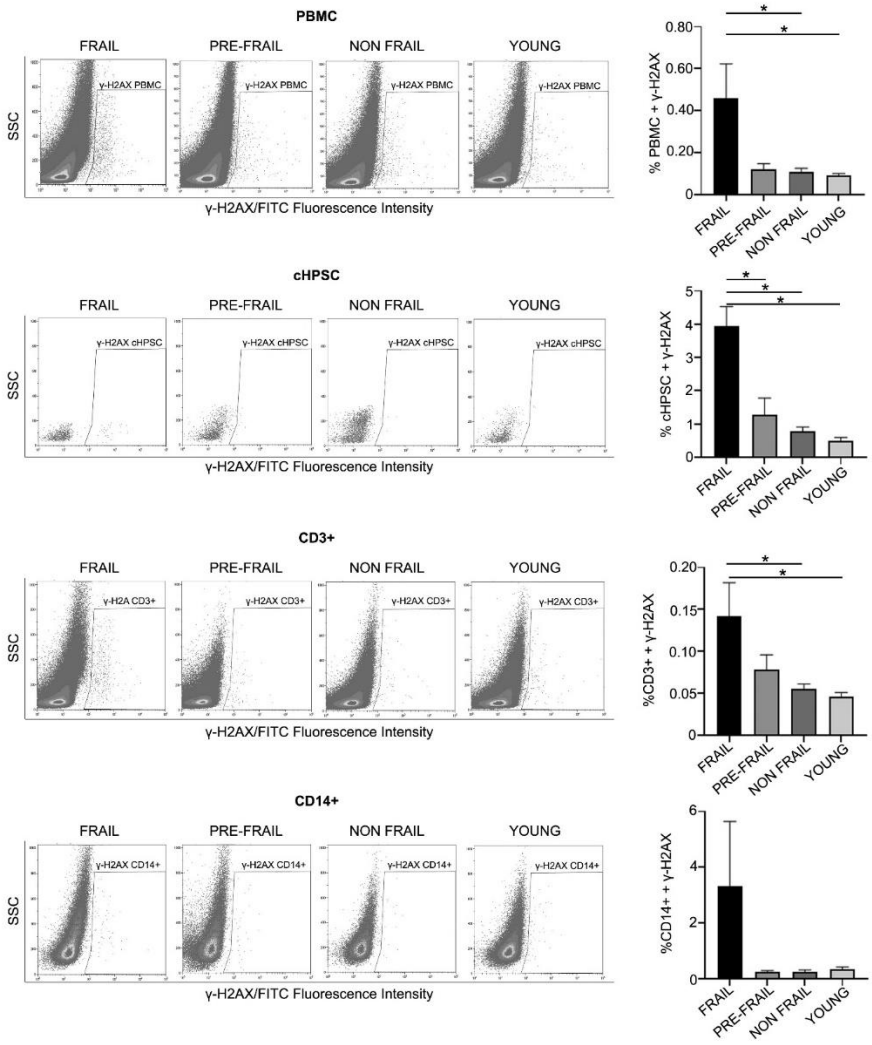
PBMC
FRAIL
PRE-FRAIL
NON FRAIL
YOUNG
γ-H2AX PBMC
SSC
γ-H2AX/FITC Fluorescence Intensity
% PBMC + γ-H2AX
cHPSC
γ-H2AX cHPSC
% cHPSC + γ-H2AX
CD3+
γ-H2A CD3+
γ-H2AX CD3+
%CD3+ + γ-H2AX
CD14+
γ-H2AX CD14+
%CD14+ + γ-H2AX

Figure 2

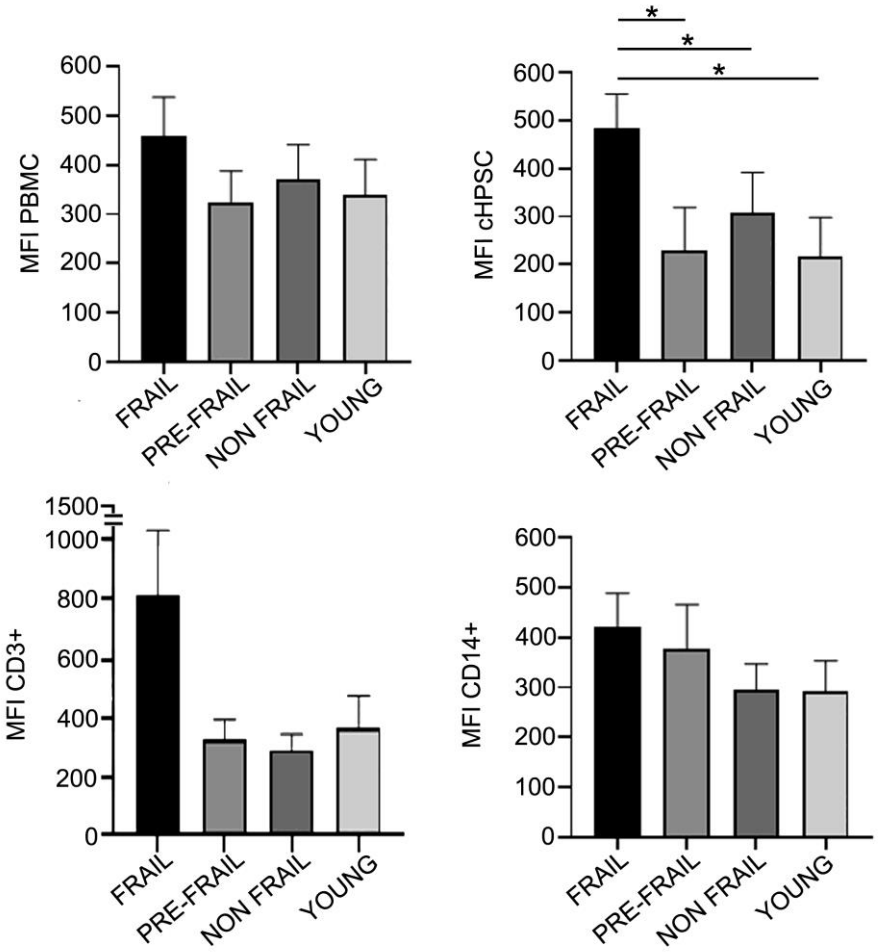
MFI PBMC
600
500
400
300
200
100
0
FRAIL
PRE-FRAIL
NON FRAIL
YOUNG
MFI cHPSC
*
*
*
MFI CD3+
1500
1000
800
600
400
200
MFI CD14+

Figure 3

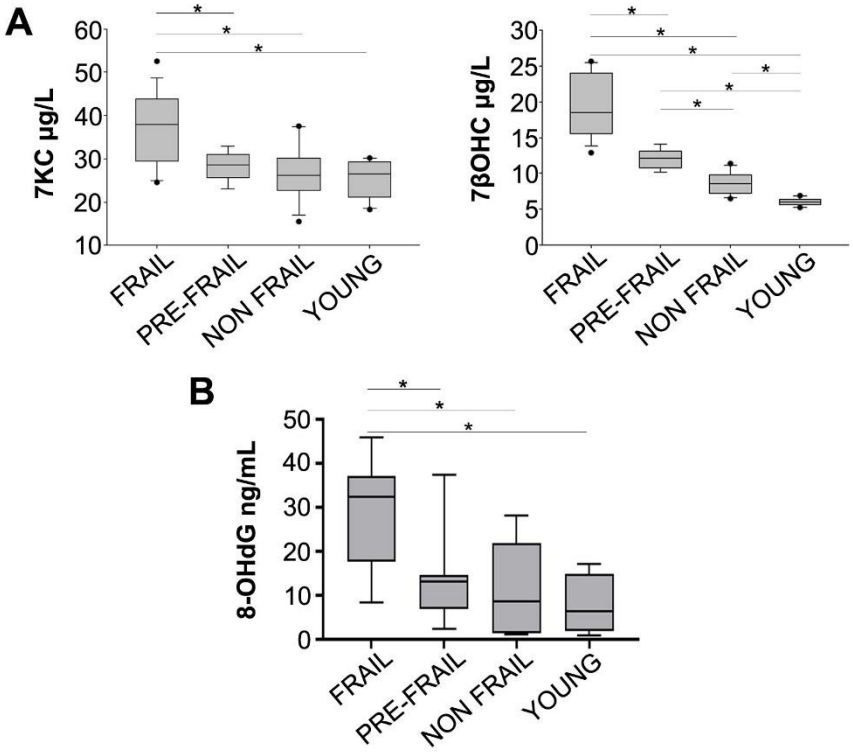
A
7KC µg/L
60
50
40
30
20
10
FRAIL
PRE-FRAIL
NON FRAIL
YOUNG
7βOHC µg/L
30
25
20
15
10
5
0
FRAIL
PRE-FRAIL
NON FRAIL
YOUNG
B
8-OHdG ng/mL
50
40
30
20
10
0
FRAIL
PRE-FRAIL
NON FRAIL
YOUNG

Supplementary Table 1. Hematological parameters of fresh blood collected in the study groups of Table 1 according to the frail, pre-frail, non-frail status and in a group of 46 young.

	Frail	**Pre-frail**	**Non-frail**	**Young**	**p value** [a]	**p value** [b]	**p value** [c]
Hemoglobin g/dL [d e]	11.1 ± 1.6	12.9 ± 1.3	14.1 ± 1.0	14.7±1.3	<.004	<.001	<.005
White blood cells, n/µl [d]	6919± 2002	6440± 2309	6350± 1213	5901± 1282	NS	NS	NS
Lymphocytes count, n/µl [f] (%)	1654 ± 658 (24,0±12.0)	1898 ± 696 (29.5±12.4)	2314 ± 508 (35.7±5.3)	1908±536 (32.5±6.6)	<.002	NS	NS
Granulocytes % Neutrophils Eosinophils' Basophils	58,6±15,5 3,2±2,7 0,6±0,5	58,4±12,6 3,3±1,1 0,8±0,7	52.6±7.1 3.1±1.2 0,5±0,4	55,0±6,4 2,9±1,6 0,8±0,3	NS	NS	NS
Monocytes %	10,2±6,5	8,3±2,1	7.8±1.6	8,8±1,9	NS	NS	NS
cHPSC Lin1-/CD45+ /CD34+ % on PBMC of fresh blood[§]	0,040±0,01	N.A	0,071±0,06	0,062±0,03		NS	

Notes. Values are expressed as mean + standard deviation. Significant differences in the comparison with young subjects are shown when positive.

[a] comparison between pre-frail vs. frail.

[b] comparison between non-frail vs. frail.

[c] comparison between non-frail vs. prefrail

[d] comparison between frail vs. young. *p < 0.05

[e] comparison between pre-frail vs. young. *p < 0.05

[f] comparison between non-frail vs. young. *p < 0.05

[§]Data obtained in randomly chosen frail (5 samples), non-frail (4 samples), young (5 samples).

N.A., not available

Supplementary Table 2. *Description of chronic diseases and classes of drugs in the study groups of Table 1 according to the frail, pre-frail, non-frail status.*

	Frail	**Pre-frail**	**Non-frail**
Chronic diseases. n (%)			
Hypertension	30 (70)	10 (76.9)	19 (59.4)
Diabetes mellitus	16 (40)	2 (15.4)	1 (3.1)
Dyslipidemia	12 (30)	3 (23.1)	12 (37.5)
Ischemic heart disease	11 (27.5)	2 (15.4)	3 (9.4)
Cerebrovascular disease	10 (25)	1 (7.7)	0 (0.0)
Renal insufficiency	10 (25)	2 (15.4)	1 (3.1)
Heart failure	8 (20)	1 (7.7)	0 (0.0)
Obstructive respiratory disease	8 (20)	1 (7.7)	0 (0.0)
Peripheral vascular disease	8 (20)	0 (0.0)	3 (9.4)
Epilepsy	3 (7.5)	0 (0.0)	1 (3.1)
Solid tumor	3 (7.5)	1 (7.7)	0 (0.0)
Rheumatic disease	3 (7.5)	2 (15.4)	0 (0.0)
Gastrointestinal disease	2 (5)	2 (15.4)	2 (6.3)
Asthma	1 (2.5)	0 (0.0)	2 (6.3)
Leukemia	1 (2.5)	0 (0.0)	0 (0.0)
Classes of drugs. n (%)			
Antihypertensives	33 (82.5)	11 (84.6)	21 (65.6)
Proton-pump inhibitors	24 (60.0)	6 (46.2)	7 (21.9)
Oral antidiabetic agents	12 (30)	2 (15.4)	1 (3.1)

Statins	12 (30)	6 (46.2)	11 (34.4)
Folic acid supplements	10 (25)	1 (7.7)	1 (3.1)
Antiepileptic drugs	3 (7.5)	0 (0.0)	1 (3.1)
Vitamin D supplements	7 (17.5)	0 (0.0)	0 (0.0)
Calcium supplements	5 (12.5)	1 (7.7)	0 (0.0)
Bisphosphonates	1 (2.5)	0 (0.0)	0 (0.0)
Antiarrhythmics	11 (27.5)	4 (30.8)	1 (3.1)
Oral anticoagulants	15 (37.5)	1 (7.7)	2 (6.3)
Antiplatelet agents	19 (47.5)	4 (30.8)	5 (156)
Benzodiazepines	7 (17.5)	0 (0.0)	2 (6.3)
Antipsychotics	6 (15)	1 (7.7)	0 (0.0)
Opioids	3 (7.5)	0 (0.0)	0 (0.0)
Non steroidal anti-inflammatory drugs	0 (0.0)	1 (7.7)	0 (0.0)
Corticosteroids	6 (15)	1 (7.7)	1 (3.1)
Drugs for the genitourinary system	8 (20)	2 (15.4)	3 (9.4)
Antidepressants	5 (12.5)	0 (0.0)	3 (9.4)
Respiratory medications	7 (17.5)	2 (15.4)	2 (6.3)

Supplemental figure legends

Supplementary Figure 1. Gating strategy of flow cytometry for the analysis of PBMC isolated by Ficoll-Paque sedimentation and the respective CD31+, CD14+ and CD34+/CD3-/CD14- cell subpopulations. γ -H2AX positive cells are also indicated. CD3 indicate the T lymphocytes, CD14 the monocytes and CD34 the cHPSCs within CD3-/CD14- cells. γ -H2AX was evaluated as a marker of DNA damage. SSC: side scatter. FSC: forward scatter.

Supplementary Figure 2. Gating strategy of flow cytometry for the analysis of cHPSC CD45+/Lin1-/CD34+in mononucleated cells (PBMC) of fresh whole blood. SSC: side scatter. FSC: forward scatter.

Supplementary Figure 3. Receiver-operating characteristics (ROC) curve. Evaluation of the comparison of percentage of DNA damaged cHPSC of 40 frail versus 32 non-frail subjects (left) and versus 13 pre-frail subjects (right). The area under the curve (AUC) and the 95% confidence interval (CI) are reported.

Supplementary Figure 1

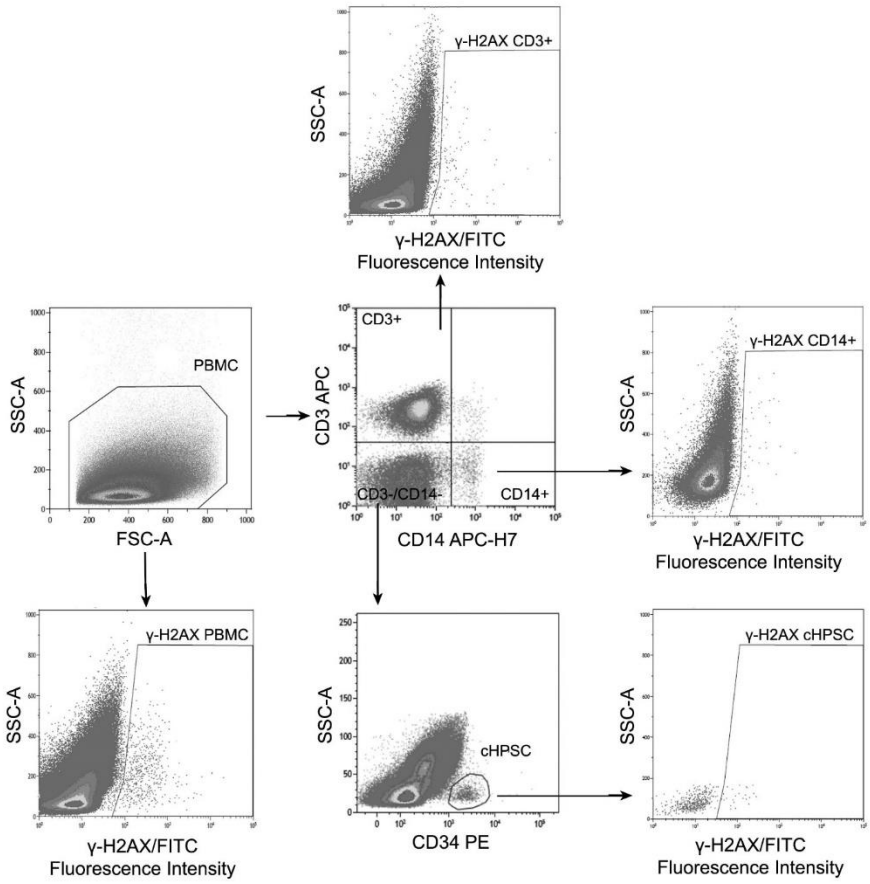

Supplementary Figure 2

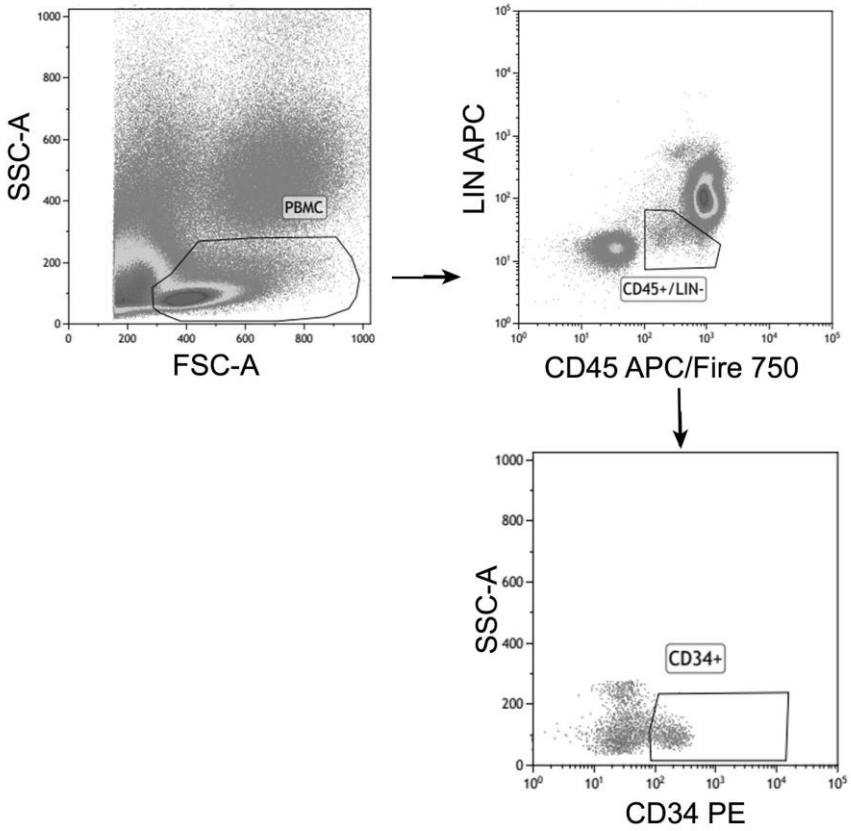

Supplementary Figure 3

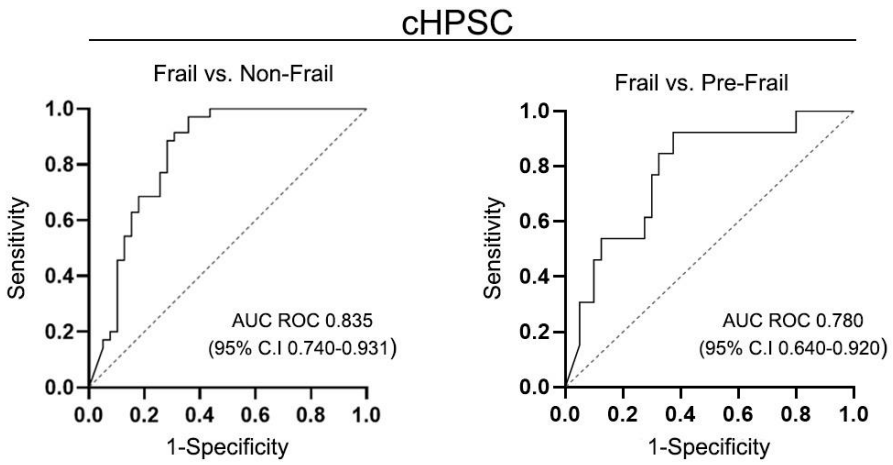

References

1. E Dent, F C Martin, H Bergman, J Woo, R Romero-Ortuno, J D Walston. Management of frailty: opportunities, challenges, and future directions. *Lancet*. 2019; 394: 1376–86. doi: 10.1016/S0140-6736(19)31785-4.

2. Vermeiren S, Vella-Azzopardi R, Beckwee D, et al. Frailty and the prediction of negative health outcomes: a meta-analysis. *J Am Med Dir Assoc*. 2016; 17: 1163.e1–17. doi:10.1016/j.jamda.2016.09.010.

3. Lang PO, Michel JP, Zekry D. Frailty syndrome: a transitional state in a dynamic process. *Gerontology*. 2009; 55(5): 539-49. doi: 10.1159/000211949.

4. Fried LP, Tangen CM, Walston J et al. Frailty in older adults: Evidence for a phenotype. *The Journals of Gerontology: Series A*. 2001; 56(3): M146–M157. doi: 10.1093/gerona/56.3.m146.

5. Collerton J, Martin-Ruiz C, Davies K et al. Frailty and the role of inflammation, immunosenescence and cellular ageing in the very old: cross-sectional findings from the Newcastle 85+ Study. *Mech Ageing Dev*. 2012; 133(6): 456-66. doi: 10.1016/j.mad.2012.05.005.

6. Mitnitski A, Collerton J, Martin-Ruiz C et al. Age-related frailty and its association with biological markers of ageing. *BMC Medicine*. 2015; 13: 161. doi: 10.1186/s12916-015-0400-x.

7. Sánchez-Flores M, Marcos-Pérez D, Costa S et al. Oxidative stress, genomic features and DNA repair in frail elderly: A systematic review. *Ageing Res Rev*. 2017; 37: 1-15. doi: 10.1016/j.arr.2017.05.001.

8. Dent E, Kowal P, Hoogendijk EO. Frailty measurement in research and clinical practice: A review. *Eur J Intern Med.* 2016; 31: 3-10. doi: 10.1016/j.ejim.2016.03.007.

9. Rattan SIS. Increased molecular damage and heterogeneity as the basis of aging. *Biol Chem*. 2008; 389(3): 267-72. doi 10.1515/BC.2008.030.

10. Siddiqui MS, Francois M, Fenech MF, Leifert WR. Persistent gammaH2AX: a promising molecular marker of DNA damage and aging. *Mutat Res Rev Mutat Res*. 2015; 766:1–19. doi: 10.1016/j.mrrev.2015.07.001.

11. Bouquet F, Muller C, Salles B. The loss of gammaH2AX signal is a marker of DNA double strand breaks repair only at low levels of DNA damage. *Cell Cycle*. 2006; 5(10):1116-22. doi: 10.4161/cc.5.10.2799.

12. Sedelnikova OA, Horikawa I, Zimonjic DB, Popescu NC, Bonner WM, Barrett JC. Senescing human cells and ageing mice accumulate DNA lesions with unrepairable double-strand breaks. *Nat Cell Biol*. 2004; 6(2): 168-70. doi: 10.1038/ncb1095.

13. Sedelnikova OA, Horikawa I, Redon C, et al. Delayed kinetics of DNA double-strand break processing in normal and pathological aging. *Aging Cell*. 2008; 7: 89–100. doi: 10.1111/j.1474-9726.2007.00354.

14. Sharma A, Singh K, Almasan A. Histone H2AX phosphorylation: a marker for DNA damage. *Methods Mol Biol*. 2012; 920:613-26. doi: 10.1007/978-1-61779-998-3_40.

15. Teixeira-Gomes A, Lage B, Esteves F et al. Frailty syndrome, biomarkers and environmental factors – A pilot study. *Toxicology Letters*. 2020; 330: 14–22. doi: 10.1016/j.toxlet.2020.04.023.

16. Valdiglesias V, Sánchez-Flores M, MSc, Marcos-Pérez D et al. Exploring genetic outcomes as frailty biomarkers. *J Gerontol A Biol Sci Med Sci*. 2019; 74(2): 168–175. doi: 10.1093/gerona/gly085.

17. Guralnik JM, Simonsick EM, Ferrucci L et al. A short physical performance battery assessing lower extremity function: association with self-reported disability and prediction of mortality and nursing home admission. *J Gerontol*. 1994; 49(2): M85-94. doi:10.1093/ geronj/49.2.m85.

18. Washburn RA, McAuley E, Katula J, Mihalko SL, Boileau RA. The physical activity scale for the elderly (PASE): evidence for validity. *J Clin Epidemiol*. 1999; 52(7):643-51. doi: 10.1016/s0895-4356(99)00049-9.

19. Cruz-Jentoft AJ, Bahat G, Bauer J et al. Sarcopenia: revised European consensus on definition and diagnosis. *Age and Ageing*. 2019; 48(1): 16-31. doi: 10.1093/ageing/afz046.

20. Kaiser MJ, Bauer JM, Ramsch C, et al. Validation of the Mini Nutritional Assessment short-form (MNA-SF): a practical tool for identification of nutritional status. *J Nutr Health Aging*. Nov 2009;13(9):782-8. doi: 10.1007/s12603-009-0214-7.

21. Folstein MF, Folstein SE, McHugh PR. "Mini-mental state". A practical method for grading the cognitive state of patients for the clinician. *J Psychiatr Res*. 1975; 12(3):1 89-98. doi: 10.1016/0022-3956(75)90026-6.

22. Mahoney FI, Barthel DW. Functional evaluation: the barthel index. *Md State Med J*. 1965; 14: 61-5.

23. Lawton MP, Brody EM. Assessment of older people: self-maintaining and instrumental activities of daily living. *Gerontologist*. 1969; 9(3): 179-86. doi.org/10.1093/geront/9.3_Part_1.179.

24. Charlson ME, Pompei P, Ales KL, MacKenzie CR. A new method of classifying prognostic comorbidity in longitudinal studies: development and validation. *J Chronic Dis*. 1987; 40(5):373-83. doi: 10.1016/0021-9681(87)90171-8.

25. Beaton LA, Marro L, Malone S et al. Investigating γ H2AX as a biomarker of radiosensitivity using flow cytometry methods. *ISRN Radiol*. 2013; 704659. doi: 10.5402/2013/704659.

26. Marcello A, Civra A, Bonotto R et al. The cholesterol metabolite 27-hydroxycholesterol inhibits SARS-CoV-2 and is markedly decreased in COVID-19 patients. *Redox Biology*. 2020; 36: 101682. doi: 10.1016/j.redox.2020.101682.

27. Brown AJ, Jessup W. Oxysterols: Sources, cellular storage and metabolism, and new insights into their roles in cholesterol homeostasis. *Mol Aspects Med*. 2009 Jun;30(3):111-22. doi: 10.1016/j.mam.2009.02.005.

28. Iuliano L. Pathways of cholesterol oxidation via non-enzymatic mechanisms. *Chem Phys Lipids*. 2011 Sep;164(6):457-68. doi: 10.1016/j.chemphyslip.2011.06.006.

29. Kulig W, Cwiklik L, Jurkiewicz P, Rog T, Vattulainen I. Cholesterol oxidation products and their biological importance. *Chem Phys Lipids*. 2016; 199: 144-160. doi: 10.1016/j.chemphyslip. 2016.03.001.

30. Diaz-De la Cruz EN, Cerillos-Gutiérrez JI, Garcìa-Sànchez A et al. The alteration of pro-inflammatory cytokines and oxidative stress markers at six-month post-living kidney donation. *Front Med*. 2020; 7: 382. doi: 10.3389/fmed.2020.00382.

31. Osorio FG, Rosendahl Huber A, Oka R, et al. Somatic mutations reveal lineage relationships and age-related mutagenesis in human hematopoiesis. *Cell Rep*. 2018; 25(9): 2308-2316. doi: 10.1016/j.celrep.2018.11.014.

32. Moehrle BM, Geiger H. Aging of hematopoietic stem cells: DNA damage and mutations? *Exp Hematol*. 2016; 44(10): 895-901. doi: 10.1016/j.exphem.2016.06.253.

33. Di Rosa F. Two niches in the bone marrow: a hypothesis on life-long T cell memory. *Trends Immunol.* (2016) 37:503–12. doi: 10.1016/j.it.2016.05.004.

34. Patel AA, Zhang Y, Fullerton JN et al. The fate and lifespan of human monocyte subsets in steady state and systemic inflammation. *J Exp Med*. 2017; 214(7): 1913–1923. doi: 10.1084/jem.20170355.

35. Yona, S, Kim KW, Wolf Y et al. Fate mapping reveals origins and dynamics of monocytes and tissue macrophages under homeostasis. *Immunity*. 2013; 38:79–91. doi: 10.1016/j.immuni.2012.12.001.

36. Lopez-Otin C, Blasco MA, Partridge L, Serrano M, Kroemer G. The hallmarks of aging. *Cell*. 2013; 153(6): 1194-1217. doi:10.1016/j.cell. 2013.05.039.

37. Park Y, Gerson ST. DNA repair defects in stem cell function and aging. *Annu Rev Med*. 2005; 56: 495-508. doi: 10.1146/annurev. med.56.082103.104546.

38. Pang WW, Price EA, Sahoo D, et al. Human bone marrow hematopoietic stem cells are increased in frequency and myeloid-biased with age. *Proc Natl Acad Sci U S A*. 2011;108(50):20012-20017). doi: 10.1073/pnas.1116110108.

39. Verovskaya EV, Dellorusso PV, Passegué E. Losing sense of self and surroundings: hematopoietic stem cell aging and leukemic transformation. *Trends Mol Med*. 2019;25(6):494-515. doi: 10.1016/j.molmed.2019.04.006.

40. Bigarella CL, Liang R, Ghaffari S. Stem cells and the impact of ROS signaling. *Development*. 2014;141(22):4206-4218. doi: 10.1242/dev.107086.

41. Flach J, Bakker ST, Mohrin M et al. Replication stress is a potent driver of functional decline in ageing haematopoietic stem cells. *Nature*. 2014, 512, 198-202. doi: 10.1038/nature13619.

42. Mani C, Reddy PH, Palle K. DNA repair fidelity in stem cell maintenance, health, and disease. *Biochim Biophys Acta Mol Basis Dis*. 2020; 1866(4): 165444. doi: 10.1016/j.bbadis.2019.03.017.

43. Rossi JD, Bryder D, Nussenzweig A, Nussenzweig A, Hoeijmakers J, Weissman IL. Deficiencies in DNA damage repair limit the function of haematopoietic stem cells with age. *Nature*. 2007; 447(7145):725-9. doi: 10.1038/nature05862.

44. Rockwood K, Howlett S E. Age-related deficit accumulation and the diseases of ageing. *Mechanisms of Ageing and Development*. 2019; 180: 107–116. doi: 10.1016/j.mad.2019.04.005.

Chapter 4

Biological conditions related to frailty and their effects on adult renal stem cells cultured as nephrospheres

Chiara Grasselli[1] et al.

[1]School of Medicine and Surgery, Milano-Bicocca University, Via Cadore 48, 20900 Monza, Italy

Funding: This research was supported by Fondazione Cariplo Milano (Italy) by the grant 2017-0577 to RAP.

Manuscript in preparation

Abstract

Frailty, an age-related syndrome closely associated with increased vulnerability to physical stressors and with multiple physiological system impairment, is common in patients with progressive decline of renal function. The aim of this study was to evaluate whether biological conditions related to frailty were able to modulate the renal stem cells (RSC) behavior giving information to clarify the high prevalence of chronic kidney dysfunction in frailty.

Nephrosphere (NS) cells, in which stem/progenitor cells are enriched, were treated with plasma of enrolled subjects (49 frail, 38 non-frail and 46 young). Only NS cells treated with plasma of frail subjects showed a significant decrease of self-renewal ability with significantly higher of both intracellular reactive oxygen species (ROS) and percentage of cells positive for DNA damage. The analysis of frail plasma, compared to non-frail and young plasma, showed a significant increase of the oxidative status and a characteristic inflammatory profile.

These results evidenced that the alterations found in the NS cells treated with frail plasma were due to the action of factors present in the frail plasma, raising the hypothesis concerning a possible role of biological mediators related to frailty in the modulation of stem/progenitor cell behavior.

The data obtained may shed light not only on the possible mechanisms that correlate frailty and kidney dysfunction but also on mechanisms that in frailty may involve overall the adult stem cell compartments. Therefore, this data might pave the way for the development of new therapeutic approaches to prevent or reduce frailty progression.

Introduction

Frailty is a multidimensional geriatric syndrome that can be associated to aging. It is defined as a state of increased vulnerability resulting from severe decline of several physiological systems, loss of homeostatic mechanisms and functional reserves. Frail persons have a reduced capacity to compensate for internal and external stressors. The WHO World Report on Ageing and Health [WHO, 2015] reported that frailty in community-dwelling older adults aged 65 or above ranges 17% and further increases considering the more advanced ages. The identification of frailty occurs through five criteria defined by Fried [Fried, 2001] based on reduced clinical and mechanical functions, so this can be possible only after the onset of clinical manifestations without the possibility of a precocious diagnosis.

A progressive decline of renal function is often present in frailty [Kojima, 2017] and it is associated in particular to chronic kidney diseases (CKD) [Shlipak, 2004]. Of note, elderly individuals with CKD are two to three times more likely to be frail than those with normal renal function and the prevalence of frailty is >60% in dialysis-dependent CKD patients. They often have a reduced energy intake that contributes to sarcopenia and a subsequent frailty [Kim, 2013], associated to progressive deterioration of kidney function [Carrero, 2013] and increased risk of early mortality [Wilhelm-Leen, 2009] In frail patients the risk of negative outcomes is proportional to the degrees of kidney dysfunction [Weiss, 2011; van Munster, 2016].

In this scenario, only few studies evaluating the relationship between frailty and its potential association with renal function are available. During aging, mitochondrial dysfunction, the alteration of the cell-cell

communication related to inflammatory mediators [Lopez-Otin, 2013] and the degenerative and functional changes in tissue-specific stem cells, and stem cell niches have been demonstrated to contribute to age-related decline [Tümpel, 2019]. Therefore, stem cell exhaustion may be considered as a hallmark of aging and in the context of renal aging stem cell exhaustion could play a role, though in human it has not been demonstrated yet.

In the current debate on frailty we want to raise the question on the relations among renal stem/progenitor cells, kidney dysfunction and frailty. Our study wants to evaluate the effects of biological conditions related to frailty, such as oxidative stress and the alteration of inflammatory mediators, on adult RSC behavior and understand whether they can modulate the renal stem/progenitor cell pool and their function. The data obtained may eventually open the way to novel methods for recognizing frailty syndrome and promoting future novel therapeutic approaches.

Materials and Methods

Study population

A group of 87 subjects (49 Frail and 38 Non-Frail) aged ≥ 65 years old were recruited from the Geriatrics Unit, San Gerardo Hospital ASST Monza. The exclusion criteria for the recruited subjects were a) illiteracy, b) psychiatric disorders, c) Parkinson's disease, d) cognitive function impairment, e) Multiple Sclerosis, f) neurodegenerative diseases, g) hip fracture or other severe trauma affecting mobility. The identification of frail phenotype in all 87 subjects was based on the five operative criteria discriminated by Fried et al. [Fried, 2001]: 1)

Unintentional weight loss over the last year (≥5%); 2) Fatigue in activity of daily living that was measured using the question "In this last month, do you have less energy to do the things of daily living you want?". This parameter was categorized as no exhaustion or yes exhaustion; 3) Reduction of the walking speed. Subjects are considered frail if they employ more than 7 seconds to cover a distance of 4 meters [Guralnik, 1994]; 4) Low physical activity. It was assessed using Physical Activity Scale for the Elderly (PASE) over one-week period. The PASE score combines information on leisure, household and occupational activity [Washburn, 1999]; 5) Reduction of muscle strength. Weakness was measured using the dynamometer handgrip strength for three consecutive times on dominant hand. The criterion is positive if the best value is less than cutoff value (<27 for males and <16 for females) [Cruz-Jentoft, 2019].

Regarding the frail phenotype, participants were considered frail if they fulfilled three or more criteria and non-frail with zero criteria scored.

Forty-six young subjects, aged between 25 and 35 years old, without functional disability, acute pathologies in progress or abuse of drugs, alcohol, smoke and with healthy life style, were recruited as control group.

The study was conducted according to the principles of the Declaration of Helsinki II and approved by the Ethics committee Brianza (Monza, Italy) code FRA-ARSC march 22nd, 2018. The sensitive information was anonymously available to the researchers. The participation in the study was voluntary, all subjects were fully informed on the aims of the study and nature of participation. Each participating subject signed the informed consent forms.

After recruitment, patients underwent a comprehensive geriatric assessment (CGA) including demographics (age and sex), life habits (smoking and alcohol consumption), and several tools to evaluate nutritional, cognitive, functional, and somatic health status. Nutritional status was evaluated using the Mini Nutritional Assessment-short form (MNA-sf) [Kaiser, 2009] and cognitive status using the Mini Mental State Examination (MMSE) [Folstein, 1975]. The functional status was assessed with the modified Barthel Index [Mahoney 1965], the Lawton and Brody's Instrumental Activity of Daily Living (IADL) [Lawton 1969] and the Short Physical Performance Battery (SPPB) [Guralnik, 1994]. Lastly, the somatic health status was assessed with the Charlson Comorbidity Index (CCI) [Charlson, 1987] and by determining the number of drugs taken at home (Table 1).

Plasma collection

Whole blood from frail, non-frail and young subjects was collected into BD Vacutainer CPT Cell Preparation Tubes with sodium heparin (Becton Dickinson, Franklin Lakes, NJ, USA). The plasma was separated by centrifugation at 1500 x g for 15 minutes using a Thermo Scientific SL 16R Centrifuge (Thermo Scientific, Waltham, MA, USA). Samples were then aliquoted and stored at -80 °C until analyses.

Tissues

Normal kidney tissue was obtained from 12 neoplastic patients (5 males, 7 females; median age 68 years; age range between 49-82 years) after nephrectomy for renal cell carcinoma (RCC). Normal kidney tissues were taken from the opposite side of the tumor and collected

only after exceeding the diagnostic needs. The procedures were approved (code FRA-ARSC march 22nd, 2018) by the institutional local Ethical Committee "Comitato Etico Azienda Ospedaliera San Gerardo" and patient informed consent was obtained. All procedures were performed in accordance with the Declaration of Helsinki, the relevant guidelines and regulations. Patients were anonymized. Nephrosphere (NS) cultures were established from fresh renal tissue samples.

Nephrosphere cultures

The renal single-cell suspension obtained after enzymatic and mechanical dissociation of the 12 different renal tissues and 24- to 48-hours adhesion step [Bianchi, 2010] were cultured as NS as described in Bombelli et al [Bombelli, 2013]. NS cultures grew as low cell density (10.000 cells/mL) in non-adherent conditions in dishes coated with poly-Hema (Sigma-Aldrich, St.Louis, MO, USA). To evaluate the effect of plasma on NS cell behavior, 10% of plasma from the recruited subjects was added to the culture medium. Floating NS were collected, after 10–12 days, and dissociated enzymatically for 5 min with TrypLE Express (Life Technologies,Waltham, MA, USA) first, and then mechanically by repetitive pipette syringing to generate a single cell suspension for further experiments [Bombelli, 2013].

Immunofluorescence

Immunofluorescence staining of cells obtained after dissociation of floating NS cells was performed on a cytospinned preparation. The slides were prepared spinning 20,000 cells at 800 x g for 15 minutes on Heraeus Multifuge 3S+ Centrifuge (Thermo Scientific, Waltham, MA,

USA), cytospinned cells were fixed in freshly buffered 4% paraformaldehyde for 20 minutes. After blocking with phosphate-buffered saline (PBS) containing 0.1% bovine serum albumin (Sigma-Aldrich), 0.3% Triton X-100 (Sigma-Aldrich) and 0.1% Saponin (Sigma-Aldrich, St.Louis, MO, USA), cells were incubated overnight at 4°C with Anti-phospho-Histone H2A.X (Ser139) (Clone JBW301; Millipore, Burlington, MA, USA; 1:100) primary antibody. After rinsing in phosphate-buffered saline (PBS), cells were incubated for one hour at room temperature (RT) with Alexa Fluor 488 conjugated anti-rabbit IgG secondary antibody (Molecular Probes Invitrogen, Waltham, MA; 1:100).

The slides were mounted with ProLong Gold Antifade with DAPI (Molecular Probes Invitrogen) for nuclear counterstain. Micrographs were taken using a Zeiss LSM710 confocal microscope equipped with Zen software version 2009 (Zeiss, Oberkochen, Germany). Percentages of labeled cells over the total nuclei (n = 10 different fields for each sample; three independent cultures), number of foci per nucleus and fluorescence intensity of foci per nucleus were evaluated. Data are reported as the average of three independent experiments ± the standard error of the mean (SEM). Number and fluorescence intensity of foci per nucleus were performed with using Count Nuclear Foci Plugin-ImageJ software version 1.53c (National Institutes of Heath, NIH, Bethesda, MD; http://imagej.nih.gov/ij).

Flow cytometry analysis

Cells obtained after NS dissociation were stained with FITC Annexin V Apoptosis Detection Kit with Propidium Iodide (PI) (Biolegend, San

Diego, CA, USA) or subjected to phospho-Histone H2AX (Ser139) staining. For the latter, cells were resuspended in PBS with 5% FBS for 15 minutes at RT and then suspended and fixed with 4% Methanol free Formaldehyde (Thermo Fisher Scientific, Waltham, MA, USA) and permeabilized with 0.1% Triton X-100 (Sigma-Aldrich, St. Louis, MO, USA). After centrifugation, 70% cold methanol was added dropwise while vortexing the cellular pellet, then the samples were stored at -20°C for 24 hours. Successively, these samples were washed and stained at 4°C with FITC-conjugated anti-phospho-Histone H2AX (Ser139) (Clone JBW301; Millipore, Burlington, MA, USA; 2.5mg/mL) for 2 hours and with eFluor 660-conjugated anti-Human Ki-67 (Clone 20Raj1; Invitrogen, Waltham, MA; 1:200) for 30 minutes. The samples were then immediately analyzed with a MoFlo Astrios cell sorter equipped with Summit 6.3 software and data analyzed with Kaluza 2.1 software (Beckman Coulter, Miami, FL, USA).

Reactive oxygen species assay

Dissociated NS cells were resuspended in 300µL of warm stem cell medium [Bombelli, 2013] added with 10 µM 2',7'-dichlorofluorescin diacetate (DCFH-DA; Sigma-Aldrich, St. Louis, MO, USA) and incubated al 37°C for 30 minutes. Successively, sample was washed with 300µL of cold PBS. After centrifugation, 300µL of cold PBS was added, then the samples were acquired with a MoFlo Astrios cell sorter equipped with Summit 6.3 software at excitation and emission wavelengths of 485 and 528 nm, respectively and data were analyzed with Kaluza 2.1 software (Beckman Coulter, Miami, FL, USA).

Evaluation of oxidative stress in plasma samples

Oxysterols were analyzed in a set of randomly chosen samples as markers of oxidative stress. The 8-hydroxy-2-deoxy Guanosine (8-OHdG) was quantified as a marker of oxidative DNA damage.

Oxysterols were analyzed by isotope dilution mass spectrometry in serum collected from frail, non-frail and young individuals. 7β-hydroxycholesterol (7βOHC), 7-keto-cholesterol (7KC), 5α6α-epoxycholesterol (5α6αEC), 5β,6β-epoxycholsterol (5β,6βEC) and 3β,5α,6β-3OH-cholesterol (triol) (3β,5α,6β-3OHC), marker of cholesterol oxidation as results of oxidative stress and cholesterol autoxidation [Brown and Jessup, 1996; Kulig, 2016], lathosterol and lanosterol, marker of cholesterol synthesis, and 27-hydroxycholesterol (27-OHC) and 24S-hydroxycholesterol (24-OHC), marker of mitochondrial homeostasis, were quantified by isotope dilution mass spectrometry [Marcello, 2020].

The 8-hydroxy-2-deoxy Guanosine (8-OH-dG) was analyzed in duplicate by enzyme-linked immunosorbent assay (ab201734, 8-hydroxy-2-deoxy Guanosine ELISA kit, Abcam, Cambridge, UK), *according to manufacturer instructions,* in plasma collected from frail, non-frail and healthy young [Diaz-De la Cruz, 2020].

Cytokines

The concentration (pg/mL) of 40 cytokines (MCP-1, MIP-1a, MIP-1B, CCL7, Eotaxin, MDC, CD40, CD40 Ligand, CX3CL1, KC, IP-10, EGF, Flt-3Ligand, G-CSF, GM-CSF, IFN-ɣ, IL-1a, IL-1B, IL-2, IL-3, IL-4, IL-5, IL-6, IL-7, IL-8, IL-9, IL-10 , IL-12 p70, IL-13, IL-15, IL-17, TNF-β, PDGFAA, TGF-α ,TNF-α,VEGF, RANTES,

PDGF-BB, CXCL9, CXCL12) was evaluated in the plasma of recruited subjects using Human Magnetic Luminex Screening Assay (Service by Labospace s.r.l). All samples were tested in duplicate.

Statistical analysis

Statistical analysis was performed with Oneway ANOVA (with Tukey's test correction). An alpha of 0.05 was used as the cut off for statistical significance. Receiver operating characteristic (ROC) curve analysis were done using one-way analysis (Wilson-Brown method) and the results were reported as fraction. The GraphPad Prism program has been used (GraphPad Software, Inc., La Jolla, CA, USA).

Results

Study population

87 subjects, 49 frail (Male 21, Female 28; average age 83.7±6.2 years), 38 non-frail (Male 24, Female 14; average age 74.5±8.2), were recruited based on the phenotype criteria of Fried et al [Fried 2001]. Forty-six young subjects (M 17, F 29; age 29.9±2.9), without functional disability or acute pathologies in progress were recruited as control group. Age was found to be significantly different among aged groups ($p=0.001$), increasing in frail subjects, confirming the expected age-dependence of frailty syndrome. Female gender was prevalent in frail group, but the opposite occurred in the non-frail group.

For subjects a multi-domain clinical evaluation has been collected. An increase of frailty was correlated to smoking or former smoking subjects. The number of alcohol consumer was statistically higher in non-frail group compared with frail subjects. Other variables related to

multidimensional geriatric assessment were evaluated. There were significantly differences in the frail group respect to non-frail, in particular: Barthel Index, IADL autonomy, Short Physical Performance Battery (SPPB), Mini Nutritional Assessment (MNA), Mini Mental State Evaluation (MMSE), Polypharmacy, Physical Activity Scale for the Elderly, PASE. It is of note the Charlson Comorbidity Index, as a weighted index to predict risk of death within one year of hospitalization for patients with specific comorbid conditions that resulted significantly different among groups; CCI > 2 was present in frail only (Table 1). These data confirmed the correlation between frailty and comorbidity, highlighted by Rockwood [Rockwood, 2006]. Drug assumption was found to be common in frail patients probably due to comorbidity. The average of the classes of drugs in non-frail group is three time lower than in frail ones (2.3 ± 1.6 non-frail vs 7 ± 2.7 frail; $p < 0.001$) (Table 1). The comorbidity and multi-drug intake can account for the increase of oxidative stress, as said below, particularly in frail patients.

Effect of collected plasma on RSC behavior

To evaluate the effects of plasma obtained from the enrolled patients we treated RSC grown as NS from 12 normal renal tissues obtained from 12 different RCC patients with 10% plasma sample of 49 subjects (17 frail, 16 non-frail and 16 young controls). Each plasma was used to treat three different renal NS cultures (Table 2).

Ten days after treatment, we first characterized RSC self-renewal capacity by analyzing sphere forming efficiency (SFE), which is the number of obtained nephrospheres divided by the number of plated

renal cells, expressed as a percentage. Confocal microscopy images and the SFE graph (Figure1 A, B) showed that there were not SFE differences in the renal cells treated with plasma of young respect to untreated controls, while the cells treated with frail plasma had a significant SFE decrement respect to the cells treated with young plasma or untreated. The non-frail-treated cells had a significant SFE decrement intermediate between that of cells treated with frail or young plasma. The proliferation of NS cells treated with plasma of the different groups was analyzed by FACS evaluating the Ki76+ cells. No differences in the differently treated cells were observed (Figure 1 C). Even Annexin V/PI staining showed no differences in cell viability, early and late apoptosis and necrosis among the different plasma-treated or untreated NS cells (Figure1 D).

These data indicated that the decrease of self-renewal ability in cell treated with plasma of frail patients is not correlated to cell death or proliferation.

Frail plasma increases DNA damage in NS cells

Several studies have shown that the phosphorylation of histone H2AX at Serine 139 (γ-H2AX) is the earliest and abundant indicator of DNA double-strand breaks (DSB). We detect γ-H2AX both by immunofluorescence staining and flow cytometric analysis in dissociated NS cells after treatment with plasma of 17 frail, 16 non-frail, 16 young subjects.

By confocal microscopy analysis, we observed a statistically higher percentage of γ-H2AX positive NS cells in NS treated with plasma of frail patients compared to the other groups (Figure 2 A, B). We then

investigated the number of γ-H2AX foci per nucleus, corresponding to the number of DSB. In the nuclei of dissociated NS cells treated with plasma of frail subjects there was a statistically higher number of foci (Figure 2C). In nuclei of NS cells treated with plasma of non-frail, young and untreated the number of foci was considerably lower and similar to each other (Figure 2 C). Of note, the γ-H2AX fluorescence intensity per nucleus was also statistically increased after treatment with frail plasma compared to the other groups (Figure 2 D).

We also detected by FACS analysis the percentage of cells positive for γ-H2AX foci in dissociated NS cells and, consistently with confocal microscopy data, we observed a statistically higher percentage of NS cells with DNA damage in those treated with plasma of frail subjects compared to the other groups (Figure 2 E).

These data suggested that in NS cells there were an increase of DNA damage in response to eventual factors present in the plasma of frail patients.

Effect of frail plasma on ROS formation in NS cells.

Among the possible factors implicated in DNA damage we considered the oxidative stress. The fluorescent cell-permeable indicator 2',7'-dichlorofluorescin diacetate (DCFH-DA) was used for detecting intracellular ROS. DCFH-DA is deacetylated by cellular esterases to a non-fluorescent compound, which is later oxidized by ROS into fluorescent 2',7'-dichlorofluorescein (DCF). The intensity of the generated fluorescent signal correlates with the intracellular level of ROS. We investigated in five NS cell cultures whether intracellular

ROS content changed when treated with a set of different plasma of enrolled subjects (6 frail, 5 non-frail and 5 young).

By cytofluorimetric analysis we detected an increased DCF fluorescence intensity in cells treated with plasma of frail patients compared with cells treated with plasma of non-frail and young, and untreated. The phenomenon, though not significant, is documented in cells treated by frail plasma by the fluorescent peak that shifted respect to the peaks of cells treated with the other plasma (Figure 3).

These results support the hypothesis that frail plasma induces an accumulation of intracellular ROS. Since this accumulation is a characteristic response to environmental stimuli, the data obtained gave a strong indication to evaluate the components of plasma of our subjects.

Evaluation of ROS in plasma samples

We evaluated the oxidative status of our enrolled subjects analyzing a set of their plasma.

We observed significant increments of auto-oxidation oxysterols, 7-keto-cholesterol and 7β-hydroxycholesterol in the frail plasma with respect to non-frail, together with 5α6α-epoxycholesterol, 5β.6β epoxycholsterol and 3β.5α.6β-3OH-cholesterol (triol) in plasma of frail subjects (Figure 4 A), which were suggestive for an increased oxidative stress in frail compared to non-frail individuals.

In support, we observed a decrease both in the quantification of sterol precursors (lathosterol and lanosterol), markers of colesterol synthesis, and in the enzymatic product of cholesterol oxidation (27-

hydroxycholesterol and 24S-hydroxycholesterol) in plasma of frail patients compared to other groups (Figure 4 A).

To support these data, in a different set of plasma, we also evaluated 8-hydroxy-2-deoxy Guanosine, in which is produced by the oxidative damage of DNA by reactive oxygen species and serves as an additional marker of oxidative stress. We observed a significant increase of 8-OHdG in frail subjects compared with non-frail subjects (Figure 4 B).

DNA damage and reduced ability to self-renewal found in NS cells treated with plasma of frail subjects could be correlated with the increased oxidative stress in frailty. To support this hypothesis, we treated dissociated NS cells with different concentrations of hydrogen peroxide (H_2O_2) (0.1mM, 0.5mM and 1mM of H_2O_2) and we observed a statistically decrease of SFE (Supplementary figure 1 A) and simultaneously a higher amount of DNA damage increasing H_2O_2 concentration (Supplementary figure 1 B).

Cytokines evaluation on human plasma samples

Even the alteration of inflammatory mediators could play a role on the NS cells behavior. We thus evaluated 40 inflammatory cytokine levels in the human plasma samples of frail, non-frail and young enrolled subjects (Table 3). In this panel of cytokines, we paid attention to the ones more expressed in aged subjects, especially in frail patients. About interleukins, IL-1α, IL-6 and IL-8 were significantly higher in frail group than in non-frail and young groups. Similarly, there was a significant increase of CX3CL1, CD40 and CXCL9 in frail subjects compared to the others (Figure 5 A).

Interestingly, some cytokines were only expressed in frail patients, such as TNF-β, IL- 1β, IL-2, IL-15 and IL-17 (Figure 5 B). IL-10 and TNF-α were expressed in elderly subjects, both frail and non-frail, but not in young controls. Most of the cytokines studied showed a trend of expression that increased in frail group and decreased both in non-frail and young groups, though not significantly, or only in young subjects (CXCL10, FLT3 LIGAND, GM-CSF, TGF-α, CCL3, IL-4, IL-7, IL-12p70, VEGF, CCL2, CCL22, CXCL1 and CXCL12) (Supplementary figure 2 A). Some cytokines are more abundant, though not significant, in the plasma of non-frail (IL-9, CCL11, CCL4, IL-13 and IFN-γ) (Supplementary figure 2 B) and young (IL-5, RANTES, PDGF-BB, PDGF-AA, EGF and CD40 LIGAND) groups (Supplementary figure 2 C).

The ROC curve was performed to evaluate how well the statistically higher inflammatory cytokines can discriminate frail from non-frail plasma. Thus, ROC curve analysis assessing the concentration of CX3CL1, CD40, IL-1α, IL-6, IL-8 and CXCL9 in our non-frail and frail subjects.

The values of the area under the ROC curve (AUC) for all the cytokines evaluated was summarized in Figure 6.

The AUC includedbetween 0.7 and 0.9 (Figure 6) indicating a good discriminating power of the concentration of cytokines to potentially discriminate between frail and non-frail plasma using the standard 95% confidence interval criteria.

These results suggest that cytokines present exclusively in the plasma of frail patients could play a role in the alteration of stem characteristics of NS cells.

Indeed, our preliminary analysis showed that the 6 cytokines significantly more abundant in frail plasma and the 5 cytokines present exclusively correlated with the highest oxidative status in the plasma and with a significant increase of DNA damage and a decrease of SFE in NS cells treated with the same frail plasma.

Discussion

Frailty syndrome is a state of increased vulnerability, closely linked to advanced age and simultaneously a controversial aspect of aging, given its ability to be reversible at the early stage [Tarazona-Santabalbina, 2016; Travers, 2019]. As reported in literature, our population of frail subjects showed a higher prevalence of comorbidity, documented by the higher CCI, high multi-drug intake, an increment of frailty with age and in females.

In our population, we tested whether in the organism of aged and frail people there were biological conditions able to change the renal stem/progenitor cells (RSC) behavior that could explain the frequent kidney dysfunction in the frail status. The SFE, which evaluates the self-renewal ability of cells that give rise to NS, was reduced after the treatment of NS cells with plasma of our frail patients, without modification of their cell viability and proliferation.

This suggested that the decrement of self-renewal ability, in NS cells treated with frail plasma, was an important response to environmental stimuli. This hypothesis was supported by the high level of the oxidative status found in the plasma of frail patients, documented by the oxysterol analysis, which suggested that cholesterol homeostasis was disturbed in frail patients following an increase in ROS. In addition,

the significant increase of 8-OHdG, marker of oxidative DNA damage, in frail plasma suggested that the eventual DNA damage in frail subjects may have an oxidative origin as we previously evidenced in circulating hematopoietic stem cells (Chapter 3, submitted manuscript).

Therefore, we can argue that the DNA damage and the decrement of SFE found in NS cells treated with plasma of frail subjects could be correlated with the increased oxidative activity of frail plasma.

Likely, this DNA damage may provoke an impairment of RSC functions, as it is often hypothesized in literature for the DNA damaged cells of others stem cell compartments [Behrens, 2014]. The reduction of self-renewal seen in NS cells treated by frail plasma may be a confirmation of this. The treatment of NS with H_2O_2 confirmed the correlation between oxidative stress, the increment of DNA damage and the reduction of SFE. In addition, we also observed an increment of intracellular ROS in NS cells treated with frail plasma. All these data let us suppose that the main alterations found in the NS cells treated with frail plasma (SFE reduction and DNA damage increment) were due to the action of factors present in the frail plasma, which had the characteristics of a high oxidative status. Interestingly, these factors were also able to increment the intracellular ROS.

Our analysis of inflammatory mediators in plasma of frail patients compared to others evidenced a peculiar cytokine profile in frail patients, in which 6 cytokines are significantly higher (IL-6, IL-8, IL-1α, IL-15, CD40, TNFβ and CX3CL1) and 5 are exclusively present (TNF-β, IL- 1β, IL-2, IL-15 and IL-17) in frails.

Preliminary analysis showed that the plasma of frail subjects with the highest levels of oxidative stress also had the cytokine profile in which

some of the 11 cytokines, mentioned above, were present. These frail plasmas were those also able to induce the highest increase of DNA damage and the significant decrease of SFE in the treated NS cells. Of note, the same frail subjects from which the plasma was collected also showed a significant increase of DNA damage in their circulating hematopoietic progenitor stem cells (cHPSC) [Grasselli et al. Submitted, Chapter 3].

The literature data report that the cytokines IL-6, TNF-β, IL- 1β, CX3CL1, IL-17 interacting with the respective receptors on different cell types are able to elicit the intracellular ROS formation [Lo, 1998; Hwang, 2004; Forcina, 2019; Dhillon, 2012; Liu, 2015; Park, 2012]. At least one or a combination of these cytokines were present in our frail plasma with the higher capacity to induce DNA damage in NS cells. This is an important aspect because it shows that the same biological situation related to frailty, the oxidative status and the intracellular ROS production, might affect every cell type including the stem cell compartment, determining DNA damage and an overall impairment in several tissues and organs.

In conclusion, we evidenced that there is a combination of oxidative stress and pro-inflammatory cytokines in plasma of frail patients that contribute to an increase of intracellular ROS and DNA damage, inducing the alteration of stem characteristics of NS cells.

This research, showing on allogenic renal stem/progenitor cells the capacity of frail plasma to damage DNA, which correlate with findings obtained on homologous cHSPC of the frail plasma donors (see Chapter 3), supported the hypothesis that in frail patients different

stem/progenitor cell compartments may be affected and induced to exhaustion.

This study can also pave the way to better understand how the organ homeostasis, in particular kidney, can be controlled acting on oxidative stress and inflammatory profile or removing damaged cells, allowing the attenuation of frailty progression with the development of new drug therapies.

Table 1. *Comprehensive Geriatric Assessment of 87 subjects, according to the operational definition of frailty [Fried et al].*

Characteristics	**Frail (n=49)**	**Non-frail (n=38)**	**p-value**
Age. Years	83.7± 6.2	74.5 ± 8.2	<.001
Females. n (%)	28 (57.1)	14 (36.8)	.090
Smoke. n (%)			
Current smoker	3 (6.1)	1 (2.6)	.397
Past smoker	12 (24.5)	7 (18.4)	
Alcohol. n (%)			
Moderate consumption	12 (24.5)	19 (50)	.014
Consumption of >1 unit (males) or >½ unit (females)	2 (4.1)	-	
History of allergies. n (%)	4 (8.2)	3 (7.9)	.868
Mini nutritional assessment - short form. Median (IQR)	11 (22.4)	14 (1)	<.001
Mini-Mental State Examination. median (IQR)	26 (53.1)	30 (2)	<.001

Modified Barthel Index. Median (IQR)	65 (30)	100 (0)	<.001
Instrumental Activities of Daily Living. Median (IQR)	4 (2)	7 (2)	<.001
Short Physical Performance Battery. Median (IQR)	5 (3)	12 (2)	<.001
Number of drugs. median (IQR)	7 (4)	3 (2.5)	<.001
Charlson Comorbidity Index. median (IQR)	2 (3)	0 (1)	<.001
Average of drug intake	7 ± 2.7	2.3 ± 1.6	<.001

Values are expressed as mean ± standard deviation unless otherwise specified. IQR = interquartile range.

p-value: comparison between frail vs. non-frail.

Table 2. *Different normal renal tissue cultures treated with plasma of frail and non-frail subjects and young controls.*

NS Tissue culture	Sex	Age	Number of plasma samples tested on NS cultures		
			Frail	Non-Frail	Young
C298	M	73	5	3	4
C299	F	66			
C300	F	50			
C302	M	71	4	5	5
C305	F	78			
C306	F	69			
C308	M	76	5	5	5
C309	F	82			
C299	F	66			
C311	M	49	3	3	2
C312	M	74			
C288	F	63			

Table 3. *Baseline inflammatory biomarker profile.*

Inflammatory Biomarkers (pg/mL)	**Frail (n=38)**	**Non-frail (n=37)**	**Young (n=37)**	**p-value [a]**	**p-value[b]**	**p-value[c]**
RANTES	19627± 2683.5	30606± 3017.5	46648.1± 9933.6	ns	<.005	ns
PDGF-BB	1997.6± 286.5	2318± 266.8	2915.66± 546.6	ns	ns	ns
CCL11	646.4± 89.9	773.1± 82.8	448± 51.5	ns	ns	<.005
CCL22	589.8± 114.7	536± 42.1	545.1± 34.5	ns	ns	ns
CX3CL1	1718.8± 220,4	989.2± 100.1	1225.2± 211.6	<.001	<.005	ns
CXCL1	210.28± 78,8	108.7± 7.2	165.9± 51.3	ns	ns	ns
CXCL10	150.2± 19,9	117.3± 17.6	56.6± 4.5	ns	<.001	<.001
EGF	36.3± 7.5	35.3± 5.1	57± 19.1	ns	ns	ns
FLT-3 LIGAND	94.5± 8.9	100.6± 3.7	71.8± 3.2	ns	<.005	<.005
G-CSF	77.8± 8.6	96.9± 17.9	56.9± 7.0	ns	ns	ns
GM-CSF	51.6± 8.5	43.1± 9.5	16.6± 2.2	ns	<.005	ns
TNF-β	134.5± 125.7	0	0	ns	ns	ns

PDGF-AA	594.1± 82.2	748.4± 76.3	737.5± 106.5	ns	ns	ns
TGF-α	7.8± 0.7	6.7±0.7	7.1±0.9	ns	<.005	ns
VEGF	41.1±5	37.4±3.9	29±3.5	ns	ns	ns
CCL2	518.4± 35.5	391.8± 26.7	255± 17.8	ns	ns	ns
CCL3	333.8± 39.7	284.7± 28.8	257.1± 49	ns	<.005	ns
CCL4	303.6± 42.7	718.5± 410.3	203.3± 49.6	ns	ns	ns
CCL7	96.6± 25.3	97.4± 16.6	201.8± 52.3	ns	ns	ns
CD40	868.2± 164.2	419.6± 34.2	302.9± 26.7	<.001	<.001	ns
CD40 LIGAND	1255.2± 213.5	1293.9± 180	1446.1± 367.8	ns	ns	ns
IFN-γ	63.9± 25.1	85.09±0	58.16± 0.9	ns	ns	ns
IL-1α	18.8± 4.5	9.7± 3.9	8.1± 2.6	<.005	<.005	ns
IL-1β	28.8±1	0	0	ns	ns	ns
IL-2	94.2±8	0	0	ns	ns	ns
IL-3	0	0	0	ns	ns	ns
IL-4	81.8± 11.6	52.1± 8	56.2± 6.5	ns	<.001	ns
IL-5	0	0	8.94±1.8	ns	ns	ns
IL-6	21.64± 7.6	70.06± 3.0	4.33± 0.1	<.001	<.001	ns
IL-7	7.923± 0.8	5.43± 0.5	6.24± 1.1	ns	ns	ns

IL-8	18.9± 3.6	11.4± 2.3	5.5± 0.6	<.001	<.001	ns
IL-9	0	151.7±0	0	ns	ns	ns
IL-10	77.4± 72.8	125.4± 96.4	0	ns	ns	ns
IL-12p	1098.2± 0	133.2± 0.5	317.21± 0	ns	ns	ns
IL-13	335.4± 34.6	2141.9± 210.7	403.7± 76.8	ns	ns	ns
IL-15	5.8± 1	0	0	<.005	<.005	ns
IL-17	149.8± 137.3	0	0	ns	ns	ns
TNF-α	21±12.7	6.4±0.2	0	ns	ns	ns
CXCL12	968.8± 204.8	785.4± 37.4	786± 60.1	ns	ns	ns
CXCL9	588.8± 126.5	518.3± 136.9	507.8± 0	<.005	<.005	ns

Values are expressed as mean of sample concentrations (pg/mL) within range where standards recovery is 70-130% ± SEM.

[a] comparison between frail vs. non-frail.

[b] comparison between frail vs. young.

[c] comparison between non-frail vs. young.

Ns: not significant.

Figure legends

Figure 1. *Plasma-mediated effects on NS cell behavior.* (A) Phase contrast images of renal cells grown as NS untreated (Ctrl) or treated for 10 days with plasma of frail, non-frail and young subjects. Scale bar: 100μm. (B) SFE data of renal cells treated with plasma of studied groups (17 frail, 16 non-frail, 16 young). (C) Percentage of NS cells positive for Ki67 after different plasma treatment, FACS analysis data. (D) Percentage of live, early, late apoptotic and necrotic NS cells after different plasma treatments. Data are expressed as mean ± SEM. *p value < 0.05 (17 frail, 16 non-frail, 16 young plasma samples, each one tested on 3 different NS cell cultures).

Figure 2. *Increase of DNA damage in dissociated NS cells after plasma treatment.* (A) Representative immunofluorescence analysis nuclei (n = 10 different fields for each sample; three independent cultures), of γ-H2AX expression in NS cells treated with plasma of enrolled subjects and untreated (Ctrl). Scale bars: 50 μm and 10 μm in the zoomed inserts. (B) Charts showing the quantitative analysis of the percentages of γ-H2AX+ cells over the total nuclei; (C) of the number of foci per nucleus; (D) of the fluorescence intensity of foci per nucleus. (E) Representative FACS dot plots of γ-H2AX in NS cells treated with plasma of the studied groups (17 frail, 16 non-frail, 16 young sample plasma). Histograms represent the percentage of NS cells positive for DNA damage (γ-H2AX) after the different plasma treatment. Data are expressed as means ± SEM. *p value < 0.05 (17 frail, 16 non-frail, 16 young plasma samples, each one tested on 3 different NS cell cultures).

Figure3. *Intracellular ROS in dissociated nephrosphere cells.* Representative flow cytometric analysis of 2', 7'-dichlorofluorescein (DCF) on dissociated NS cells treated with plasma of enrolled subjects (6 frail, 5 non-frail and 5 young); DCF Fluorescence intensity quantification (bar graphs). Data are representative of five independent NS cultures. Ctrl = untreated cells.

Figure 4. *Representation of oxidative status in different plasma.* (A) Level of 7βOHC, 7KC, 5α6αEC, 5β,6βEC, 3β,5α,6β-3OHC, lathosterol, lanosterol, 27-OHC and 24-OHC in 17 frail, 18 non-frail and 10 young samples. (B) Level of 8-OHdG in 10 frail, 10 non-frail and 10 young samples. Data are expressed as means ± SEM. *p value < 0.05.

Figure 5. *Evaluation of cytokine concentrations in plasma samples.* (A) Scatter-plots showing mean cytokine concentrations (pg/mL) of IL-6, IL-8, CXCL9, IL-1α, CX3CL1 and CD40 from the enrolled plasma samples (38 frail, 37 non-frail and 37 young) evaluated by Human Magnetic Luminex Screening Assay. (B) Scatter-plot showing mean values of TNF-β, IL- 1β, IL-2, IL-15 and IL-17, cytokines present only in the plasma of frail subjects.

Figure 6. *Receiver-operating characteristics (ROC) curve.* Evaluation of ROC curves for IL-6, IL-8, CXCL9, IL-1α, CX3CL1 and CD40 concentration as discriminator between frail and non-frail plasma. Data are expressed as means ± SEM. *p value < 0.05.

Figure 1

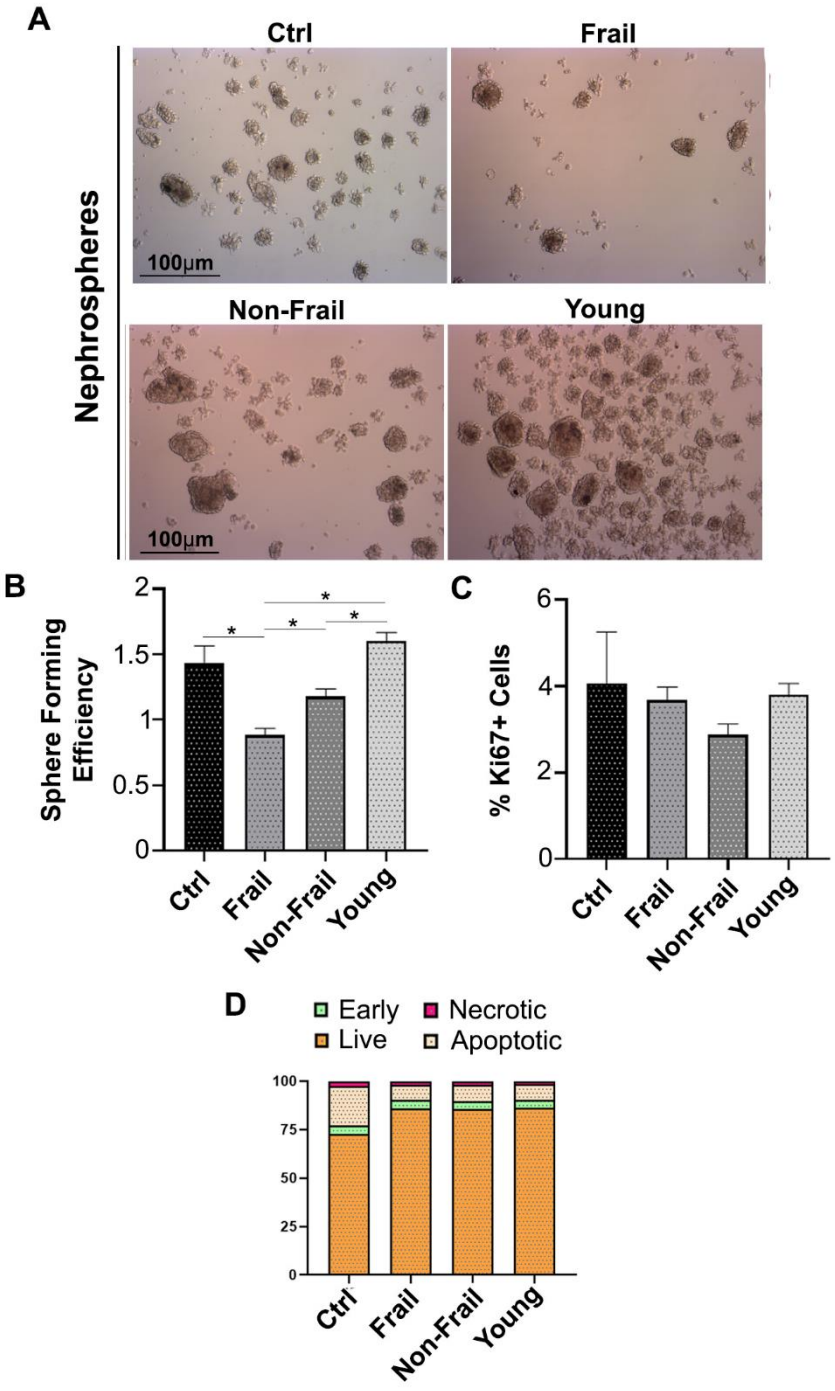
A
Ctrl
Frail
Nephrospheres
100µm
Non-Frail
Young
100µm
B
Sphere Forming Efficiency
2
1.5
1
0.5
0
*
*
*
*
Ctrl
Frail
Non-Frail
Young
C
% Ki67+ Cells
6
4
2
0
Ctrl
Frail
Non-Frail
Young
D
Early
Necrotic
Live
Apoptotic
100
75
50
25
0
Ctrl
Frail
Non-Frail
Young

Figure 2

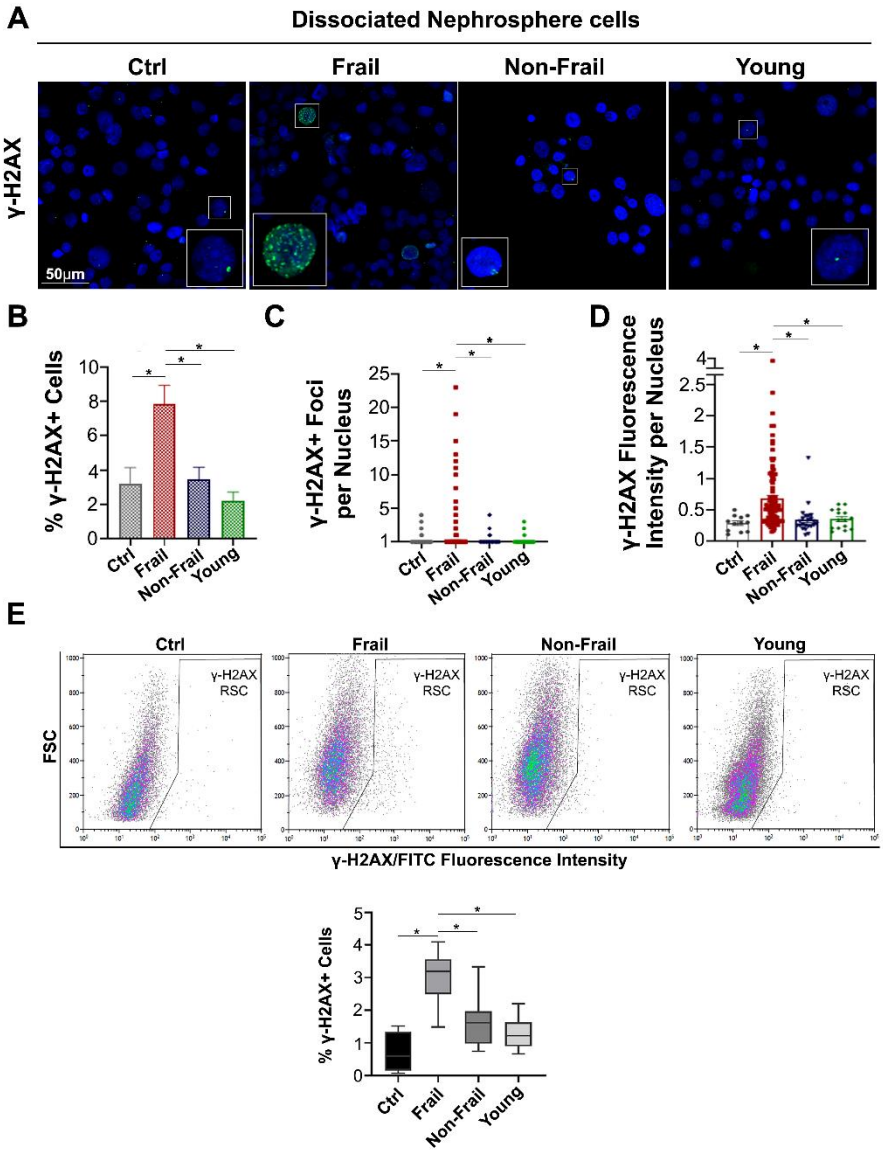
A
Dissociated Nephrosphere cells
Ctrl
Frail
Non-Frail
Young
γ-H2AX
50μm
B
% γ-H2AX+ Cells
C
γ-H2AX+ Foci per Nucleus
D
γ-H2AX Fluorescence Intensity per Nucleus
E
FSC
γ-H2AX RSC
γ-H2AX/FITC Fluorescence Intensity
% γ-H2AX+ Cells

Figure 3

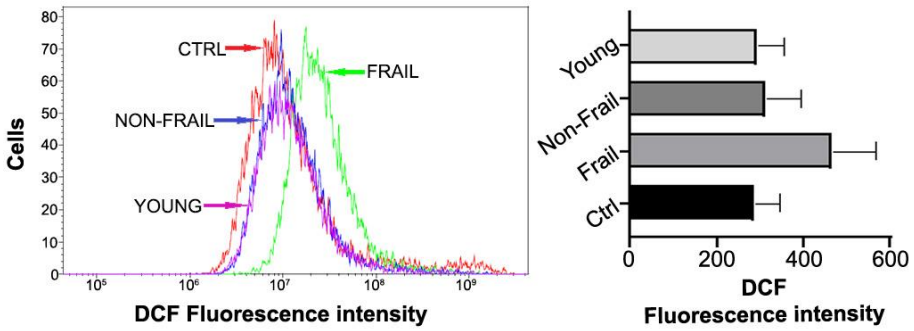
Cells
CTRL
FRAIL
NON-FRAIL
YOUNG
DCF Fluorescence intensity
Young
Non-Frail
Frail
Ctrl
DCF
Fluorescence intensity

Figure 4

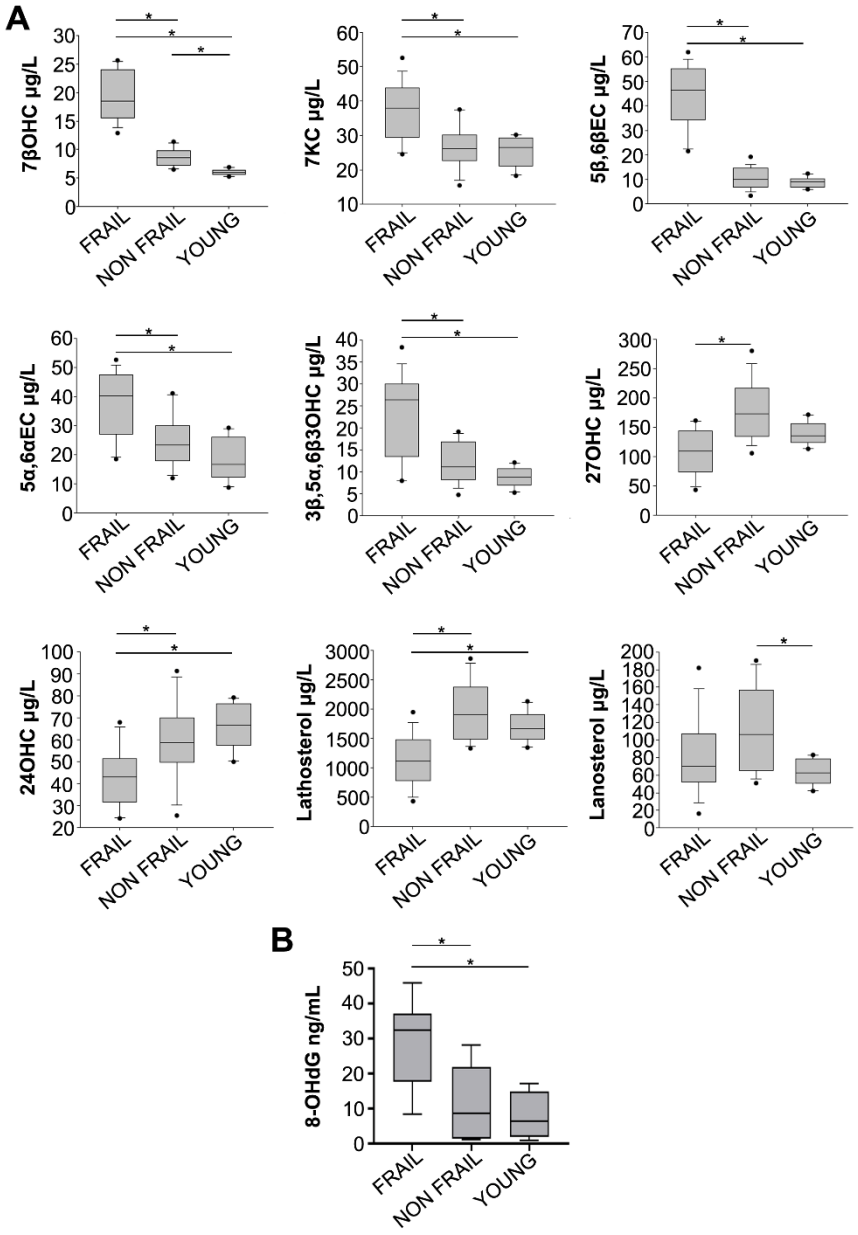
A
7βOHC µg/L
7KC µg/L
5β,6βEC µg/L
5α,6αEC µg/L
3β,5α,6β3OHC µg/L
27OHC µg/L
24OHC µg/L
Lathosterol µg/L
Lanosterol µg/L
FRAIL
NON FRAIL
YOUNG
B
8-OHdG ng/mL

Figure 5

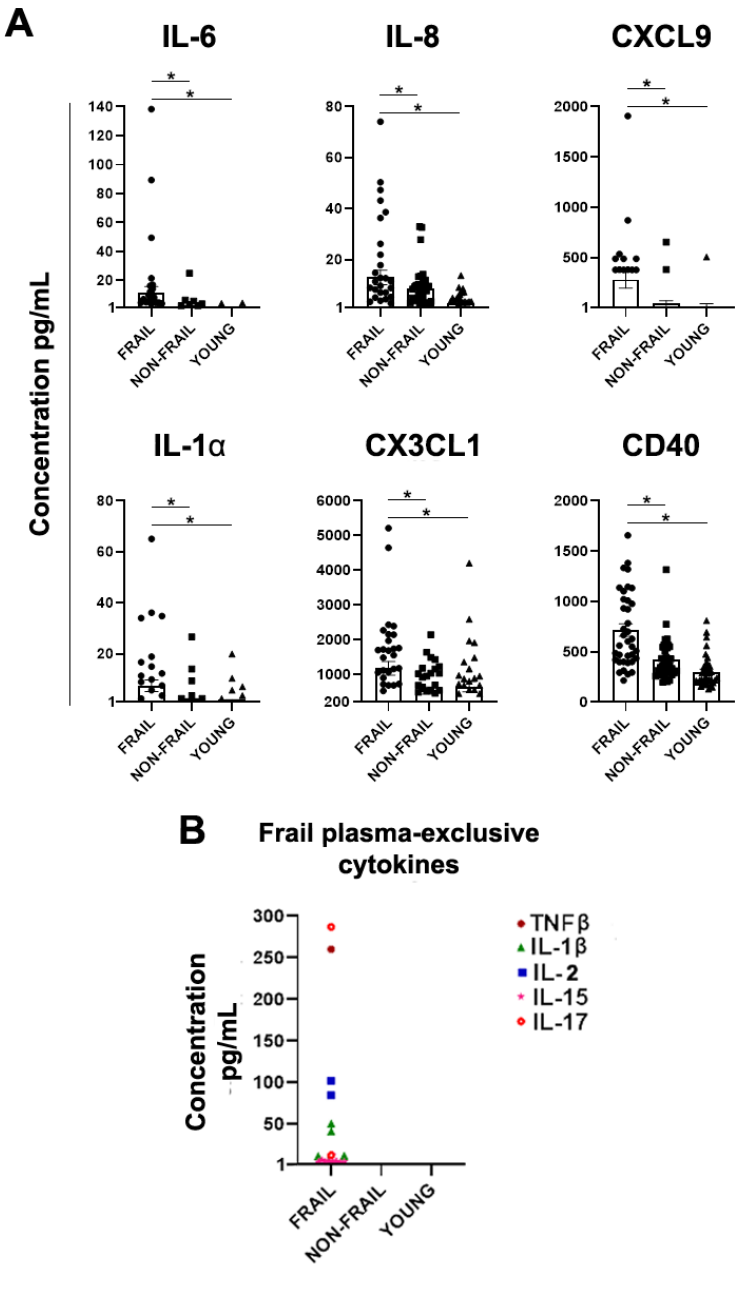
A
IL-6
IL-8
CXCL9
IL-1α
CX3CL1
CD40
Concentration pg/mL
FRAIL
NON-FRAIL
YOUNG
B
Frail plasma-exclusive cytokines
Concentration pg/mL
TNFβ
IL-1β
IL-2
IL-15
IL-17

Figure 6

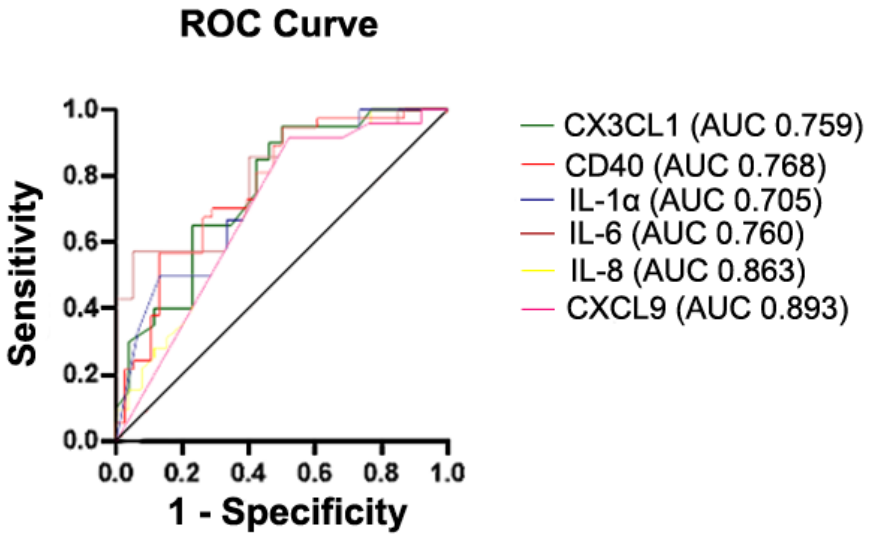
ROC Curve
Sensitivity
1 - Specificity
0.0
0.2
0.4
0.6
0.8
1.0
CX3CL1 (AUC 0.759)
CD40 (AUC 0.768)
IL-1α (AUC 0.705)
IL-6 (AUC 0.760)
IL-8 (AUC 0.863)
CXCL9 (AUC 0.893)

Supplemental figure legends

Supplementary figure 1. *Evaluation of the behavior of NS cells after hydrogen peroxide treatment.* (A) SFE with different concentrations of H_2O_2 (0.1mM, 0.5mM and 1mM). (B) Percentage of NS cells positive for DNA damage (γ-H2AX) after treatment with different concentrations of H_2O_2. Data are expressed as means ± SEM. *p value < 0.05.

Supplementary figure 2. *Evaluation of an additional 24 cytokine concentrations in plasma samples.* (A-C) Scatter-plots showing mean cytokine concentrations (pg/mL) of CXCL10, FLT3 LIGAND, GM-CSF, TGF-α, CCL3, IL-4, IL-7, IL-12p70, VEGF, CCL2, CCL22, CXCL1, CXCL12, IL-9, CCL11, CCL4, IL-1, IFN-γ, IL-5, RANTES, PDGF-BB, PDGF-AA, EGF and CD40 LIGAND from the enrolled plasma samples (38 frail, 37 non-frail and 37 young) evaluated by Human Magnetic Luminex Screening Assay.

Supplementary figure 1

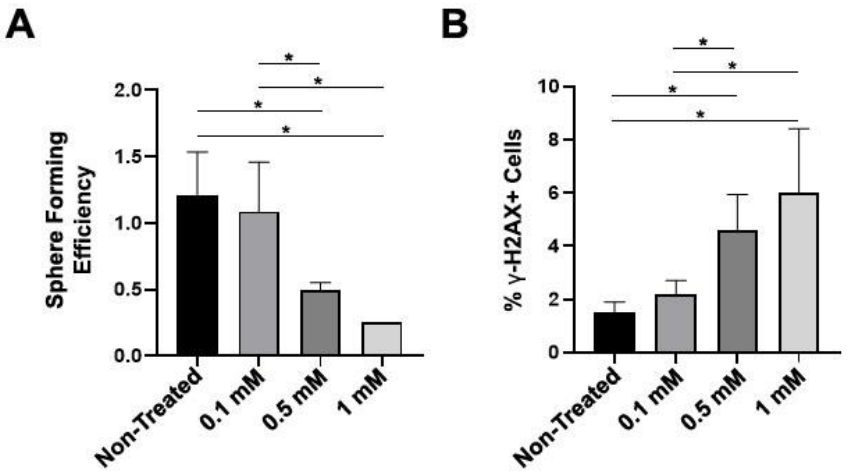

Supplementary figure 2

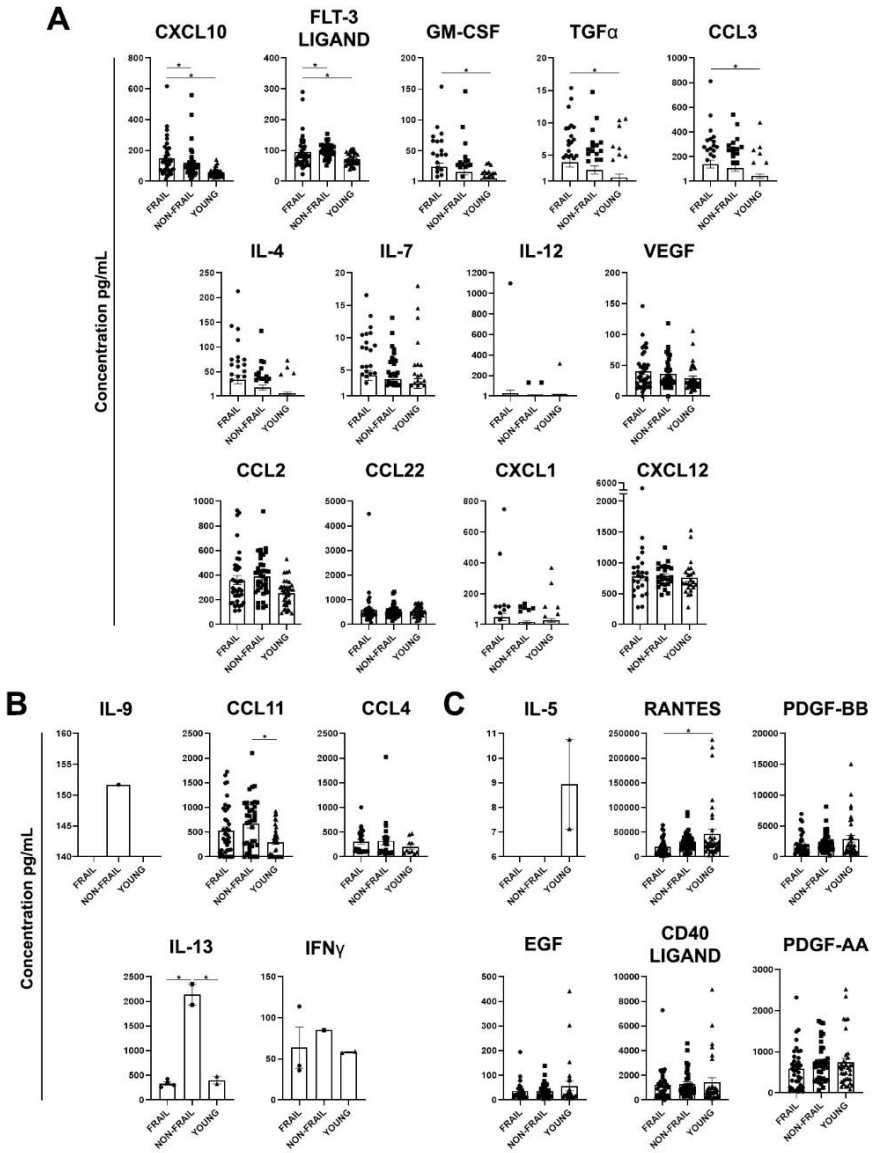

References

Fried LP, Tangen CM, Walston J et al. Frailty in Older Adults: Evidence for a Phenotype. The Journals of Gerontology: Series A. 2001; 56(3): M146–M157.

Kojima G. Prevalence of frailty in end-stage renal disease: a systematic review and meta-analysis. Int Urol Nephrol. 2017; 49(11): 1989-1997.

Shlipak MG, Stehman-Breen C, Fried et al. The presence of frailty in elderly persons with chronic renal insufficiency. Am J Kidney Dis. 2004; 43(5): 861-7.

Kim JC, Kalantar-Zadeh K, Kopple JD. Frailty and protein energy wasting in elderly patients with end stage kidney disease. J Am Soc Nephrol. 2013; 24: 337–351.

Carrero JJ, Stenvinkel P, Cuppari L et al. Etiology of the protein-energy wasting syndrome in chronic kidney disease: a consensus statement from the International Society of Renal Nutrition and Metabolism (ISRNM). J Ren Nutr. 2013; 23: 77–90.

Wilhelm-Leen ER, Hall YN, Tamura MK et al. Frailty and Chronic Kidney Disease: The Third National Health and Nutrition Evaluation Survey. Am J Med. 2009; 122(7): 664–71.

Weiss CH, Moazed F, McEvoy CA et al. Prompting physicians to address a daily checklist and process of care and clinical outcomes: a single-site study. Am J Respir Crit Care Med. 2011; 184(6): 680-6.

Van Munster BC, Drost D, Kalf A, Vogtlander NP. Discriminative value of frailty screening instruments in end-stage renal disease. Clin Kidney. 2016; 9(4):606-10.

López-Otín C, Blasco MA, Partridge L et al. The hallmarks of aging. Cell .2013; 153(6):1194-217.

Tümpel S, Rudolph KL. Quiescence: good and bad of stem cell aging. Trends Cell Biol. 2019; 29: 672- 685.

Guralnik JM, Simonsick EM, Ferrucci L et al. A short physical performance battery assessing lower extremity function: association with self-reported disability and prediction of mortality and nursing home admission. J Gerontol. 1994; 49(2): M85-94.

Washburn RA, McAuley E, Katula J et al. The physical activity scale for the elderly (PASE): evidence for validity. J Clin Epidemiol. 1999; 52(7):643-51.

Cruz-Jentoft AJ, Bahat G, Bauer J et al. Sarcopenia: revised European consensus on definition and diagnosis. Age and Ageing. 2019; 48(1): 16-31.

Kaiser MJ. Bauer JM. Ramsch C. et al. Validation of the Mini Nutritional Assessment short-form (MNA-SF): a practical tool for identification of nutritional status. *J Nutr Health Aging*. Nov 2009;13(9):782-8.

Folstein MF. Folstein SE. McHugh PR. "Mini-mental state". A practical method for grading the cognitive state of patients for the clinician. J Psychiatr Res. 1975; 12(3):1 89-98.

Lawton MP. Brody EM. Assessment of older people: self-maintaining and instrumental activities of daily living. Gerontologist. 1969; 9(3): 179-86.

Charlson ME. Pompei P. Ales KL. MacKenzie CR. A new method of classifying prognostic comorbidity in longitudinal studies: development and validation. J Chronic Dis. 1987; 40(5):373-83.

Bianchi C, Bombelli S, Raimondo F et al. Primary Cell Cultures from Human Renal Cortex and Renal-Cell Carcinoma Evidence a Differential Expression of Two Spliced Isoforms of Annexin A3. Am J Pathol. 2010; 176(4): 1660–1670.

Bombelli S, Zipeto MA, Torsello B et al. PKHhigh cells within clonal human nephrospheres provide a purified adult renal stem cell population. Stem Cell Res 2013, 11: 1163-1177.

Brown AJ, Jessup W. Oxysterols: Sources, cellular storage and metabolism, and new insights into their roles in cholesterol homeostasis. *Mol Aspects Med*. 2009 Jun;30(3):111-22. doi: 10.1016/j.mam.2009.02.005.

Kulig W , Cwiklik L, Jurkiewicz P, Rog T, Vattulainen I. Cholesterol oxidation products and their biological importance. *Chem Phys Lipids*. 2016; 199: 144-160. doi: 10.1016/j.chemphyslip. 2016.03.001.

Marcello A. Civra A. Bonotto R et al. The cholesterol metabolite 27-hydroxycholesterol inhibits SARS-CoV-2 and is markedly decreased in COVID-19 patients. Redox Biology. 2020; 36: 101682.

Diaz-De la Cruz EN. Cerillos-Gutiérrez JI. Garcìa-Sànchez A et al. The alteration of Pro-inflammatory Cytokines and Oxidative Stress Markers at Six-month Post-living Kidney Donation. Front Med. 2020; 7: 382.

Rockwood K, Mitnitski A, Song X et al. Long-term risks of death and institutionalization of elderly people in relation to deficit accumulation at age 70. J Am Geriatr Soc. 2006; 54(6): 975-9.

Tarazona-Santabalbina FJ, Gómez-Cabrera MC, Pérez-Ros P et al. A Multicomponent Exercise Intervention that Reverses Frailty and Improves Cognition, Emotion, and Social Networking in the Community-Dwelling Frail Elderly: A Randomized Clinical Trial. J Am Med Dir Assoc. 2016; 17(5): 426-33.

Travers J, Romero-Ortuno R, Bailey J et al. Delaying and reversing frailty: a systematic review of primary care interventions. Br J Gen Pract. 2019; 69(678): e61-e69.

Behrens A, Van Deursen JM, Lenhard Rudolph K, Schumacher B. Impact of genomic damage and ageing on stem cell function. Nat Cell Biol. 2014; 16(3): 201–207.

Lo YY, Conquer JA, Grinstein S, Cruz TF. Interleukin-1 beta induction of c-fos and collagenase expression in particular chondrocytes: involvement of reactive oxygen species. J Cell Biochem. 1998; 69(1): 19-29.

Hwang YS, Jeong M, Park JS et al. Interleukin-1β stimulates IL-8 expression through MAP kinase and ROS signaling in human gastric carcinoma cells. Oncogene. 2004; 23: 6603–6611.

Forcina L, Miano C, Scicchitano MS et al. Increased circulating levels of Interleukin-6 affect the redox balance in skeletal muscle. Oxidative Medicine and Cellular Longevity. 2019; 13.

Dhillon P, Wallace K, Herse F et al. IL-17-mediated oxidative stress is an important stimulator of AT1-AA and hypertension during pregnancy. Am J Physiol Regul Integr Comp Physiol. 2012; 303(4): R353–R358.

Liu R-M and Desai LP. Reciprocal regulation of TGF-β and reactive oxygen species: A perverse cycle for fibrosis. Redox Biol. 2015; 6: 565–577.

Park J, Song KH, Ha H (2012) Fractalkine increases mesangial cell proliferation through reactive oxygen species and mitogen-activated protein kinases. Transplant Proc 44:1026–1028

Chapter 5

Summary, conclusions and future perspectives

Summary

Frailty is a geriatric syndrome that can be defined as an age-related progressive impairment of multiple physiological systems, resulting in a significantly reduced capacity to compensate for external stressors. Consequently, the frail subject is at risk for poor clinical and functional outcomes [Lang, 2009].

Fried and colleagues proposed a phenotype characterization of frailty through five clinical criteria, but this can be possible only after the onset of clinical manifestations without the possibility of a precocious diagnosis.

Several studies report a high prevalence of frailty in individuals with chronic kidney disease (CKD), and frailty can further increase with advancing age and progressive decline of renal function towards end-stage renal disease [Kojima, 2017]. Elderly individuals with CKD are two to three times more likely to be frail than those with normal renal function. However, the relationship between kidney dysfunction and frailty is still unclear [Chowdhury, 2017].

There are increasing evidences that the aging process can have adverse effects on stem cells, in fact their self-renewal ability declines and their differentiation potential into the various cell types is altered [Tümpel, 2019]. Aging-induced exhaustion and deterioration of stem cell pool may play a key role in the pathophysiology of aging-associated diseases, including kidney dysfunction.

In this scenario, participating to a project (2017-0577) funded by Fondazione Cariplo, I was involved during my 3-years PhD course in the characterization of adult renal stem/progenitor cells.

Our group isolated a population of multipotent renal stem-like cells by a functional approach [Bombelli, 2013], taking advantage from the ability of renal stem/progenitor cells (RSC) to grow as nephrospheres (NS). Investigating the expression of renal progenitor markers described in literature (CD133 and CD24) [Bussolati, 2005; Sagrinati, 2006], our group identified in NS a PKH^{high}/CD133+/CD24- cell population displaying in vitro stem-cell properties [Bombelli, 2013], able to repopulate human decellularized renal scaffold [Bombelli, 2018].

At the beginning of my PhD I participated in the characterization of multipotency of RSC [Bombelli, 2020], as described in Chapter 2 of this Thesis.

Successively, for the project in which I was involved, we tested whether in the organism of elderly and frail people there were biological conditions able to alter RSC behavior, justifying the kidney dysfunction often present in the frail status. The development of the funded project had in view the recruitment of frail, pre-frail, non-frail subjects and young controls, and collection of whole blood separated into plasma and PBMC. I contributed to study DNA damage in both PBMC and circulating hematopoietic stem/progenitor cells (cHSPC) of frail patients, observing a statistically higher percentage of cells positive for DNA damage [Grasselli et al. Submitted, Chapter 3].

Given these premises, to assess whether there were biological conditions related to frailty able to affect the properties of adult RSC present in NS cultures, I contributed to study the action of frail plasma on RSC as described in Chapter 4.

Conclusion and application to translational medicine

In conclusion, we found that frail plasma affected the self-renewal property of RSC but not the cellular proliferation and vitality. Interesting findings were also the high oxidative status of frail plasma and the capacity of these plasma to elicit in NS cells the highest ROS and DNA damage. The latter was also correlated with the highest DNA damage in the cHSPC of the donors of frail plasma. Lastly, the frail plasma had an inflammatory profile that showed a characteristic presence of 11 cytokines over the 40 studied. In literature for some of these 11 cytokines is described their capacity to induce intracellular ROS. In our experiments their presence in the frail plasma correlated with the plasma high oxidative status and with the highest DNA damage and reduction of SFE induced in NS cells treated with this plasma.

It is possible to argue that there are correlations between the exhaustion of renal stem cells functions and the frailty status, due to the increase of oxidative stress and pro-inflammatory cytokines in the plasma of frail patients, which lead to increment of DNA damage, intracellular ROS and impairment of self-renewal abilities. The impairment of allogenic RSC, treated with frail plasma, recall the situation seen with the homologous cHSPC of the donors of frail plasma. However, it is likely that the adult stem cell compartment of the different tissues may suffer the same situation which can lead to a functional decline of different organs and result into frailty.

From a translation point of view, the obtained findings may contribute to a better comprehension of frail pathophysiology and could help the development of novel therapies to modulate the oxidative status, reduce

DNA damage or eliminate the damaged cells. This would be important not only in relation to kidney dysfunction but, in a more general way, in all frail patients for attenuating frailty progression, improving their quality of life and reducing the national healthcare costs.

Future Perspectives

In the future development of this research, it will be important to investigate whether the plasma of frail patients can influence the differentiation potential of NS cells and in particular the RSC PKH+/CD133+/CD24- of our NS cells. We will use the differentiation media described in Bombelli et al [Bombelli, 2013] supplemented with 10% plasma obtained from frail and non-frail patients to perform epithelial, endothelial and podocytic differentiation. It would also be interesting to evaluate DNA damage in these differentiated cultures to compare and correlate all the data. We expect to observe a correlation in the alteration of self-renewal, DNA damage and differentiation when NS cells are cultured in presence of plasma of frail patients, confirming that high oxidative stress and inflammatory mediators can influence the RSC function. It will be also important as a future perspective, to test analytically the role of inflammatory cytokines on NS cells and on RSC PKH+/CD133+/CD24- treating them with exogenous cytokines selected from those that have been found to be significantly present in plasma of frail patients and evaluating their role on oxidative stress, DNA damage, self-renewal and differentiation.

To translate the results obtained in this research into *in vivo* settings, we could do parabiosis studies, in which old and young mice are surgically

joined so they share a circulatory system to study the effects of circulating factors in driving disease. Heterochronic parabiosis, involving the pairing of young and old mice, have been well used to investigate whether exposure to a circulatory system could act as a source of rejuvenation for an older animal as well as a source of aging in young mice [Rebo, 2016; Villeda, 2011; Smith, 2015]. We could examine young mice heterochronically paired with both old fit mice and frailty mice models and vice versa, and young isochronic pairings and old isochronic pairings as controls, to determine if circulating factors can modulate and interfere with stem cells compartment, causing DNA damage and an impairment of physiological systems, especially in kidneys.

References

Lang PO, Michel JP, Zekry D. Frailty syndrome: a transitional state in a dynamic process. Gerontology. 2009; 55(5): 539-49.

Kojima G. Prevalence of frailty in end-stage renal disease: a systematic review and meta-analysis. Int Urol Nephrol. 2017; 49(11): 1989-1997.

Chowdhury R, Peel NM, Krosch M et al. Frailty and chronic kidney disease: a systematic review. Arch Gerontol Geriatr 2017; 68: 135-142.

Tümpel S, Lenhard Rudolph K. Quiescence: Good and Bad of Stem Cell Aging. Trends Cell Biol. 2019; 29(8):672-685.

Bombelli S, Zipeto MA, Torsello B et al. PKHhigh cells within clonal human nephrospheres provide a purified adult renal stem cell population. Stem Cell Res 2013, 11: 1163-1177.

Bussolati B, Bruno S, Grange C et al. Isolation of renal progenitor cells from adult human kidney. Am. J. Pathol. 2005, 166, 545–555.

Sagrinati C, Netti GS, Mazzinghi B et al. Isolation and characterization of multipotent progenitor cells from the Bowman's capsule of adult human kidneys. J. Am. Soc. Nephrol. 2006, 17, 2443–2456.

Bombelli S, Meregalli C, Scalia C et al. Nephrosphere-Derived cells are induced to multilineage differentiation when cultured on human decellularized kidney scaffolds. Am J Pathol. 2018; 188(1):184-195.

Bombelli S, Meregalli C, Grasselli C et al. PKHhigh/CD133+/CD24− Renal Stem-Like Cells Isolated from Human Nephrospheres Exhibit In Vitro Multipotency. Cells. 2020; 9: 1805.

Rebo J, Mehdipour M, Gathwala R et al. A single heterochronic blood exchange reveals rapid inhibition of multiple tissues by old blood. Nat Commun. 2016; 7: 13363.

Villeda SA, Luo J, Moscher KI et al. The ageing systemic milieu negatively regulates neurogenesis and cognitive function. Nature. 2011; 477: 90‑4.

Smith LK, He Y, Park J et al. beta2-microglobulin is a systemic pro-aging factor that impairs cognitive function and neurogenesis. Nat Med. 2015;21:932‑7.

Publications

Grasselli C, Ferrari D, Zalfa C, Soncini M, Mazzoccoli G, Facchini FA, Marongiu L, Granucci F, Copetti M, Vescovi AL, Peri F, De Filippis L. Toll-like receptor 4 modulation influences human neural stem cell proliferation and differentiation. Cell Death & Disease. 2018; 9: 280. DOI: 10.1038/s41419-017-0139-8.

Zalfa C, **Grasselli C**, Santilli G, Ferrari D, Lamorte G, Vescovi AL and De Filippis L. GFAP Delta as divergent marker of human glial progenitors. Stem Cell Research and Therapy. 2018; 8: 9. DOI: 10.4172/2157-7633.1000437.

Grasselli C, Carbone A, Panelli P, Giambra V, Bossi M, Mazzoccoli G, De Filippis L. Neural stem cells from Shank3-ko mouse model autism spectrum disorders. Mol Neurobiol. 2020; 57(3):1502-1515. DOI: 10.1007/s12035-019-01811-6.

Bombelli S, Meregalli C, **Grasselli C**, Bolognesi MM, Bruno A, Eriani S, Torsello B, De Marco S, Bernasconi DP, Zucchini N, Mazzola P, Bianchi C, Grasso M, Albini A, Cattoretti G and Perego RA. $PKH^{HIGH}/CD133^{+}/CD24^{-}$ renal stem-like cells isolated from human nephrospheres exhibit in vitro multipotency. Cells. 2020; 9, 1805. DOI: 10.3390/cells9081805.

Bombelli S, Torsello B, De Marco S, Lucarelli G, Cifola I, **Grasselli C**, Strada G, Bovo G, Perego RA, Bianchi C. 36-kDa Annexin A3 isoform negatively modulates lipid storage in clear cell renal cell carcinoma cells. Am J Pathol. 2020;190(11): 2317-2326. DOI: 10.1016/j.ajpath.2020.08.008.

Conference Communications

Grasselli C, Bombelli S, Mazzola P, Eriani S, Bolognesi M, Rossi F, Antolini L, Cattoretti G, Annoni G, Perego RA. "A pilot study to assess the correlation between frailty and DNA damage in hematopoietic stem cells". XXXVII CONFERENZA NAZIONALE DI CITOMETRIA (GIC). Aggiornamenti e Innovazioni della Citometria nella Applicazioni Cliniche e di ricerca. Capaccio Paestum (SA). 28-31 May 2019.

Bombelli S, **Grasselli C**, Bolognesi M, Bruno A, Eriani S, Torsello B, De Marco S,Bianchi C, Strada G, Zucchini N, Albini A, Cattoretti G and Perego RA. "$PKH^{HIGH}/CD133^{+}/CD24^{-}$ stem-like cells isolated from human nephrospheres exhibit in vitro multipotency". 22^{nd} Nephrogenesis Workshop. UCL Great Ormond Street Institute of Child Health Development Biology and Cancer. London. 14 June 2019.

Grasselli C, Bombelli S, Mazzola P, Eriani S, Bolognesi M, Rossi F, Antolini L, Cattoretti G, Annoni G, Perego RA. "DNA damage in haematopoietic stem cells from frail subjects: a pilot study". Young Scientists Meeting, SIPMeT. pathobiology: from molecular disease to clinical application. Plesso Didattico Morgagni-Università Degli Studi Di Firenze. 12-13 September 2019.

De Marco S, Bianchi C, Torsello B, Minutiello E, Bombelli S, **Grasselli C**, Eriani S, Zucchini N, Viganò P, Strada G and Perego RA. "Molecular interactions among Arg/Abl2, TGF-β1, Lox and functional role in clear cell Renal Cell Carcinoma (ccRCC) progression". Young Scientists Meeting, SIPMeT. pathobiology: from molecular disease to clinical application. Plesso Didattico Morgagni-Università Degli Studi Di Firenze. 12-13 September 2019.

De Marco S, Torsello B, Minutiello E, Bombelli S, **Grasselli C**, Eriani S, Zucchini N, Strada G, Bianchi C and Perego RA. "Molecular interactions among TGF-β1, Lox and Arg/Abl2 in clear cell Renal Cell Carcinoma (ccRCC) and in its progression". 2nd joint EACR-MRS Conference on Seed and Soil Mechanisms of metastasis. Berlin. 07-09 October 2019.

Mazzola P, Bombelli S, **Grasselli C**, Eriani S, Bolognesi M, Rossi F, Antolini L, Cattoretti G, Annoni G and Perego RA. "Correlation between frailty and DNA damage in hematopoietic stem cells: a pilot study". Gerontological Society of America (GSA) 2019 Annual Scientific Meeting. Strength in age: Harnessing the power of networks. Austin, Texas. 13-17 November 2019.

De Marco S, Torsello B, Minutiello E, Bombelli S, **Grasselli C**, Eriani S, Zucchini N, Viganò P, Strada G, Bianchi C, Perego RA. TGF- β1, Lox and Arg/Abl2 interact to promote clear cell renal cell carcinoma progression. Congresso Nazionale Società Italiana di Urologia (SIU). Roma (IT). 17/10/2020 – 18/10/2020.

Torsello B, De Marco S, Bossi M, Bombelli S, **Grasselli C**, Zucchini N, Bianchi C, Perego RA. Abl2 is required for TGF β1-induced invasion of clear cell renal cell carcinoma cells. EACR 2021: Innovative Cancer Science. Virtual. 14/06/2021 – 18/06/2021.

Grasselli C, Bombelli S, Mazzola P, Eriani S, Bolognesi M, Rossi F, Antolini L, Cattoretti G, Annoni G, Perego RA. "DNA damage in adult stem cells: a possible marker for frailty?". AMP Europe 2020. Milano (MI). 14-18/06/2021.

De Marco S, Torsello B, Minutiello E, Bombelli S, **Grasselli C**, Bianchi C, Perego RA. "Abl2 knockdown affects TGF β-mediated 3D invasion of ccRCC cells". AMP Europe 2020. Milano (MI). 14-18/06/2021.

Bombelli S, Eriani S, **Grasselli C**, Bolognesi M, Rossetti G, Ranzani V, Torsello B, De Marco S, Bianchi C, Pagani M, Cattoretti G, Perego RA. Molecular characterization of nephrosphere-derived PKH /CD133+/CD24- stem-like cells evidenced possible new markers for renal stem cells in situ identification. AMP Europe 2020. Milano (MI). 14-18/06/2021.

De Marco S, Torsello B, Bombelli S, **Grasselli C**, Zucchini N, Strada G and Perego RA, Bianchi C. Clear cell renal cell carcinoma invasion is modulated by TGF-ß1/ARG interaction. European urology. Riccione (RN). 17/10/2021.

Grasselli C, Bombelli S, Eriani S, Mazzola P, Bolognesi M, Rossi F, Antolini L, Grasso M, Zucchini N, Bellelli G, Perego RA. Biological conditions related to frailty and their effects on adult renal stem cells cultured as nephrospheres. MOLECULAR PATHOLOGY: FROM BENCH TO BEDSIDE - SIPMeT Young Scientist Meeting 2021. Perugia (PG). 10-11/12/2021.